S.Yu. Sapronova, V.P. Tkachenko,
O.V. Fomin, I.I. Kulbovskiy, E.P. Zub

RAIL VEHICLES: THE RESISTANCE TO THE MOVEMENT AND THE CONTROLLABILITY

monograph

Dnipro
2017

UDC 629.4.072:629.1.072

C 19

This monograph is recommended for printing by the Science Council of DUIT STATE UNIVERSITY OF INFRASTRUCTURE AND TECHNOLOGY (protocol No 1 dd 8.12.2017).

Reviewers: ***Miamlin S.V.*** – doctor of Technical Sciences, Professor, Vice-Rector on Scientific Work of Dnipropetrovsk National University of Railway Transport named after academician V. Lazaryan
Gorbunov M. I. – doctor of Technical Sciences, Professor, Head of Railway Transport, Automobile Transport and Lifting-Transporting Machines of Volodymyr Dahl East Ukrainian National University

S.Yu. Sapronova, V.P. Tkachenko, O.V. Fomin, I.I. Kulbovskiy, E.P. Zub.

C19 Rail Vehicles: The Resistance to the Movement and the Controllability: Monograph. Dnipro: Ukrmetalurginform STA, 2017. – 160 p.

ISBN 978-966-921-163-7

The monograph substantiates the existence and determines the origin of the constituent element of the resistance to the movement within rail carriages; the constituent is determined by the control of the wheel pairs within the railway track. In this book, we suggest the method to analyze closed power circuit in mechanical power transmission applied to rolling stock. The method of mathematical modeling for two-point contact of the wheel with the rail has also been developed. The characteristics of the kinematic resistance to the movement for a number of types of rolling stock have been obtained. There are power factors which control the rail carriages and their analysis is very important, therefore we address to it in the book as well. Based on the decrease in the circulation ratio within the closed power circuits of the control system created for carriages by the railway track, we also suggest the principles of designing the rolling stock truck arrangement with low resistance to the movement.

The monograph is intended for scientists, engineers and technicians working in the field of design and research for railway transport as well as for masters and postgraduate students of specialty 273 - «Railway transport».

UDC 629.4.072:629.1.072

ISBN 978-966-921-163-7

CONTENTS

INRODUCTION 6

1. STUDY ON THE RESISTANCE TO THE MOVEMENT OF THE ROLLING STOCK 9

1.1. Historical Review on the Studies of the Movement Resistance with the Railway Rolling Stock 9

1.2. Structure of the Resistance to the Movement of Rail Carriages 30

1.2.1. Resistance in the Axle Equipment 30

1.2.2. Loss of Power in the Traction Drive 33

1.2.3. Resistance to Wheels Rolling on Rails 33

1.3. The Choice on the Calculation Schemes for Simulating the Carriages Control by the Railway Track 39

1.3.1. The Nature of the Resistance to the Movement Based on the Control of the Wheel Pairs by the Railway Track 39

1.3.2. Closed Power Circuits in the Contacts of Wheels with Rails 40

1.3.3. Closed Power Circuits of Wheel Pairs 41

2. STUDY ON CONTROLLABILITY AS THE PROCESS OF GUIDANCE FOR THE CARRIAGE BY THE RAILWAY TRACK 44

2.1. The Concept of Controllability in the Railway Transport 44

2.2. The Study on the Guidance Force Generated by the Track for Wheel Pairs 48

2.3. Theories of Wheel-Rail Adhesion 49

2.4. Study of Adhesion Characteristics 51

2.5. The Guidance of the Carriage by the Railway Track 56

2.5.1. The Role of Wheel Flange Reactions in the Wheel Pairs Control and the Coefficient of the Derailment Resistance 56

2.5.2. The Kinematics of the Wheel Pairs Contact with Rails 61

2.5.3. Power Interaction of the Wheel Flanges and the Rail 63

2.5.4. The Criterion of the Derailment Prevention 64

3. THEORETICAL STUDY ON RESISTANCE TO THE MOVEMENT ASSOCIATED WITH THE CONTROL OF THE CARRIAGE BY THE RAILWAY TRACK 66

3.1. The Choice on the Calculation Schemes for Modeling the Carriages Control by the Railway Track 66

3.1.1. The System of Coordinates and the Simulation Features for the Rail Carriages 66
3.1.2. The Calculation Models of the Carriages under the Study 69
3.2. Differential Equations of the Carriage Movement 73
3.2.1. Equations of the Wheel Pairs Movement 73
3.2.2. Equations of the Truck Frame Movement 75
3.2.3. Equations of the Body Movement 76
3.3. Mathematical Models of Locomotives 76
3.3.1. Mathematical Models of Frame Locomotives 77
3.3.2. Locomotives with Linked Carriages 79
3.3.3. Six-Axle Carriages with the Axial Formula of 3o-3o 84
3.3.4. Multiaxial Locomotives Based on Two-Axle Carriages 87
3.4. Models of Electric Trains, Diesel Trains, Passenger Carriages, Trams and Underground Carriages 93
3.5. Mathematical Models of Freight Carriages 96
3.6. Simulation of the Contacting Parts of the Carriage 100

4. SIMULATING THE EXTERNAL CONTROL ACTION 103
4.1. Generalized Contact and Axle Equipment Reactions 103
4.2. Analysis on the Control of Power Factors 108
4.2.1. Structure of the Power Factors Affecting Wheel Pairs 108
4.2.2. Power Factors for Rolling Stocks Control when Interaction between Wheel Pairs and Tracks 109

5. MODELING THE KINEMATIC RESISTANCE TO THE MOVEMENT 114
5.1. The Nature of the Resistance to the Movement Associated with the Control of the Wheel Pairs by the Railway Track 114
5.2. Mathematical Modeling for Carriages Control by Rails in the Curve .. 118
5.2.1. Calculation Scheme of Truck Guiding into the Curve of the Track ... 118
5.2.2. The System of Equations for Truck Equilibrium when Guided into the Curve 121
5.2.3. Calculation Results of the Resistance to the Movement Associated with the Control of Wheel Pairs by Rail Tracks: A Study on the Carriages of 18-100 Type 122
5.3. Method to Calculate the Kinematic Resistance to the Movement 126
5.3.1. Reduction of Forces and the Moments of the Movement Resistance 126
5.3.2. Impact of Carriage Truck Parameters on the Kinematic Movement Resistance 127

6. WAYS TO IMPROVE CONTROLABILLITY AND REDUCE THE RESISTANCE TO THE MOVEMENT OF RAIL CARRIGES 131
6.1. Linked Carrieges Design Development 132
6.2. Carriages with Radial Installation of Wheel Pairs 133
6.2.1. HTCR-II Trucks Locomotives Developed by Electro-Motive Diesel 134
6.2.2. Truck of 2TE25k Locomotive Being Studied 134
6.2.3. Wheel Blocks of Talgo High-Speed Spanish Electric Trains 136
6.2.4. Technical Solutions for Designs of Wheels with Radial Installation of Wheel Pairs 137

CONCLUSIONS AND RESULTS 147

REFERENCES 150

INRODUCTION

For more than 30 years, one of the main and most resource-intensive problems of railway transport is the problem of heavy wear of wheels rolling surfaces and rails in curved sections of tracks. Significantly greater wear of wheels and rails in curves in comparison with straight lines is explained by the fact that the rolling stock in the curves is guided by the horizontal forces, which are necessary for doing work against the frictional forces between wheels and rails. The track curved sections make up more than 40% of the total length of the main Ukrainian railways, and 60-70% in the field of industrial and municipal transport. Taking this into account it becomes obvious that the urgency of the research studying for the processes of carriages guiding by railway tracks is beyond doubt. The main reason for the resistance to the movement associated with the control of wheel pairs by railway tracks is the frictional interaction in the contacts of wheels with rails caused by sliding. Moreover, the contact sliding is the main cause of the wheel-rail rolling surfaces wear in curved sections of tracks.

The resistance to the movement is one of the most important technical and economic characteristics of the railway carriages. The practical experience of the railway transport operation shows that from 1/3 to 1/4 of the total energy consumed by the railway rolling stock traction is used for doing work against the friction.

The forces of the resistance to the movement of trains or separate units of the rail transport are regarded as the external forces acting on it and directed, as a rule, against their movement. As the traction forces, they are conditionally reduced to the contact points of wheels with rails. The forces of the resistance to the movement are subdivided into the main ones acting constantly during the movement and the additional ones emerging only when moving along the certain sections of the track or at certain periods of time.

The sum of the forces of the main resistance (W_o) and the additional resistance (W_d) is called the total resistance of the train (W). The train movement resistance consists of the resistance to the locomotive movement (W') and the resistance to the train carriages movement (W''). In calculations, the specific forces of the

resistance to the movement are used, i.e. the absolute resistance forces taken relative to the weight of the corresponding unit of the rolling stock. They are measured differently across the countries, for example: *N*/*kN*, kg/ton, lb[1]/ton, etc.

The main resistance to the movement (W_o) acts in case of the movement in straight horizontals of tracks when there is no wind and it consists of the following components associated with the following processes:

- friction in the box bearings of the rolling stock;
- friction and sliding wheels on rails;
- impacts on rails irregularities;
- aerodynamic resistance of the air medium.

The forces of the additional resistance to the movement are of the resistance forces operating under certain conditions. Moreover, the additional resistance to the movement can be composed by the components associated with the following movement conditions:

- slopes gradients of the track;
- curved sections of the track;
- operation of undercar generator in passenger carriages;
- resistance forces that emerge at low air temperatures;
- additional resistance when starting;
- contrary or cross winds.

The traction effort of the locomotive is necessary for doing work against the movement resistance of both the locomotive and the train. If the traction force is greater than resistance, the train is accelerated in accordance with Newton's motion law. If the traction force is equal to the resistance, the train moves at a constant speed. If the traction force is lower than the resistance, the train slows down.

The traditional design of the truck arrangement of the rolling stock and, in particular, that of the wheel pairs with the wheel rigid connection through the axle is the cause of the specific dynamic processes, which are often found with railway transport only.

Their main feature is reciprocal effect of the wheels and the wheel pairs through the axle, the truck frame and the rail track on the distribution of torque between the wheels, in case of the group drive this distribution is between the axles as well.

The common knowledge says that the control over, or guidance of railway carriages by tracks is carried out under the influence of the horizontal forces which occur when wheels contact with rails. The rigid linking of the wheels

[1]lb – pound (from Latin *libra* – scales) – unit of the mass and the force in the English-speaking countries

1 pound ≈ 0.454 kg

in the wheel pair and the variable radii of the wheel profiles provide classical advantages of the rigid wheel pair: ability to direct the uncontrolled movement in the transverse direction within the gap of the railway track and self-centering respectively the axis.

The concepts of the controllability are widely used in the theory of the movement of wheeled and track-type machines, ships and aircrafts, spacecraft, i.e. wherever controlling influence comes from the part of the control bodies. Based on the analysis of the controllability of these means of transport, the authors suggested the generalized term for the controllability.

In its turn, the controllability is defined as a property of a vehicle to be under trajectory and/ or a course guidance, that is to preserve, or to change the magnitude and the direction of the motion speed under the influence of the control effect.

If we consider machines with control systems, their controllability is determined by the reaction of the machine to the controlling effort coming from the control body, the reaction shows itself in the form of the changes in the track parameters, in the course parameters or in the lateral kinematic parameters. For example, in the case of an automobile, this is a steering wheel turning, in the case of a ship or an aircraft, these are a helm and a control wheel respectively.

As it is known, there are no trajectory control bodies within the railway carriages because they are guided or directed by lateral reactions from the rail track.

In the current monograph, the authors have shown that the horizontal effect of the carriage on the track and the kinematic resistance to the movement are interconnected and interdependent; the carriage with a lower kinematic resistance to the movement has a lower horizontal dynamic effect on the track. The book suggests the approach which regards the guidance of carriages by the railway track as a controlled phenomenon; this allows us to create the general approaches to the design of truck arrangements on the basis of the comprehensive methodology for evaluation of the quality indicators of the railway carriages controllability.

The monograph is intended for scientists, engineers and technicians who work in the field of design and research of the dynamics of railway carriages as well as students studying for their Master's degrees and post-graduate students of specialty 273 "Railway transport".

1 STUDY ON THE RESISTANCE TO THE MOVEMENT OF THE ROLLING STOCK

1.1. Historical Review on the Studies of the Movement Resistance with the Railway Rolling Stock

Starting the review from the first studies on the resistance to the movement, dated back as far as the earliest ages of the railways development, and including the recent ones, one cannot help noting that almost all the researches of this kind have been experimental and conducted with the objective to obtain the formulas for the traction calculations. In general, the whole period of time devoted to the studies of the resistance to the movement can be divided into the main and the additional ones.

In 1818, George Stephenson, the inventor of the first famous steam locomotive called Rocket, conducted the first experiments to determine the resistance of wagons to the movement in England.

In 1825, Czech engineer Franz Anton Ritter von Gerstner, later built the first Tsarskosilska Railroad in the Russian Empire, revealed that the resistance of the wagon to the movement when transferring goods on the rails was seven times higher than in case of its movement on natural soil road.

In 1835, when the first railway of the Russian Empire was only being designed, P. Melnikov, the Minister of Communications of the Russian Empire in 1865-1896, wrote a book where he described the experiments on determining the rolling stock resistance to the movement.

In 1858, Russian engineer A. Dobronravov in *General Theory of Steam Engines and Theory of Steam Locomotives* [1] considered in detail the constituent elements of the resistance to the train movement. A. Dobronravov raised the question of interaction between the locomotive traction power, the train weight, the profile of the track and "ability to drive a locomotive".

In Russia, the first attempts to determine the force of traction by research were made by professor M. Okatov. In 1869, he made the experiments on "sliding"

(determining the limitation of the traction force by the adhesion) on the section of Peterburg-Luban of the Mikolaiv railway.

A large series of the experimental studies on the rolling stock resistance to the movement, the traction force, the water and fuel consumption was carried out in 1877-1879 under the supervision of Russian engineer V. Lopushinskyi on the Morshansk-Syzran railway [2].

The experiments proved the necessity to take into account the kinetic energy of the train in case of traction calculations. According to the results of the experiments, the first empirical formulas were derived for determining the main specific resistance of passenger carriages, freight carriages and locomotives, the additional specific resistances in curved sections of tracks, as well as the dependence of the traction effort on the adhesion and the dependence of the steam flow on the train speed. The numerous studies resulted in the fundamental formula expressing the dependence between the movement resistance and the speed:

$$W = A + BV + CV^2, \tag{1.1}$$

where W – the absolute movement resistance in the force units;
V – the movement speed.

Coefficients A and B describe the influence of the mass movement on the resistance and the mechanical component of the interaction with the track. Coefficient C defines the effect of the movement aerodynamic resistance or the air resistance on the resistance.

Later, the triangular quadratic parabolas became the most common forms of describing the main resistance of the rolling stock:

$$w_o'' = a + \frac{b + c \cdot V + d \cdot V^2}{q}, \tag{1.2}$$

where q – the average weight of the rolling stock unit.

Even during the first experiments, the influence of "injurious or parasitic carriage movement" on the resistance was the issue of concern and was determined in a lower value for the passenger carriages than for the freight ones. This was the first mention of the kinematic resistance to the carriage movement.

In paper *Determination of Fuel Consumption by Locomotives* (1877), L. Ermakov, a professor of the Moscow Institute of Railway Engineers (Russian Empire), scientifically developed the fundamentals of traction calculations to determine the train weight, the movement time, the permissible speeds for trains at braking, the consumption of water and fuel. Thus, for defining the economic benefit of the train acceleration before the up-hill, the accumulated kinetic energy of the train was taken into account. In his paper *Data and Calculations Relating to Locomotives Operation* (1883), the distribution of the movement resistance

forces acting in the train is considered in the aspect as follows: the resistance to the movement on the straight horizontal track, the resistance to the movement of tenders, the resistance to the movement on up-hills and the resistance in curves of tracks [3].

In 1881, Ukrainian engineer A. Borodin expressed the idea of creating artificial conditions during experiments on locomotives and was the first who proposed to relocate the experiments from the railway track into the laboratory, where the locomotive at any constant mode transfers its work to the transmission or through the rollers to brakes. In 1882 in Kiev workshops, he created the world's first engine laboratory, where complex machines were tested [4].

In 1889, on the basis of the theoretical and experimental studies of the Moscow-Kursk and Vladikavkaz railways, professor N. Petrov and engineer V. Lopushinskyi (Russia) suggested the calculation formulas to define the resistance of the rolling stock [5] as a function of the motion speed:

• for two-axle freight carriages

$$w_o'' = 1.8 + 0.073 \cdot V + 0.001 \cdot V^2, \tag{1.3}$$

• for two-axle passenger carriages

$$w_o'' = 1.8 + 0.083 \cdot V. \tag{1.4}$$

The forces creating the resistance to the movement have been studied both experimentally and theoretically. The theoretical work of professor N. Petrov in the field of friction became classical and is still being studied by the specialists working over the issues of the resistance to the movement of the rolling stock. In lecturing course *Locomotives* and in his other papers [6-8], he systematized the researches on the theory of the trains traction. Professor N. Petrov considered in detail the causes of the wheels resistance to the movement at the junctions, and the cases of the air resistance to the movement of the train.

The hydrodynamic theory of friction developed and published in 1883 by professor N. Petrov explained the phenomena occurring in the axle boxes of wheel pairs and helped to cast light on the problem of the movement resistance in a new approach.

N. Petrov is considered to be the founder of the theory of the train traction. He developed a formula to determine the main specific resistance to the movement of two-axle freight carriages. This formula is interesting by its structure, namely, by the presence of two main factors that affect the resistance to the movement: the speed and the loading degree of carriages.

The formula by professor N. Petrov for two-axle freight carriages was as follows:

$$w = 1.2 + \frac{0.9 \cdot V}{q} + \frac{0.0012 \cdot V^2}{q} + \frac{0.03 \cdot V^2}{Q}, \quad (1.5)$$

where w – the main specific resistance of the train (kg/t);

q – the average weight of the loaded carriage (tones);

Q – the weight of all the carriages in the train (tones).

The studies of N. Petrov and V. Lopushinskyi gave an opportunity to improve the methods of train traction calculations and proved the inaccuracy of the calculation formulas developed by Meyer, Geigard, and Franco.

In 1895, S. Smirnov, engineer and director of the Petersburg Putilov factory, outlined the foundations of the method of "minimum" for defining the directional forces of rails in the curves [9].

In 1898, Russian engineer Yu. Lomonosov began the operational tests on the stream locomotives within the trains by the order of the Traction Department of the Kharkiv-Mykolaiv railway. In paper *Traction Calculations and Appendixes with Graphical Methods* [10], Yu. Lomonosov substantiated the necessity to reject the purely theoretical approach in determination of the traction force and the resistance to the movement of the rolling stock with further transition to the experimental practice.

In 1904, American professor W.J. Davis published in *the Street Railway Journal* an article based on his experimental research of the first electric locomotives [11]. The first complex tests to determine the resistance of electric locomotives at high speeds and the influence of the carriage number on the resistance were carried out in 1900 at section Buffalo & Lockport, the maximum speed reached 60 mph. Utilizing the experimental data, W.J. Davis suggested the following formula for calculating the resistance of trains with the electric traction:

$$w = b = c \cdot V^2 + \frac{d \cdot V^2}{T} \cdot \left[A_1 + m\left(A_2 + A_3 + \ldots + A_n \right) \right], \quad (1.6)$$

where w – the specific resistance to the movement (lb/ton);

V – the motion speed (ml/h);

T – the train weight (ton);

c – the complex friction coefficient when sliding and rolling;

d – the wind pressure coefficient;

m – the proportionality coefficient showing the effect of each carriage on the overall aerodynamic movement resistance;

$A_1, A_2, \ldots, A_n$ – the cross-sectional areas of the locomotive $\left(A_1\right)$ and carriages $\left(A_2, \ldots A_n\right)\left(lb^2\right)$.

If all carriages in the train are the same, the formula is simplified as written:

$$w = b = c \cdot V^2 + \frac{d \cdot A \cdot V^2}{T} \cdot \left[1 + m\left(n-1\right)\right], \tag{1.7}$$

where n – the number of carriages in the train;

$b = 3.5$ – for freight trains;

$b = 4.0$ – for standard passenger train carriages and long electric trains;

$b = 5.0 - 6.0$ – for electric trains light in weight;

$c = 0.11$ – for heavy track constructions;

$c = 0.13$ – for the average construction of the track;

$d = 0.0035$ – for open platforms;

$d = 0.0024 - 0.0030$ – for the connection of carriages of electric trains;

$m = 0.10$.

During the period of 1908-1916, a large series of experiments was carried out in the experimental laboratory of *the University of Illinois* (USA) under the guidance of Professor E. Schmidt and engineer N. Dunn for determining the resistance of the freight and the passenger trains with the steam and the electric traction. The results were obtained in the range of speeds between 10-55 mph during the experimental travel. The results of the research were published in a series of the publications of the bulletin of *the Engineering Experiment Station* of the University of Illinois, Urbana during 1910-1927 [12-16].

In 1927, Edward C. Schmidt summarized the results of the many years of the research on the resistance of freight trains in track curved sections [17] and assumed that the additional resistance to the movement per the curve or the specific resistance could be measured in kg per ton of weight per 1 degree of the curve.

One of the issues which does not have the mainstream agreement is the authorship of the quadratic form of the movement-resistance function of the speed. It is attributed to many researchers. Sometimes it is called *Petrov-Lopushinskyi formula*, sometimes – as *Borries Formel*, sometimes – *Leitzmann Formel* formula, or *Function de Barbier* [18]. Moreover, there are references to several more author's formulas on the dedicated issue in the scientific literature. We consider it is reasonable to mention them below.

The formula by *A. H. Armstrong* (1910) [19]:

$$w = \frac{50}{\sqrt{Q}} + 0.03 \cdot V + \frac{0.002 \cdot a \cdot V^2}{Q}. \tag{1.8}$$

Westinghouse formula*:*

$$w = 4 + \frac{V}{10} + \frac{10 \cdot S^2}{36 \cdot Q}. \tag{1.9}$$

Mailloux formula (1904):

$$w = 3.5 + 0.15 \cdot V + \left[\frac{0.02 \cdot N + 0.25}{N \cdot Q} \right] \cdot V^2. \tag{1.10}$$

Cole formula (1909):

$$w = 5.4 + 0.002 \cdot (V - 15)^2 + \frac{100}{(V + 2)^2}. \tag{1.11}$$

In formulas (1.8)–(1.11) read as follows:

w – the main specific movement resistance (lb/ton);

V – the motion speed (ml/h);

Q – the train weight (ton);

a – the cross-section of the carriage (lb^2);

N – the number of carriages in the train.

However, the most commonly, the fundamental formula for the movement resistance is still called *Davis equation*. In 1926 in brochure [20], Davis suggested an improved empirical formula to calculate the train resistance at straight horizontal tracks in the form as follows:

$$w = 1.3 + \frac{29}{Q} + 0.045 \cdot V + \frac{0.0005 \cdot a \cdot V^2}{Q \cdot N}, \tag{1.12}$$

where w – the train resistance to the movement (lb/ton);

Q – the axial loading (ton);

N – the number of the axes;

a – the cross-section of the locomotive (m^2).

For many decades, Davis's original formula for the movement resistance has remained unchanged in principle, but there were developed many variants how to alter its coefficients as the new types of the rolling stock entered the scene, the modernizations of the old rolling stock occurred or the speed increase took place.

Great importance was also paid to the accuracy of the traction calculations and therefore the Davis formula has been constantly completed and improved by the efforts of hundreds of researchers.

Thus, based on long experiments in 40-50 years of the 20th century, *American Association of Railway Engineers* (AREA), modified the Davis equation in the form as follows:

$$w_u = 0.6 + \frac{20}{q} + 0.01V + \frac{KV^2}{qn}, \tag{1.13}$$

where w_u – the resistance to the movement (lb/ton);

q – the axial loading (ton);

n – the axes number;

V – the speed (ml/h);

K – the coefficient of the aerodynamic resistance.

The values of coefficient K are the following: K = 0.07 for covered carriages; K = 0.0935 for containers; K =0.16 for trailers on railway platforms.

The resistance to the movement in the curved sections of the track is greater than in the straight lines. This statement is beyond any doubt and confirmed by a large number of experiments. However, it is the least studied phenomenon, and the results obtained are contradictory in comparison with other components of the movement resistance. Meanwhile, it is generally accepted that the movement resistance in the curve is inversely proportional to the radius of the curve.

In 1912, under the Ministry of Communications of the Russian Empire, *the Office of Experiments on the Types of Stream Locomotives* was established. In 1918, it was transformed into *the Experimental Institute of Railways*, and in 1935 - into the All-Union Research Institute of Railway Transport headed by Yu. V. Lomonosov. Let us consider some of the activities of this organization with long traditions in the railway industry. In 1915, they developed the document of *Rules for Comparative Tests on Types of Steam Locomotives*, which described the obligatory procedures for testing locomotives intended for operation at the railways belonging to the state. On the basis of the tests, the technical passports of the stream locomotives of almost all the series operated on the railways of Tsarist Russia were issued. Based on the experiments, they approved *Temporary Rules for Traction Calculations* [3], which were grounded on so-called *Formula of Kharkiv-Mikolaev Railway*. These rules had been used for the traction calculations of the resistance to the movement with the biaxial carriages for the long period of time.

In 1908-1916, under the guidance of G. Lebedev, Russian railway engineer, a series of experiments with four-wheel freight carriages on trucks was conducted and a formula for main specific resistance to the movement was suggested as written:

$$w_o'' = 2.8 + \frac{q - 12 \cdot V}{700} + 0.00144 \cdot V^2. \qquad (1.14)$$

Despite the use of a large amount of the experimental data, the formula was not proved by the subsequent studies and these calculations were not applied in practice.

Based on the results of the tests with the trains composed of the four-wheeled passenger carriages and with the steam locomotive traction, Russian engineers V. Lubimov and N. Dadaev developed the dependences for the movement resistance under summer and winter operating conditions. They are respectively shown as follows:

$$w_0'' = 1.2 + 0.01v + 0.003v^2, \qquad (1.15)$$

$$w_0'' = 1.5 + 0.005v + 0.005v^2. \quad (1.16)$$

Professor Yu. V. Lomonosov [21] believed that dependence (1.15) corresponds to the ideal operation conditions, and therefore for four-axle ones he proposed the dependence, which was widely used for the calculations of the resistance to the movement until 1937.

$$w_0'' = 1.4 + 0.02v + 0.002v^2. \quad (1.17)$$

Before 1937, the main specific resistance to the movement of two-axial and three-axial carriages was determined as follows:

$$w_0'' = 1.6 + 0.0027v + 0.0003v^2. \quad (1.18)$$

However, in 1958, Russian engineer B. Karachan found the new dependence for the main specific resistance of four-wheel freight carriages [22]:

$$w_0'' = \frac{65 + v}{12 + 0.55q}. \quad (1.19)$$

The above mentioned dependence showed a slight error between the theoretical and the experimental data.

The study of *Research Institute of Railway Transport* based on dependence (1.19) gave the opportunity to obtain the other formula for two-axle freight carriages; this formula has been used for traction calculations up to date and is as written:

$$w_0'' = 1.4 + 0.2v + \frac{0.5v}{q}. \quad (1.20)$$

In 1937, the *Central Scientific Research Institute of the Ministry of Transport and Communications* conducted the test travels on the main line of the Zhovtneva Railway with the objective to determine the main resistance of four-wheel carriages and they resulted in the dependence below:

$$w_0'' = 1.4 + 0.012v + 0.0003v^2. \quad (1.21)$$

At the same time, the test travels were carried out with the two-axle and the four-axle passenger carriages and they allowed the researches to receive the dependence of the main specific resistance on the speed in the form as given:

$$w_0'' = 1.4 + 0.017v + 0.0003v^2. \quad (1.22)$$

This dependence is also currently used in the practice of the traction calculations.

In 1947, Soviet professor P. Gurskyi conducted the another series of the test travels with the four-axle tanks [23] and developed the dependence of the resistance to the movement for the loaded and the empty tanks respectively:

$$w_0'' = 1.3 + 0.04v, \tag{1.23}$$

$$w_0'' = 1.3 + 0.06v. \tag{1.24}$$

In 1947-1948 the Ural and Siberia railway test travels were carried out with the freight trains of different weights in order to determine the influence of low temperatures on the resistance to the movement [24]. The results were expressed in the dependence of the main specific resistance of the freight four-axle carriages:

$$w_0'' = 0.65 + \frac{14 + 0.2v^2}{q_0} + 0.0002v^2. \tag{1.25}$$

The further research on the main resistance for four-wheel freight carriages were conducted by *the Transport Problems Scientific Researches Section of the USSR Academy of Sciences* [25]. Thus, the main specific resistance for this type of carriages was determined as the following expression based on the theoretical studies:

$$w_0'' = 0.51 + \left(0.044 + 0.00004v^2\right)n^2 + 125\varphi + \frac{11k_c \cdot q_0}{\sqrt{I \cdot u}} + \frac{0.0564v^2}{q_0}, \tag{1.26}$$

where n – the wheel pair running on the rolling track (cm);

φ – the friction coefficient for the axle sets in bearings;

k_c – the coefficient of the resistance from the elastic deflection of the track;

I – the moment of rail inertia relative to the horizontal axis passing through the center of the rail cross-section (cm^4);

u – the elastic modulus of the rail base (kg/cm^2).

In 1953-1955, in *Central Scientific Group of the Ministry of Internal Affairs*, the comparative tests with the passenger carriages equipped with axle boxes on roller bearings and friction bearings were carried out. The experiments allowed the further development of the formula for passenger carriages with roller bearings [26], it is given below:

$$w_0'' = 1.15 + 0.0102v + 0.0003v^2. \tag{1.27}$$

In 1956, P. Gursky [27] on the basis of the data processing obtained from the tests on the traction and the heat of the courier locomotive of 2-3-2 type (Kolomenskyi plant), determined the main resistance to the movement of the train with 10 passenger carriages equipped with the axle boxes on the roller bearings:

$$w_0'' = 1.4 + 0.012v + 0.00026v^2. \tag{1.28}$$

The dependence developed as the result of this work was known as the most accurate one for the calculations of the passenger carriages resistance at speeds

faster than 90 km/h, however, the fact that it was developed with a small number of the test travels and with the carriages and the tracks of old types could not be neglected.

The next step was made by A. Baranov [28] who suggested a generalized formula for passenger trains to be as follows:

$$w_o = 0.53 + \frac{10.7 + b \cdot V + \left(b + \frac{8}{n_o} \right) \cdot 10^{-2} \cdot V^2}{q_o}, \tag{1.29}$$

where $b = 0.75 \cdot l \cdot 10^{-2}$;

l – the carriage length;

n_o – the number of axles in the train.

In the Ukrainian *Rules of Traction Calculations for Train Operation* [29] (hereinafter referred as *RTC*), the formulas for determining the approximate value of the additional resistance to the movement in curves are as follows:

а) on condition that the length of the train is less than the length of the curve, the following can be applied:

$$w_r = \frac{700}{R}, \tag{1.30}$$

or

$$w_r = 12.2 \cdot \frac{\alpha^0}{s_{cr}} \tag{1.31}$$

where R – the radius of the curve (m);

α^0 – the angle length of the curve (degree);

s_{cr} – the linear length of the curve (m);

б) if the length of the train is more than the length of the curve, they use as written:

$$w_r = \frac{700}{R} \cdot \frac{s_{cr}}{l_t}, \tag{1.32}$$

or

$$w_r = 12,2 \cdot \frac{\alpha^0}{l_t}, \tag{1.33}$$

where l_t – train length (m).

Furthermore, in several countries (USA, Italy, England and China), a formula similar to (1.30) is used for the traction calculations but with the different coefficients (refer to Table 1.1).

However, Germany, Austria, Switzerland, the Czech Republic, Slovakia, Hungary and Romania use the formulas, where instead of the radius of curve R there is the difference of (R-b) in the denominator of formula (1.30) while b is considered a constant value:

$w_r = 650/(R-55)$ – for curves with radius $R > 300$ m;
$w_r = 500/(R-30)$ – for curves with radius $R < 300$ m.

Table 1.1

Formulas for Approximate Estimation of the Additional Resistance to the movement in the Curve

Countries	Formula for Movement Resistance in Curves
USA	$w_r = 446/R$
Italy	$w_r = 800/R$
England	$w_r = 600/R$
China	$w_r = 573/R$

The fact that the values of the movement resistance for R = 300 m differ by more than 30% shows that all these formulas are approximate in the best case.

In Ukraine, for more accurate calculations for the additional resistance to the movement, *RTC* [29] recommends to use the following formulas:

a) if the length of the train is less than the length of the curve, there should be applied as written:

$$w_r = \frac{200}{R} + 1.5 \cdot \tau_c, \tag{1.34}$$

or

$$w_r = 3.5 \cdot \frac{\alpha^0}{s_{cr}} + 1.5 \cdot \tau_c; \tag{1.35}$$

b) if the length of the train is more than the length of the curve, there should be applied as given:

$$w_r = \left(\frac{200}{R} + 1.5 \cdot \tau_c \right) \cdot \frac{s_{cr}}{l_t} \tag{1.36}$$

or

$$w_r = \left(3{,}5 \cdot \frac{\alpha^0}{s_{cr}} + 1.5 \cdot \tau_c \right) \cdot \frac{s_{cr}}{l_t}. \tag{1.37}$$

Here, τ_c – the unbalanced radial (centrifugal or centripetal) acceleration of the carriages movement in the curve (m/s):

$$\tau_c = \frac{V^2}{R} - \frac{h \cdot g}{s}, \tag{1.38}$$

where V – the train movement speed (m/s);
h – the height of the outer rail (m);

g – acceleration of gravity (9.81 m/s²);

s – distance between the rolling circles of the wheel pair (for tracks of 1520 mm, s = 1600 mm).

Recalling (1.38) we obtain the following:

$$w_r = \left[\frac{200}{R} + 1.5 \cdot \left(\frac{V^2}{R} - \frac{h \cdot g}{s}\right)\right], \tag{1.39}$$

or

$$w_r = \left[3.5 \cdot \frac{\alpha^0}{s_{cr}} + 1.5 \cdot \left(\frac{V^2}{R} - \frac{h \cdot g}{s}\right)\right] \cdot \frac{s_{cr}}{l_t}. \tag{1.40}$$

Figure 1.1 shows the dependencies developed with formula (1.36).

As it can be seen from Figure 1.1, according to formulas (1.31) and (1.33), the values of the resistance to the movement become negative for some curve radiuses, the increase of the outer rail obtains the negative values as well. This does not correspond to our perceptions of the physics of the process. If a carriage moves with an equilibrium speed in a curve, then the total centrifugal force in the transverse direction is to be zero.

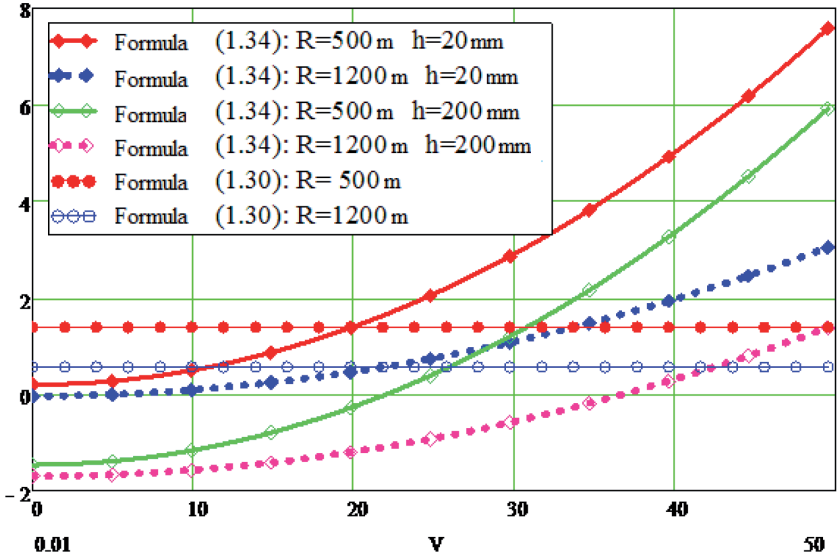

Figure 1.1. The Dependencies of the Specific Resistance to the Movement of the Rolling Stock in a Curve on the Speed. Constructed per Formulas (1.34) and per Formula by *RTC* (1.30)

The equilibrium speed is defined from the condition as written below:

$$\frac{V^2}{R} - \frac{h \cdot g}{s} = 0 \tag{1.41}$$

from which we obtain:

$$V = \sqrt{\frac{R \cdot h \cdot g}{s}} \tag{1.42}$$

The equilibrium speed is limited with unbalanced centripetal acceleration, which meeting the condition of comfort for passengers, cannot exceed 0.7 m / c^2. At the equilibrium speed, it is possible to hope for the minimum side effect produced by wheel flanges on rails and respectively the minimum value of the component composing the resistance to the movement, it depends on the flange friction, which occurs on rail lateral faces.

With the increase or the reduction in the speed, the equilibrium lateral force influencing rails increases. Moreover, when the speed increases, the force influencing the outside rail increases while the reduction of speed means the increase in the force acting on the inside rail. These causes were described, in particular, by E. Schmidt in 1927 in the weekly *Bulletin of Engineering Experimental Laboratory of the University of Illinois* [30].

The same was supported by S. Amelin and G. Andreyev, the professors of *the Leningrad Institute of Railway Transport*, in their book *Railway Design and Operation* (1986) [31].

The fact, that there exists the minimal dependency of the resistance to the movement in the curve on the speed, finds its confirmation by several experimental studies. Thus, within the researches of this kind one can name the results presented by the English researchers: A. Armstrong and J. L. Koffman. In 1910, A. Armstrong with his book *Standard Handbook for Electrical Engineers* (*Electric Traction*) provided the dependencies [32]. We show them in figure 1.2 as the scanned copies. Later, in 1961-1964, J. L. Coffman conducted a big series of experimental work on the resistance to the movement on the British railroads [77-79]. According to the research program, the analysis was carried out to reveal the dependency of the resistance to the movement on the following factors: roughness of rail lines; rolling friction of wheels; joints of rails; hunting oscillations and parasitic movements of trucks (truck hunting); friction in the flange contacts of wheels with rails; hunting and the characteristics of springs and hunting dampers. From the results of the research, J. L. Coffman drew the conclusion that the resistance to the movement needs to be predicted at the project stage of the rolling stock development. The special attention is to be paid to the issues of the interaction between the train (the locomotive and the carriages) and the track that depends on the static and the dynamic parameters of the track, the design of

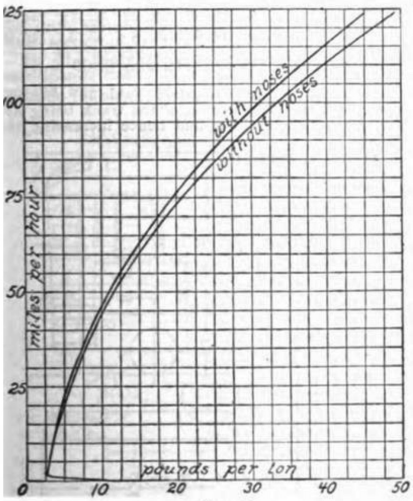

Fig. 2.

Fig. 2.—Train resistance (Berlin-Zossen tests 1903; 206400 lb.; area 130 sq. ft.

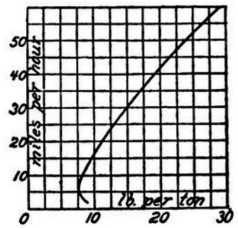

Fig. 4.—Train resistance (General Electric tests); weight 68,800 lb.

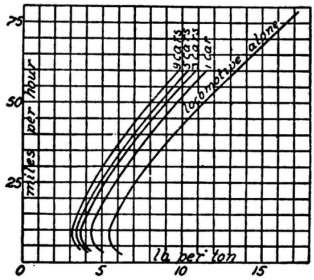

Fig. 6.—Train resistance runs (N. Y. C. locomotive and train).

Figure 1.2. Dependencies of the Resistance to the Movement in a Curve on the Speed. Provided by *Standard Handbook for Electrical Engineers* by A. Armstrong (Scanned Copies from Book [32])

wheels, the profile of flanges, the characteristics of springs and spring suspension hunting dampers, such as torque transmission. In particular, J. L. Coffman notes the essential difference in the resistance of the movement for the locomotives with different type of spring suspension: laminated springs and spiral springs.

A large contribution to the experimental studies on the resistance to the movement of different types of trains belongs to Soviet researcher P. Astakhov.

In monograph *Tractive Resistance of the Rolling Stock* (1966) [39], P. Astakhov systematized the results of the long-term experimental research on the resistance to the movement with locomotives and carriages, which were conducted by Central Scientific and Research Institute of Railway Transport of the Ministry of Railways. The monograph demonstrates technical, economic and power aspects of the problem of the resistance to the movement with the rolling stock, a short survey of the researches, the calculation formulas of the main and the additional resistance, and describes the methods of the experimental research with the magnitudes of the resistance to the movement.

On the experimental test loop[1] of the *All-Russian Research Institute of Railway Transport* (hereafter referred as VND ZT) in 1960-1962, P. Astakhov

[1]Test loop of *the All-Russian Research Institute of Railway Transport. Tscherbinka Station* of Moscow Railway.

and P. Stromsky obtained the results concerning the dependency of the resistance to the movement in curves on the speed, which also confirms the existence of the minimum in the equilibrium speed zone. Figure 1.3 presents the scanned copies from the article by P. Astakhov and P. Stromsky [33], here we can observe the research results on the resistance to the movement in curves.

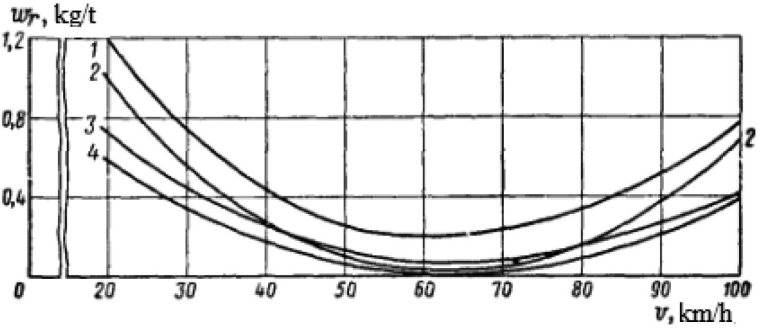

The Additional Specific Resistance of Four-Axle Freight Wagons on the Test Loop Curve with the Dependence of the Speed:
1) - empty tank wagon (q=6.1 m); 2) - empty open wagons (q=6 m);
3) - loaded tank wagon (q=19.1 m); 4) - loaded open wagons (q=20.5 m)

Figure 1.3. Dependency of the Resistance to the Movement in Curves on the Speed. The Research Results on the Test Loop of the *All-Russian Research Institute of Railway Transport* (the Scanned Copy from Book [33] with the Indication of the Original Figure Number)

G. Astakhov in monograph [39] based on the analysis of the previous researches suggests to improve formula (1.31) for the resistance to the movement in curves and to use it as followings:

$$w_r = \frac{200}{R} + 1.5 \cdot |\tau_k| \qquad (1.43)$$

Figure 1.4 shows a graphic interpretation of formulas (1.43) and (1.30).

It should be also mentioned, that the test loop railroad VND ZT has the constant radius of 955 m and the outside rail lift of 60 mm. The calculated equilibrium speed received with formula (1.39) equals 18.7 m/s or 67 km/h that coincides with the results of the experiments described in article [33] and monograph [39].

The American Railway Engineering and Maintenance-of-Way Association (AREMA) suggested the following formula for more exact calculation of the additional resistance to the movement in curved sections of tracks (2000) [34]:

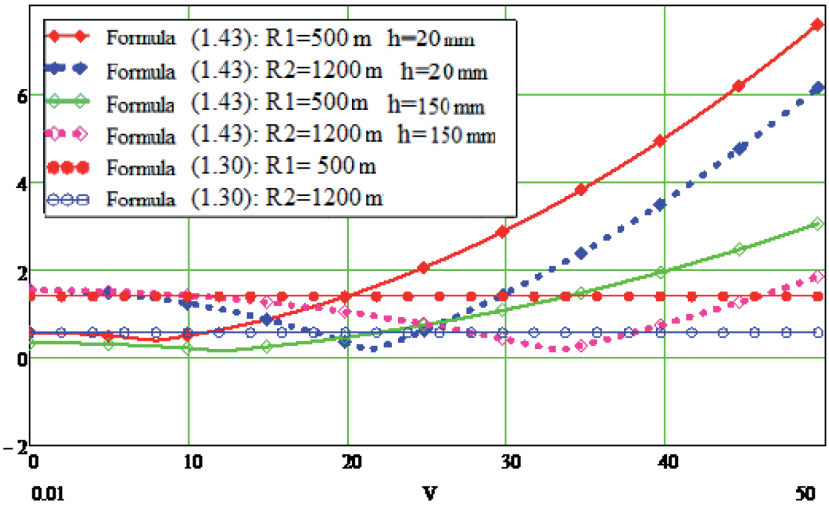

Figure 1.4. The Dependencies of Specific Resistance to the Movement on the Speed. The Rolling Stock in Curves. Constructed per Astakhov's Formula (1.43) and with Formula of RTC (1.30)

$$w_r = 0.01\frac{k}{R} \tag{1.44}$$

where w_r – the resistance to the movement in curves (kN/ton);

k – the magnitude-free parameter which depends on the type of truck arrangement of the rolling stock: it varies from 500 to 1200 with the mean value of 800;

R – curve radius in meters (m).

Similarly, in [35] it is noted that the following values for the resistance to the movement in curves are sufficient in their accuracy:

• 0.04% (approximately 0.8 of a pound per ton by a curve degree) of the main resistance to the movement;

• 0.05% (approximately 1.0 pound per ton by a curve degree) for small values of speeds (1-2 pounds per ton by a curve degree).

French professor Pierre Fayet in his doctoral dissertation (2008) [36] provides the description how to incorporate the resistance to the movement occurring in curves as the "equivalent" inclination.

The equivalent inclination was defined from the condition of the equal resistance to the movement in the curve and on that section where the equivalent inclination was equal to $800/R$ $^{o}/_{oo}$. For example, for the curve with the radius of 800 m, the equivalent inclination equals to 1 $^{o}/_{oo}$.

His paper [36] gives the formula for the resistance to the movement of the train calculated through the equivalent inclination. This formula is shown below:

$$W_r = m \cdot g \cdot \sin(\iota), \tag{1.45}$$

where W_r – the absolute resistance of the train in the curve (kN);
m – the mass of the train (t);
$g = 9.81$;
ι – the equivalent inclination (radian): $\iota = 800/1000R$;
R – the radius of the curve (m).

Further, it [36] addresses the example of dependency graph (1.45) for French TGV-Dasye with the weight of 380 t (refer to figure 1.5).

T. J. Mlinarić and K. Ponikvar (Slovenia) in their 2011 article [37] suggested the original simplified formulas for determining the specific resistance to the movement in curves. For the curves with the radiuses smaller than 300 мб they provide the formula as given:

$$w = \frac{500}{R - 30}. \tag{1.46}$$

For the curves with smaller curvature, they suggest the following:

$$w = \frac{12.2 \cdot \alpha}{l}, \tag{1.47}$$

where α is the central angle of the curve;
l – train length.

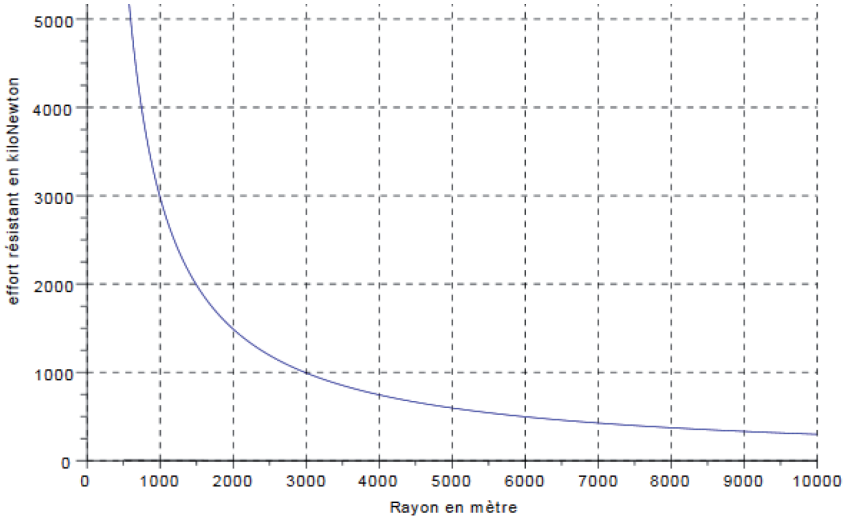

Figure 1.5. Dependency of the Resistance to the Movement of TGV-Dasye (French Train) on the radius of the curve [36]

Moreover, the last formula completely coincides with formula (1.30) recognized by *Rules of Traction Calculations for Train Operation* (*Ukrzaliznytsia*) [29].

The Canadian railroad in 1990 implemented the national version of Davis formula, the use of which is believed to be more reliable in terms of the calculation accuracy for of the resistance to the movement and the mass of the train [38]. The new Canadian version of Davis's formula is shown below:

$$w = 1.5 + \frac{18 \cdot N}{P} + 0.03 \cdot V + \frac{C \cdot a \cdot V^2}{10000 \cdot P}, \tag{1.48}$$

where w – the specific resistance to the movement (lb/ton);
P – the general weight of the locomotive or the carriage (ton);
C – the empirical coefficient.

Davis equation has been modified in order to apply it for high-speed movement, in particular, for Japan Shinkansen, Series 200. B. P. Rochard and F. Schmid) [18] suggested the modification as shown:

$$w = 8.202 + 0.10656 \cdot V + 0.0119322 \cdot V^2. \tag{1.49}$$

In recent years, the assumptions have been made that the initial Davis equations had the tendency to exaggerate the resistance value, and therefore the correcting coefficient is sometimes applied for them:

$$W_{adj} = K \cdot w_D, \tag{1.50}$$

where W_{adj} – the corrected value of the resistance to the movement;
w_D – the resistance to the movement, defined by Davis formula;
K – the correcting coefficient for upgrading the Davis resistance values.

The coefficient value of K correction is based on the testing under controlled conditions, namely:

$K = 1.00$ – for the rolling stock applied before 1950;
$K = 0.85$ – for the rolling stock applied before 1950;
$K = 0.95$ – for platforms with containers;
$K = 1.05$ – or hopper-cars;
$K = 1.20$ – for the empty covered wagons;
$K = 1.30$ – for the loaded open wagons;
$K = 1.90$ – for the empty open wagons;

D. Armstrong and P. Swift worked over the problem how to make the calculations of aerodynamic component for the railway trains more accurate, taking into account the varieties in train constructions.

Their articles [40], in particular, explain the phenomenon of the specific resistances to the movement of the empty and loaded wagons. It is provided by

the fact that the resistance to the wind of empty or slightly loaded wagons in the train is the same as that of the completely loaded ones.

As the wind resistance becomes dominating at high speeds, the specific resistance to the movement per the train weight unit is higher if the train is with empty wagons. In the case of open wagons or the wagon with open tops, the resistance to wind of the empty wagons is not higher than that with loaded wagons due to the increase in the air turbulence inside and around the empty wagon body.

In many countries, the calculation formulas of the resistance to the movement differ significantly. In table 1.2, the calculation formulas for the main resistance to the movement of the rolling stock are demonstrated. They are accepted for calculations at the railroad of various countries.

Table 1.2

The Calculation Formulas for the Main Resistance to the Movement of the Rolling Stock Applied in Various Countries

Railway	Calculation Formulas for the Main Resistance to the Movement
Chinese National Railway (N/kN): • loaded wagon • empty wagon	 $0.92 + 0.0048 \cdot V + 0.000125 \cdot V^2$ $2.23 + 0.0053 \cdot V + 0.000675 \cdot V^2$
Czech Railway: loaded wagon (daN/ton)	$1.3 + 0.00015 \cdot V^2$
German Railway: loaded wagon (daN/ton)	$1.0 + 0.0001 \cdot V^2$
Serbian Railway «new formula» (daN/ton)	$0.0483 + 0.0183 \cdot V + 0.00001 \cdot V^2$
French National Railway (daN/ton): • loaded wagon • empty wagon	 $1.0 + V^2 / 400$ $1.2 + V^2 / 400$
Australian Railway (N/ton): • loaded wagon • empty wagon	 $5.17 + 0.010997 \cdot V + 0.00051 \cdot V^2$ $18.74 + 0.1111 \cdot V + 0.00372 \cdot V^2$

In figure 1.6, we show several dependences of the main specific resistance to the movement on the speed. In various countries of the world, they used for traction calculations.

One of the latest suggestions concerning the accuracy of the formulas for the resistance to the movement was made in 2005 by A. Radosavić, an engineer of *the Belgrade Institute of Transportation* (CIP).

On the basis of the experimental studies, the formula of the main resistance to the movement for the wagons and mixed train with JZ 643 diesel locomotives was improved, the results of the tests were reported in article [41].

Furthermore, there are the issues which deserve our special attention: *Why is the locomotive resistance to the movement in the stopping regime is greater*

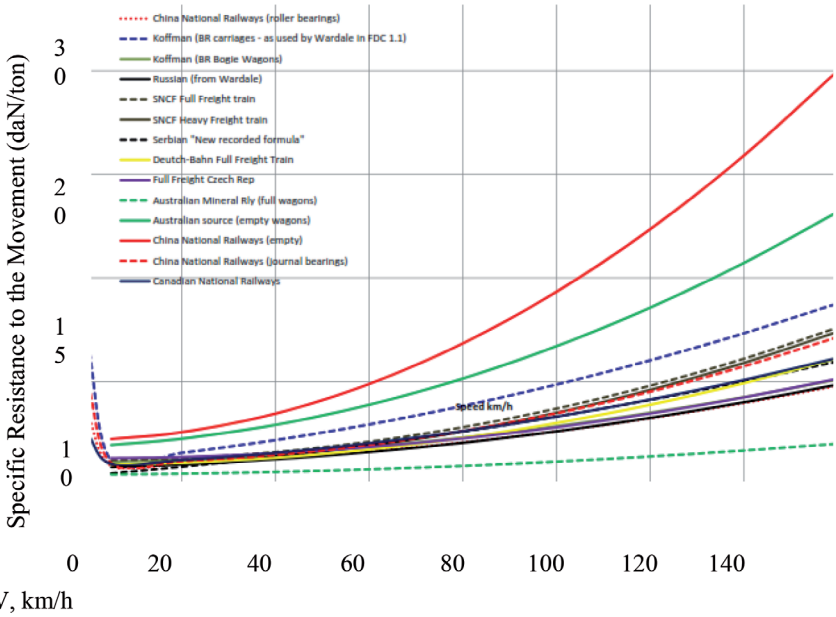

Figure 1.6. The Dependencies of the Specific Resistance to the Movement of Wagons on their Speeds, Used for Traction Calculations in Some Countries of the World

than in the traction mode? For example, RTC for locomotives (diesel-electric locomotive and electric locomotives) recommends the different formulas for the stopping regime and the traction mode (the junction-free track):

• for the traction mode the following is applied:

$$w_o^{'} = 1.9 + 0.008 \cdot V + 0.00025 \cdot V^2; \qquad (1.51)$$

• for the stopping regime, the other calculation technique is applied:

$$w_x^{'} = 2.4 + 0.009 \cdot V + 0.00035 \cdot V^2. \qquad (1.52)$$

The significant difference in the formulas coefficients (1.48)-(1.49) is the consequence of the conditional division of the locomotive main resistance to the movement into two parts: one of which considers the locomotive resistance to the movement as that of the truck, the other one regards this phenomenon as that for the as machines. When the locomotive is regarded as a machine, its resistance to the movement is caused by the power loss occurring within the locomotive due to the friction in the gear motor and the traction motor support bearings. When moving at traction mode, that is when the torque is transmitted from the traction motor to the wheel pairs, these power losses are not included into the

general resistance to the movement but are taken into account for the tractive characteristics. At the stopping regime, when the tractive effort does not occur, the locomotive resistance to the movement as that of a machine is considered as the resistance incorporated into the general resistance to the movement of the locomotive.

G. Boschetti and A. Mariscotti, the researchers of *the University of Genoa* (Italy), in their report at XX IMEKO World Congres Metrology for Green Growth [45] substantiated the need of the further research in the direction of simulation, measurement and search for the ways to reduce the mechanical resistance to the movement of the rolling stock.

The analysis has shown that the overwhelming majority of the researches on the resistance to the movement of the rolling stock were experimental, devoted only to revealing the dependencies of the resistance to the movement on the speed, they were necessary for traction calculations.

The resulting formulas allowed calculating the mass of trains, the movement speed and the time at the railroad section, the brake way, etc. During the many decades, the project development stage for the rolling stock of new types was deprived of analyzing the resistance to the movement. As the exception, one can name many researches of the aerodynamic resistance to the movement which became urgent during creation of high-speed trains.

In the course of the development of the truck arrangement for the locomotives and wagons, there have been revealed lots of problems related to the dynamics and the train insertion into the curve of small radius. They were often solved by introduction of various elastic dissipative elements into the train parts without consideration of the possible deterioration for the characteristics of the resistance to the movement connected with the straightness of the railway track that sometimes led to the increase in the horizontal loads due to the frictional contacts of wheels with rails, acting at the same time as the frictional dampers with high level of energy dispersion.

The indirect prove for the above mentioned is the data on the increased wheel surface wear at operation of new multiaxial locomotives [42-44]. Especially, it should be noted that the intensive undercut of flanges and side wear of rail tops are mostly the result of the forces of the resistance to the movement.

In some cases, at operation the train in the curves with small radiuses, the wearing is so intensive that between-repairs operation of locomotives is only 5... 7 thousand kilometers due to the wheel flange undercut.

1.2. Structure of the Resistance to the Movement of Rail Carriages

In figure 1.7, we show the structure of the resistance to the movement presented with the respective share for the each component though such a division is quite conditional because the number of components can be simultaneously regarded both as the main resistance constituents and as those belonging to the additional resistance.

As for the shares of the constituents of the resistance to the movement, they vary drastically depending on speeds, railway track characteristics, wind speeds and directions, meteorological conditions, design features of various trains.

At this, especially important is the aerodynamic resistance, which with the speeds higher than 30 … 40 m/s reaches as much as 65% of the main resistance to the movement.

1.2.1. Resistance in the Axle Equipment

The stated in the chapter component of the main resistance to the movement is connected with the friction which occurs at rolling (in case of rolling bearings) or at sliding (in case of sliding bearings) in wheel pair axial bearings [26, 28].

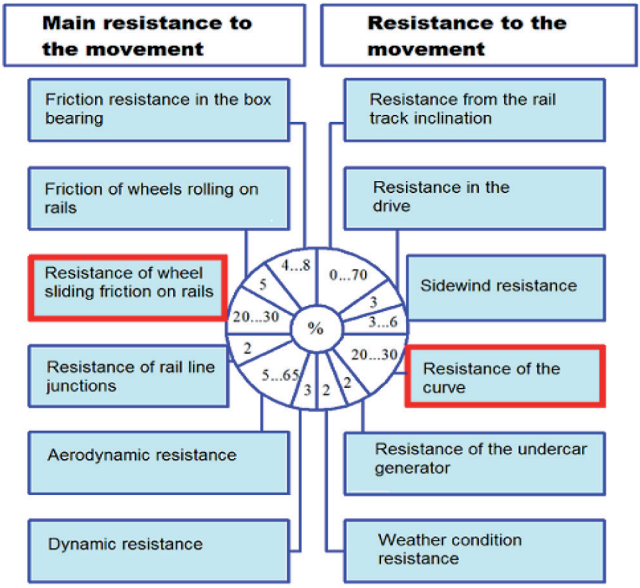

Figure 1.7. Structure of the Resistance to the Movement in Rail Trains (Main Resistance and Additional Resistance)

The friction force moment on the axis neck when sliding bearings is defined from the formula as follows:

$$M_1 = f_L \frac{d_n}{2} \tag{1.53}$$

where f – the friction coefficient for friction between the bearing neck and the bearing insert;

L – the load of the axis neck;

d_n – the diameter of the axis neck.

The resistance force acting on the wheel rim is given below:

$$F_{\hat{i}} = \frac{fLn_n}{D_w} \tag{1.54}$$

where D_w – the wheel diameter per tread.

The specific resistance to the movement due to the friction in axle-boxes of sliding bearings equals as below:

$$w = 1000 f \frac{d_n}{D_w}. \tag{1.55}$$

The friction coefficient in axle-box sliding bearings is defined by the formula as written:

$$f = A \sqrt{\frac{\mu n}{p_{avg}}} \sqrt{4\lambda + 1}, \tag{1.56}$$

where A – the coefficient, which depends on the bearing deviation from the central position. Its average value for the rolling stock equals 0.005;

n – the rotation frequency of the wheel pair axis;

λ – the relation of the neck diameter (d_n) to the neck length;

r_{av} – the specific pressure within the bearing.

Almost complete replacement of axle-box sliding bearings for rolling bearings in the rolling stock led to the reduction in energy consumption spent for train traction as much as 4.2 … 4.6% [24].

The sliding friction coefficient for metals, in most cases, is 0.05 … 0.25 while the rolling friction coefficient for the same conditions is within 0.0001 … 0.001. The losses due to the friction caused by rolling are often neglected in calculations. However, the energy which is spent for overcoming the rolling resistance is absorbed mainly in the upper layers of the material applied and is consumed for intensive cyclic re-deformation of material.

The heating of the working elements in the assembly leads to gap redistributions, losses in the accuracy and in run smoothness, as well as other violations of the normal work of the bearing assembly. Generally, the losses of energy in roller bearings are formed from the following constituents:

1) the losses for friction in the rotating elements of the bearings in the surrounding, including lubricating medium, which additionally to its main function plays the role of the viscoplastic body [46] preventing the relative displacement of the elements of the bearing and creates the resistance to the movement;

2) the losses on the working areas of cages, which appear as the result of their friction on the guiding plates of rings and the friction of the rolling bodies on the seat walls;

3) the losses which occur when rollers running in the ring bearing race.

Among the reasons of these losses we can name the following:

- relative elastic slipping of the conjugate surfaces, which occurs thanks to the differences in their curvatures and according to the difference in the values of the elastic shears in the body surfaces within the contact zones when they hit each other;
- sliding of the rollers on the guiding plates of rings related to roller bearings;
- the general slipping of the rolling bodies assembly with respect to the guiding ring, which appears at the loss of the adhesion between them;
- imperfect elasticity of the material;
- molecular interaction of the contacting surfaces, which prevents from their contingence on the front edge of the contact and from their separation on the back edge.

The moment of friction of the roller bearing can approximately be defined with the formula shown below:

$$M = f_L P \frac{d}{2}, \tag{1.57}$$

where f_L – the multiple friction coefficient;
d – the diameter of the bearing seat opening;
P – the load on the bearing.

$$P = \sqrt{F_r^2 + F_a^2}, \tag{1.58}$$

where F_r, F_a – the radial and the axial constituents of the load.

The frictions in the journal axial thrusts, seals, lubricating devices (for example, journal packings) are also related to the losses in the axle assembly. When the axial thrust is in the sliding thrust bearing, the friction losses can reach the significant values.

The research data evidence that the main resistance to the movement of the rail vehicles can be reduced as much as 20% if the roller bearings are used, while 5…6% reduction is observed when the train starts to move at the average speeds [26, 28].

1.2.2. Loss of Power in the Traction Drive

The disputable problem is how to regard the locomotive resistance to the movement. The presence of the transmission elements, which are not disconnected from the wheel pair in the stopping regime, predetermines the emergence of the forces resisting to the drive, which occur only in locomotives. This kind of the resistance, called the resistance of the locomotive as a machine, is the result of the mechanical losses in traction motors, the friction losses in the interacting parts of the machine located separately plus transmission element of the motor.

When the locomotive movement is provided or supported by electricity, the specific resistance due to the friction in the driving gear, the motor and the axial bearings, drive shaft and axial motors, is considered as the part of the locomotive traction characteristic, that is, the resistance to the movement is regarded in the aspect of the peripheral forces. Logically, here it is necessary to incorporate also the resistance in the bearings of the axle boxes. At the idle running, the above mentioned high resistances are treated as the part of the main resistance, therefore the losses are not compensated by the power supply units. Such approach to the measurements of the resistance to the movement results in the evidence that the locomotive main specific resistance at the stopping regime is greater than that in the traction mode. This does not display the physical essence of the phenomena because the actual increase in the resistance to the movement does not occur, but on the contrary we are to expect its decrease due to the lower power losses for the friction in the unloaded transmission element [47].

The connection between the main specific resistance of the locomotive, regarded as the truck, $\left(w_o'\right)$ and the resistance at the idle run $\left(w_x\right)$ is defined with the following dependence:

$$w_x = w_o' + w_з,$$

where $w_з$ – the constituent of the main specific resistance when the idle run, it is stipulated by the losses spent for the friction in the traction drive and the gear.

The resistance to the carriage movement produced by undercar generator could be incorporated into this kind of resistance.

1.2.3. Resistance to Wheels Rolling on Rails

The resistance to the wheel rolling on rails has the complex nature, which is still under study. When rolling, there are three types of friction present, they differ by their descriptions in terms of rolling friction, sliding friction and friction of rotation (or spin).

There are several theories which explain how the resistance forces are formed when rolling.

Professor O. Yu. Ishlinskiya, for example, considering the rigid body rolling on the viscoelastic medium, analytically studied the resistance to rolling and explained this phenomenon existence with the imperfection in the materials elasticity [48]. The scientist proposed the solutions of the problem related to the absolutely rigid rolling by two types of the medium: relieving and viscoelastic. The appearance of the rolling resistance was explained by the distribution asymmetry of the medium reaction to the rolling rigid body. According to O. Yu. Ishlinskiya, this medium is ground and its calculation characteristics show the residual subsidence on the rear edge of contact patch of the medium unlike the zero subsidence on the front edge of contact before the wheel. The following formula is recommended for the calculation of this rolling resistance:

$$W = 0.2\sqrt[3]{18}\,\frac{\nu}{V}\,\frac{P^{\frac{5}{3}}}{\sqrt[3]{kbR}} \tag{1.59}$$

where V – the speed of rolling;

P – the vertical load;

ν, b, k – the characteristics of the surface for rolling (medium);

R – the radius of the surface for rolling.

The other aspect of the problem of elastic imperfections is related to the elastic hysteresis of the medium. It was studied by A. Palmgren [49]. On the basis of the results of the tests conducted on thrust bearings and spheric bearings, A. Palmgren concluded that the losses on the elastic hysteresis in these cases are quite insignificant if compared against the general losses in the bearing. The main losses are represented by the losses connected with relative slipping of contacting surfaces.

On the contrary, D. Tabor in article [50], proves that the elastic hysteresis possesses the leading role in formation of resistance forces to rolling. By rolling steel balls on the flat media with different hysteresis properties, D. Tabor received the results which show that depending on the properties of the medium, the energy losses can increase more than by 8 times at all loads applied. However, the author specifies that these conclusions are fair for rather soft materials such as rubber. Thus, when rolling the balls made from phosphorous bronze, aluminum and ball-bearing steel, the energy losses could be as much as 10:5:1.

The analytical dependency received by D. Tabor for the forces of the resistance to rolling is as written:

$$F = c\alpha\, N\frac{a}{R}, \tag{1.60}$$

where N is the normal load in contact;

a – the half-width contact patch in the direction of rolling;

R – the radius of the cylinder or the sphere;

c, α – the empirical coefficients [50].

Studying the resistance to the rolling with the sample made from hard steel, J. A. Tomlinson [51] identified the coefficient of the resistance caused by intermolecular interaction between the surfaces at the expenses of the attraction and the repulsion, manifested as the friction force. According to J. A. Tomlinson, the work of these forces can be expressed as follows:

$$N \cdot W = \mu \cdot F \cdot P \cdot n, \tag{1.61}$$

where μ – the friction coefficient;

F – the relative displacement of the molecule cluster under the study;

N – the total number of the interacting molecules in their movement path x;

n – the number of cycles (the attraction and the repulsion) for a molecule;

P – the interaction force of two molecules.

Then, the coefficient of the resistance to rolling is as follows:

$$\lambda = \frac{3}{4}\frac{qW}{bP}, \tag{1.62}$$

where q – the static constant, which depends on the material structure;

b – the half-width of the contact patch.

The values of $\lambda = (2\ldots4) \cdot 10 - 5$ were found experimentally.

S. V. Pinegin, making the experiments similar to J. A. Tomlinson, came to the conclusion that the molecular component of resistance to rolling is 2 … 3 orders lower than the power hysteresis losses [52, 53].

Further, A. S. Akhmatov also notes that under practical conditions of the wheel contact with the rail, there occurs formation of molecular bonds of adhesion, which is very complex due to the instant inclusion oxides and adsorbed substances into the surface [54].

The research team headed by B. V. Deryagin [55] explained the resistance to the movement, as the result of the electrostatic attraction of the rolling pair elements due to the opposite charges which arise behind the continuously revealed contact. In order to determine the role of the molecular effect in the general resistance to rolling, many researchers applied the appropriate experimental plants at which the sliding in the wheel and rail contact was minimized. Such researches were conducted by Yu. Blokhin [56, 57], D. Tabor [50], J. A. Tomlinson [51], R. C. Drutovski [58].

Some of the results, namely, the dependency between the molecular component of the resistance (W_m) and damping component of the resistance (W_d) are stipulated by effect of the hysteresis of the contact pressure (refer to figure 1.8). In the case

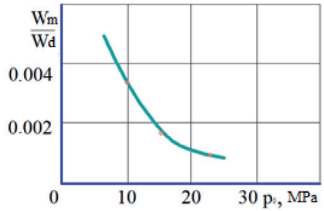

Figure 1.8. The Relation between the Molecular Constituent (W_m) and the Damping Constituent (W_d) of the Resistances to Rolling. Contact Pressure Case

of the wheel and rail contact, the part of the molecular component in comparison against the slipping and the hysteresis is small within the general resistance to rolling.

The results of the researches conducted by many authors witness that the damping constituent is more influential in the resistances to rolling. It is known that the hysteresis with the related elastic shears and the plastic shears is defined by physical and mechanical characteristics of the materials, the level of the contact stress, the shape of the contacting surfaces and the shear velocity. On studying the rolling phenomenon of the disks made from high-strength cast iron and chromium alloyed steel, Yu. G. Blokhin [56, 57] received different dependencies of the resistance to rolling on the rolling speed for cast iron (W_{ci}) and for steel (W_{st}). These dependencies are shown in figure 1.9.

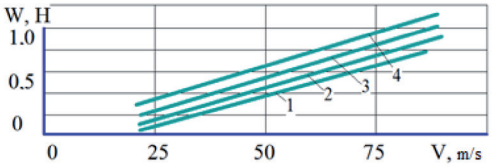

Figure 1.9. Relative (1) and Absolute (2,3) Power Losses due to Hysteresis for Cast Iron (2) and for Steel (3). Dependence on the Wheel Rolling Speed on the Rail

In the course of the researches on the dependency of the resistance to rolling in the contact aspect, a number of the authors pointed out the sharp increase in the resistance when reaching the certain stress threshold and the unstable results which depended on the number of the wheel passes with one and the same medium. Some explanations for these phenomena are suggested by K. L. Johnson [59]: after several repeated contact loads, the material reaches the fitness limit, when plastic shears actually do not exist and the new elastic state enters the scene.

This phenomenon occurs on condition as given below:

$$p_o \le 4 \cdot \tau_{ys}, \tag{1.63}$$

where p_o – the maximum contact pressure;

τ_{ys} – the ultimate yield stress when shear.

The limit of the material fitness depends on the material properties and approximately could be defined from the dependence of the Brinell hardness provided as below:

$$p_o \leq HB.$$

The number of passes, after which the resistance to rolling is stabilized, also depends on the material hardness. According to N. A. Korolyova [60], for mild steels with HRC hardness = 61... 62, it is sufficient to carry out 15... 20 passes, while the number of passes for harder ones reaches 1 000 times. The sharp increase in the resistance to rolling depends on the motion speed and is observed at V> 350 km/h (97 m/s), which is becoming an important issue for the contemporary rail transport. The dependency of the resistance to rolling on the motion speed is shown in figure 1.10 [60].

Japanese researchers Tadao Ohyama and Seigo Uchida proved that the shape of the contacting surfaces influences the stress distribution on the contact patch, the volume of the deformed material and the shape of the contact patch [61].

The experiments made by R. C. Drutovski [62] for the ball and the cylinder rolling on the other cylinder show that with the identical diameters of the bodies, the identical contact pressures and the identical rolling speeds, there are the significant differences in the resistance to rolling thanks to the different volumes of the deformed metal and, consequently, and different hysteresis losses. The dependencies of the resistance to the movement on the rolling speed for cylinders (1) and balls (2) are shown in figure 1.11.

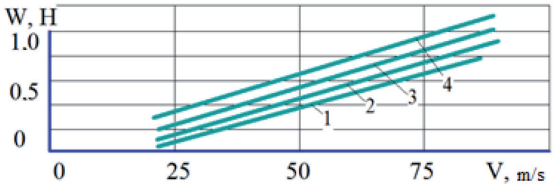

Figure 1.10. Dependency of the Resistance of Two Steel Balls Mutual Rolling on Speed

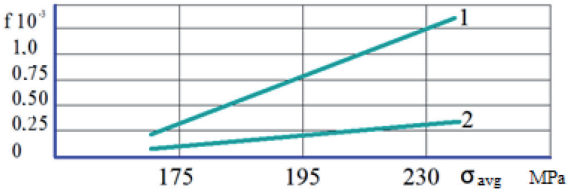

Figure 1.11. Dependency of the Resistance Coefficient to Rolling on Average Stress in the Contact: 1 – for Cylinders; 2 – for Balls

The fatigue nature of wearing at sliding friction was noted first in the papers by D. V. Konvisarov in 1952 [63, 64]. This author explains the reasons of the fatigue in the surface layers of the parts by the repeated movements or the reversal movements of sliding joints in the machine parts.

The similarity in the surface tearing and scratches with various pointed parts are not considered as wearing in the comprehensive sense of this term. D. V. Konvisarov has concluded that wearing of the rigid bodies at friction is similar to the fatigue failure. Each contact patch undergoes the heat and mechanic influences from the other contact patches many times. This results in the crack within the material, its further development and finally the surface failure. D. V. Konvisarov has checked these ideas by the tests at the pendulum device of the conventional design. The dedicated tests were conducted on the steel quenched samples with the cylindrical surfaces of different curvature at their rolling motion.

The reported above conclusions by D. V. Konvisarov are significant in importance as it was the first attempt to explain why the resistance to rolling exists and it was done by means of simultaneously influencing factors of the actual operation, which had not been mentioned before. Moreover, the samples for the Konvisarov's experiment were manufactured from the typical material applied in the machine-building sphere. This also adds to the importance of the results obtained.

The examples of the complex consideration on the influence of the volumetric and surface effects on the resistance to the movement are the scientific papers by G. Goryacheva and L. A. Galina (1973-1980) [65-67]. Their contributions as well as many others allow us to conclude that the main components of the resistance to the rolling is the friction component, stipulated by slipping in the contact of wheels and rails. The kinematic resistance to the movement addressed in this work is also of the friction failure nature.

According to the Reynolds longitudinal slide, the difference in the material medium tensions and rolling within the contact zone produce the sliding effect [68].

The surface shears at rolling are accompanied by the difference in the displacement but for sliding there are the opportunities for the shear in the contact. The sliding of surfaces is accompanied by the friction, which stipulates the resistance to the rolling. Obviously, the additional resistance to the movement may incorporate the resistance related to the pressure transmitted to rails for preventing wheel pair slip. Its high value and the data on the increase in the resistance to the movement at pressure supply in the zone of the rail-wheel contact give evidences on the necessity of the further theoretical and experimental researches of this problem.

1.3. The Choice on the Calculation Schemes for Simulating the Carriages Control by the Railway Track

1.3.1. The Nature of the Resistance to the Movement Based on the Control of the Wheel Pairs by the Railway Track

The first railway carriages were equipped with the cylindrical wheels, they were rolling on rails with flanges to guide them. However, for the first Stephenson steam engine in 1821, the rail flanges were turned into the wheel flanges.

The conventional design of the wheel pairs requires the wheel flanges, the rigid connection of wheels into the wheel pair and conical profiles of the wheel rolling surfaces. This specific character of the wheel pair design is more than 200 years old and it provides the dependable guiding of carriages by rail tracks.

The most complete work studying the issues of railway carriages guiding by rail tracks is the book by Kh. Kheyman [69] who writes that the deviations from the rolling path for both free wheel pairs or ones connected with the truck frame can be observed only as sliding. According to the researcher, the longitudinal sliding occurs owning to the rigid connection within the wheel pair by the axle. Despite the detailed information on the problem of the carriage guiding into the curves, Kh. Kheyman does not touch the resistance to the movement related to the indicated phenomenon.

When moving within the curves, the wheel pair construction allows the rails to decrease the guiding forces between the wheel flanges. However, in the curves of medium or small radiuses, the insufficient conicity of the surface for rolling causes the slip of the wheels in the longitudinal direction. The forces of the longitudinal direction contribute to the increase in the deviation of the wheel pair axle when steering around the curve and the increase in the angle of the wheel head overlap with the rail top. The latter increases the transversal reactions of the rail and the resistance to the movement. The prove of the said information is the typical scraping noise and skirr when the carriage moves within the curved section of the railroad [70].

The movement in the straight sections, especially at high speeds, may have the intensive hunting oscillations with the wheel pair and periodic contacts of the wheel flange and the rail due to track curvatures and conical surface of the wheel rolling [71].

High-speed movement generates the increase in the transversal loads on the rails.

The transversal forces acting on the rails can reach the great values [72], which causes the intensive wearing in the zone of the wheel flanges and higher resistance to the movement.

The authors of the current book propose that the constituent of the resistance to the movement related to the wheel pair guiding by the track to be terms as the kinematic resistance to the movement.

According to the widely recognized classification, the kinematic resistance to the movement has the properties of both the main resistance and the additional one [73, 74]. Therefore, the named type of the resistance should be conventionally regarded as the constituent of the main resistance when the train moves on the straight sections of the railway, while on the curved sections, it is considered to be the constituent of the additional resistance.

The reasons why the kinematic resistance occurs are the kinematic inconsistence of the wheel rolling surface geometry and the kinematic parameters of the movement.

The kinematic resistance to the movement is the result of the parasitic slipping in the closed power circuits which are generated in the system of the wheel pair guiding by the rail. The mechanical energy to be lost for overcoming the friction of the parasitic slipping is the energy of the kinematic resistance to the movement. In the system of the carriage truck guiding by the rail track, one can distinguish several closed power circuits.

1.3.2. Closed Power Circuits in the Contacts of Wheels with Rails

Publications [75, 76] write that when two-point contact between the rail and the wheel, the closed power circuit is generated with two centers within the main contact and the wheel flange contact. In this circuit, the differential slipping is born and is the reason for the additional kinematic resistance to the movement owing to the increase in the rolling resistance. The differential slipping and the related resistance to rolling was first mentioned by H. L. Heathcote in the research devoted to the kinematics of ball bearings [77].

In figure 1.12, there is the example of the possible scheme of the natural distribution of reactions (N_1, N_2) and adhesion forces (S_1, S_2) in two point wheel flange contact between the carriage wheel and the rail. F_t is the outer longitudinal reaction of the truck to the wheel. Reaction F_t is the force of the resistance to the movement to be overcome for the wheel to make a rotation. The distribution of normal reactions N_1, N_2 depends on many factors: the speed of the movement, the radius of the curve, the lift of the outer rail, the wheel pair position in the track, the truck design, the profile of the wheel surface of rolling, etc.

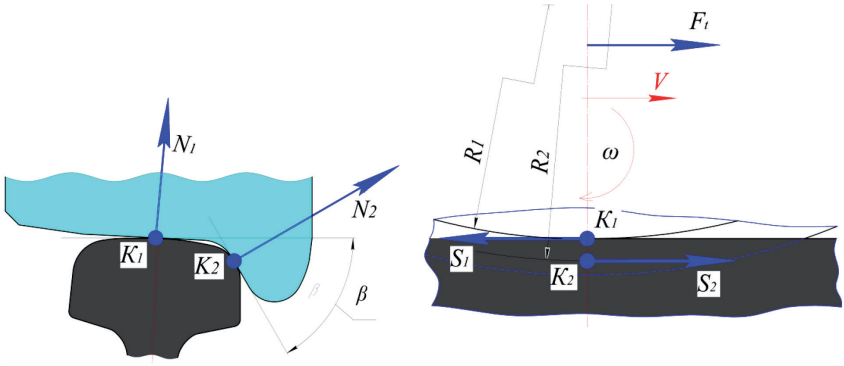

Figure 1.12. Distribution of Normal Reactions (N_1, N_2) and Adhesion Forces (S_1, S_2) at Two-Point Wheel Flange Contact of the Railway Carriage Wheel with the Rail

Based on figure 1.12, the following system of equations for the equilibrium can be derived:

$$\begin{cases} \sum M = S_1 \cdot R_1 - S_2 \cdot R_2 = 0; \\ \sum F = S_2 - S_1 + F_t = 0\ . \end{cases} \tag{1.64}$$

Equations (1.64) allow us to obtain the value of the kinematic resistance to the movement (W_k)

$$W_k = F_t = S_1 \left(1 - R_1 / R_2\right). \tag{1.65}$$

The reported information gives as the opportunities to conclude that the force of the resistance to the movement ($W = F_t$) is never to be equal to zero if there is the presence of the wheel flange contact with the rail.

1.3.3. Closed Power Circuits of Wheel Pairs

The wheel pairs together with the railway track also make up closed power circuits. The absence of the longitudinal slipping in the wheel and rail contact is possible only in the ideal case, when a single wheel pair can freely roll without touching with its wheel flange. Under real conditions of the wheel pair movement within the truck frame there always occurs slipping at the wheel and rail contact due to the existence of the axle box longitudinal reactions.

The illustration how the simplified scheme could be presented for the adhesion forces (S_1, S_2) and axle boxes reactions (F_{b1}, F_{b2}), which influence the wheel pair, is shown in figure 1.13. The wheel pair is installed with transversal shear Δy

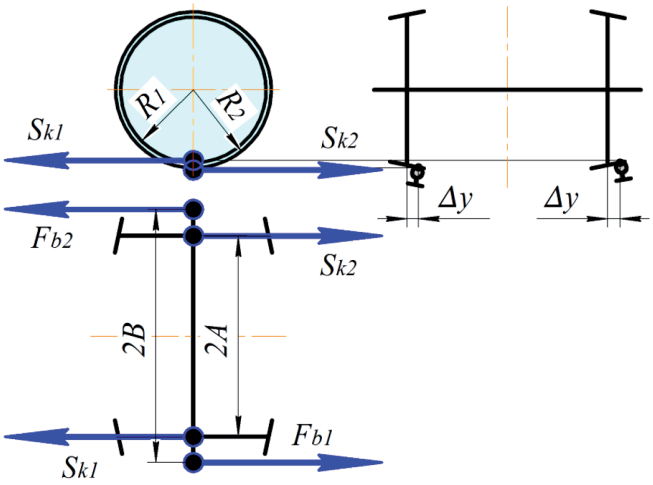

Figure 1.13. Simplified Scheme of Adhesion Forces (S_1, S_2) and Axle Boxes Reactions (F_{b1}, F_{b2}) to Act on the Wheel Pair

respectively the track axis and it rolls on rails without the hunting effect suppressed by axle equipment reactions F_{b1}, F_{b2}.

Figure 1.13 allows to obtain as follows:

$$\begin{cases} (S_{k1} + S_{k2}) \cdot A - (F_{b1} + F_{b2}) \cdot B = 0; \\ S_{k1} \cdot R_1 - S_{k2} \cdot R_2 = 0; \\ F_{b1} - F_{b2} - S_{k1} + S_{k2} = 0. \end{cases} \quad (1.66)$$

Equation (1.66) is capable of providing the value for the kinematic resistance to the movement:

$$W_k = S_{b1} - S_{b2} = S_{k1}(1 - R_1 / R_2). \quad (1.67)$$

The analysis witnesses that the majority of the papers and researches devoted to the resistance to the movement of the rolling stock have been experimental ones. They pursuit the same aim of revealing the dependency between the resistance to the movement and the speed. These dependencies were used for calculating train mass, speed, movement time at a section, brake-way, etc. For many decades of developing new types of rolling stock, nobody has analyzed the characteristics of the resistance to the movement at the stage when the main design decisions are made by the engineering team. As an exception one may consider a number of researches on the aerodynamic resistance to the movement, which are of vital importance for high-speed trains.

When developing the truck arrangements for locomotives and carriages, the issues of dynamics of guiding the train in the curves with small radiuses were often solved by introducing various springy-dissipative parts into locomotive underframes without taking into account possible deterioration of the resistance to the movement characteristics connected with directing wheel pairs by rail tracks. Sometimes, this resulted in increasing horizontal loads on frictional contacts of wheels with rails which acted as frictional dampers with a high level of energy dissipation during this process.

The indirect confirmation for this is found in the data related to the increase of surface wear of the wheel rolling when operating the new types of heavyweight locomotives [78]. Especially, we should outline the intensive flange undercut and the rail top side-drift as they are the result of the action of the forces generated due to the resistance to the movement.

The surface profiles of the rolling wheels determine the various radiuses of the tread circles. The spatial distribution of the contact forces and sliding speeds leads to the appearance of differential sliding motions in the contacts, creating parasitic frictional forces which are the reason of the additional kinematic resistance to the movement. This type of the resistance appears to be especially strong when two-point flange contact.

The recognized classification of the resistances to the movement does not encourage the development of the researches regarding the processes of guiding carriages by rail tracks. This statement is based on the fact that frictional processes in the contacts of wheels with tracks are studied separately both for the main and the additional resistances to the movement.

The materials of the analysis we are reporting above allows us to define a new research area of decreasing the resistance to the movement of rail carriages owing to the factors which are uncovered sufficiently in the world's science and actual practice. This research direction is based on a hypothesis that the guiding of wheels pairs by rail tracks is fulfilled entirely at the expense of the additional resistance to the movement. Moreover, the authors of the current publication propose to term this additional resistance to the movement related to the carriage guiding by rail tracks as the kinematic resistance to the movement. The offered approach to the movement may serve as a foundation for extensive research on the resistance to the movement with the aim of saving energy resources for the haulage of trains.

2 STUDY ON CONTROLLABILITY AS THE PROCESS OF GUIDANCE FOR THE CARRIAGE BY THE RAILWAY TRACK

2.1. The Concept of Controllability in the Railway Transport

It is commonly known that pure wheel pair rolling is possible only if it rolls freely along rails and is not connected with any truck frame. When driving the wheel pair in a real case with the wheel pair mounted in a frame, there always occurs the axle box reaction. The movement is the result of the interaction with the other wheel pairs and with the body while the turning of a separate wheel pair by a truck frame is manifested in the additional sliding of the wheels, which causes opposite directed friction resistance. These resistances could be suppressed at the expense of the directed efforts, which are always associated with the resistance to the movement.

The horizontal impact on the track is revealed as the total effect of all horizontal reactions occurring in the contacts of wheels with rails.

A certain reduction in the impact on the track can be achieved, for example, by installing counter battens in steep curves, application of wheel flange lubricators and rail-lubricators, introduction of new profiles of wheel rolling surfaces, optimization of the rolling stock truck arrangement parameters, etc. Given the fact that the curves make up about 30% in the total length of the Ukrainian railways and that the influence of the truck arrangement on the track in the curves is greater than in the straight sections (at the same speeds), the topical character of the research aiming at controlling the train guidance into the track curves becomes obvious.

The horizontal interaction of trains and tracks is described in several thousands of works, which makes it impossible to review them in detail.

Thus, the theoretical basis for the study of the horizontal dynamics of the rail transport saw the sunrise of its development at the end of the last century.

For geometric framing, the methods by Roy, Pouchet, Vogel, Maistre, Plass, Jakobi, later improved by K.Koroliov, I.Nikolaiev, V.Panskiy and A.Slomianskiy were used.

The fundamentals of the dynamic guiding for trains into curves were laid by S. Smirnov. They are based on the idea of finding the center of the train rotation at the intersection of its longitudinal axis and the perpendicular, dropped from the center of the curve. The principles of the least resistance to the carriage turn in curves and the formula for determining the force of wheel flange pressing on rails were proposed by A. Holodetsky. Currently, to study a steady movement of a carriage in curves, they use the method by K. Tseglynsky modified by K. Korolev. This method takes into account the elasticity of the track and the horizontal dynamics coefficients for calculating the lateral forces.

The graphical and analytical method by Kh. Kheyman was based on minimizing the moments of the resistance of the carriage rotation in the curve and was not disseminated for the practices of calculations due to its complexity [69]. Kh. Kheyman examined how the trucks of Bissell, Helmholtz, Lotter, and Eckard behaved in curves, and has noted that the leading wheel pair, mounted in front of the truck, often climbs on the outer rail and never has a free run regularity, since it is unstable. The rear wheel guides, on the contrary, almost always have a free run regularity. In this connection, Kh. Kheyman points out the important role of reverse torque device for guiding wheel pairs, which should have a sufficiently large reverse moment for reliable installation without jamming in the track.

In order to make the calculations for the dynamic steering of the carriage into the curve more accurate, S. Kutsenko examined the new characteristics of the wheel profiles, the distribution of sliding in the contacts and the forces of the resistance to the movement in the curve [79].

Developed by O. Yershkov, the generalized method for determining the transversal forces acting in a curve is based on the assumption of the linear dependency between the level of lateral forces and the unbalanced centripetal acceleration, it incorporates three important characteristics: the speed, the curve radius, and the outer rail elevation [80].

In the analysis of the motion of the rolling stock in the curves, there have been widely used quasi-static methods with idealizations typical for them: the ideal curve and the constant coefficients of friction slip in the wheel and rail contacts.

On analyzing the design and principles of the most common reverse torque devices, D. Minov proposed their classification, according to which the reverse torque should have high stiffness at small deviations of trucks or leading wheel pairs. This provides the increased stability of the movement in the straight sections of the track as well as the fixation of the leading wheel pair in the middle position. At vast deviations of the truck, the values of the reverse torque are to sharply decrease [81].

As a rule, the requirements to the characteristics of carriages in terms of the minimum impact on the track in its straight and curved sections are contradictory. The discussion of these issues has led to the recognition of the need for controlled guiding of the carriages by rail tracks. A. Kravchenko formulated the principles of minimizing the directing forces by means of controlling the angular moment with regard to the body link with the truck and outlined the main ways of implementing the idea of controllability of the movement [82].

Performed by V. M. Kashnikov detailed analysis of the known systems of the controlled movement of the rail carriages [83-85] allowed the conclusion that the opportunities to decrease the directing efforts by optimizing the parameters of the truck arrangement are practically exhausted and the solution of the problem is possible only through the application of the systems of controlled movement. These systems can be divided into active and passive ones. The passive control systems include:

- the controlled displacement of the truck rotation center and the inherent decrease in directing efforts of the overrun axle [86];
- radial arrangement of the truck axes by means of the mechanism, which uses the unbalanced centrifugal forces [87];
- changes which depend on the radius of the directing length curve for the carriage by means of the pneumatic cylinders, which affect the running axes;
- trucks with turntable wheel pairs;
- the use of a controlled connection between trucks: the joining forces for the front and the rear trucks create the moment which is directed opposite to the moment of the friction forces of wheels against rails;
- horizontal balancing of axes.

Within the systems of active direction, the principles are implemented with the distinguishing feature: the use of automatic devices for power control over the parameters and over the configuration of the trucks, for example, those to create the angular connection between the truck and the body using pneumatic, hydraulic, electric or other drives.

In accordance with the direction of this work, it should be noted that the control over the carriages by the track is a prerequisite for a significant reduction in the resistance to the movement by decreasing the horizontal reactions in the wheel and rail contacts.

If to conduct the research of the rolling stock controllability in the context of the theory of the wheeled vehicle motion, then the problem to determin the dedicated controllability quantitative parameters seems to be a trivial task, because the result of the control action is almost always known in advance (except in emergencies), as we are dealing with the control per the tight program in this case. One of such quantitative characteristics is, in particular turnability, defined

by a minimum curve radius, in which it is possible to steer the vehicle with the acceptable levels of lateral pressure. The term of *turnability* is similar to the term of *insertion* by K. Ju. Tseglynsky and K. P. Koroliov [92, 93].

The aforementioned theory does not take into consideration the qualitative parameters of the controllability of the rail carriage movement. It was proposed to evaluate the quality of this control by the amount of the additional influence of the track on the carriage. First of all, this is a horizontal effect on the track. It is necessary to distinguish between two modes of nonrectilinear motion at the track control over the carriage: *the kinematic insertion mode* (in which none of the wheel pairs of the carriage has wheel flange contact with the rail) and *the power insertion mode* (which is characterized by the guiding of wheel pairs accompanied by wheel flange touch).

Obviously, in *the kinematic insertion mode*, the level of the impact of the carriage on the track is much lower than that in *the power insertion* mode.

When a carriage moves in a circular curve, the main vectors of the external force influence on wheel pairs, namely, main force vector $(\vec{F}_y)$ and main vector of moments $(\vec{M})$ are equal to zero:

$$\vec{F}_y = \vec{F}_i + \vec{F}_k; \quad \vec{M} = \vec{M}_i + \vec{M}_k, \tag{2.1}$$

where $\vec{F}_i$ is the main vector of the horizontal forces of inertia acting on the carriage;

$\vec{F}_k$ – the main vector of moments of the horizontal forces of inertia acting on the carriage;

$\vec{F}_k$ – the main vector of horizontal forces in the contacts of wheels with rails;

$\vec{M}_k$ – the main vector of moments of horizontal forces in the wheel and rail contacts.

In the ideal case with the constant movement of the carriage in the curve at the equilibrium speed, the horizontal effect on the track should be absent, but in practice it always takes place. The value of the horizontal contact reactions depends on the quality of controllability.

Another qualitative parameter of controllability is the additional resistance to the movement associated with the control, that is, the guiding of the wheel pairs by the track. In the course of the carriage guiding by the track, there occurs a phenomenon of the power flows circulating in closed circuits, the flows are formed by the elements of the truck arrangement, the drive and the wheel pairs. Although the circulating power flows are related to the steering function of wheel pairs, they are, as a rule, parasitic, causing the significant additional slipping in the wheel and rail contacts, mechanical losses and the increased resistance of the movement, especially in curved sections of the track.

Further, any additional slipping, unrelated to the traction effort, sharply decreases the threshold values of the adhesion coefficient, that is, it worsens the traction dynamic and braking performance of the rolling stock. The aforementioned resistance to the movement, which the authors refer to as a kinematic resistance, is closely connected to the directing efforts and the frictional interaction between wheel pairs and rails.

According to the generally adopted idea, the trucks with those wheel pairs, which radially arrange themselves in curves, have a number of advantages over the carriages with conventional "rigid" wheel pairs. The latter create considerably more load on rails. Many theoretical and experimental studies have proved that the radial installation of wheel pairs can significantly reduce the parasitic slipping in the contacts, as well as the load on the wheel flange contacts and, consequently, reduce the wear of the wheel flanges along with the resistance to the movement [85-91].

2.2. The Study on the Guidance Force Generated by the Track for Wheel Pairs

For the theoretical study on the track directing forces acting on wheel pairs, an accurate description of the peripheral force and adhesion forces is required.

In the early period of railroad development, the issue of the wheel and rail adhesion was raised solely in connection with the adhesion qualities of the traction rolling stock. A large number of the research works is devoted to increasing the maximum traction power of adhesion in the wheel and rail system for a more complete realization of its function as a driving train. However, the problem of the wheel and rail adhesion is much deeper than its analysis in terms of traction. The adhesion must be considered throughout the whole complex, taking into account the complete picture of the horizontal forces of interaction between the carriage and the track, given that the horizontal constituents of the contact forces determine the horizontal dynamics of the carriage. From the standpoint of this sense, it would be appropriate to single out neither the longitudinal phenomena nor the transversal ones as the individual problems associated only with the adhesion qualities and horizontal transversal dynamics respectively, but to consider these phenomena jointly within the scope of complex horizontal dynamics. The attempts to address the longitudinal and transversal adhesion issues separately or, at best, as partially related, often lead to the adverse effects. For example, the beneficiating activates that improve the dynamic performance may lead to deterioration in the other indicators such as the resistance to the movement, the intensive wear of the contact surfaces, etc.

2.3. Theories of Wheel-Rail Adhesion

At the beginning of the twentieth century in connection with the rapid development of the transport technology, the several scientific theories appeared at the same time reflecting the physical laws of wheel-rail adhesion. Among them the most developed are as follows:

- plastic deformation theory;
- elastic incompleteness theory;
- molecular theory;
- molecular-mechanical theory.

The pseudosliding theory or creep theory by O. Reynolds [68] was widely used in practices of adhesion force calculations. The Reynolds theory was applied by F. Carter when developing the technique for theoretical determination of the amount of wheel slip relative to the rail [94]. By representing the surface of a rail top in the form of a plane and the surface of a rolling circle in the form of a cylinder, F. Carter suggested the formula known today as the creep formula:

$$\varepsilon = \mu \cdot \sqrt{8 \cdot P / ER(1-\sigma^2)} \cdot (1 - \sqrt{1 - F / F_{\max}}), \qquad (2.2)$$

where R – the wheal rolling radius;

μ – the coefficient of the sliding friction;

P – the vertical load per a width unit of the contact surface;

E –the modulus of elasticity of the wheel material;

σ – Poisson's ratio of the wheel material;

F, $F_{\max}$ – the tangential force per a width unit on the contact surface and its maximum value in terms of the adhesion, respectively.

K. L. Johnson generalized Carter's plane theory to the three-dimensional case of rolling of two spheres with taking into account of longitudinal and lateral creep [95]. According to his idea, the contact surface of two bodies is divided into two asymmetric areas, namely the slide area and the adhesion area. The latter has the ellipse shape, which touches the contact ellipse by apex forward in the direction of the motion. However, Johnson's theory as a generalized Carter's theory is limited to a case study of a pure longitudinal and lateral creep, i.e. the case of the absence of a turning creep or a spin.

The strip theory by J. Halling [96], D.J. Hainess and E. Olerton [97] can also be regarded as the further development of Carter's theory. Their theory considers pure longitudinal creep with the elliptical area of the contact. In this case, the contact patch is divided into a series of strips parallel to the direction of rolling each of which was studied according to Carter's theory without any interrelation between each other.

It should be noted here that the data of the theoretical studies obtained by publications [96, 97] are in good agreement with the experimental work.

The great contribution to the development of the adhesion theory was made by J.J. Kalker, who developed a linear creep theory, according to which at small creep values, the area of the contact patch where the slide occurs is so small that it can be neglected if we regard the entire contact area as an adhesion zone [98]. According to this theory, as the particles of the wheel surface fall into the contact area, they interact at the front edge of the contact area. While moving along the contact, the traction effort is generated due to the lack of sliding. J.J. Kalker suggested to express the ratio between the creep (longitudinal, lateral or angular in case of slide) and the forces and the creep moment (spin) in the form of simplified linear functions [99].

The explanations of the friction nature as a result of the deformation of certain volumes of the contacting bodies when they penetrate each other are given by the deformation theories of friction according to which the friction arises due to the deformation wave, which travels in front of each penetrating protrusions.

This theory has been developed in Andreev's works[1].

The absorption and the dispersion of the energy in the process of formation and destruction of the frictional bonds due to the thermodynamic hysteresis are described in the energy theory of friction developed by V.D. Kuznetsov[2], and P.A. Rebinder[3].

Moreover, the development of this theory in the form of an entropy-energy theory of friction is presented in the work by L.I. Bershadsky[4].

According to the Structural-Energy Theory of Friction, all friction processes arise and develop as a result of two influencing phenomena: on the one hand, the increase in the free energy in the friction system (activation), on the other hand, its decrease (passivation).

Furthermore, A.V. Chichinadze[5] laid the foundations of the thermal dynamics of friction and further developed by M.V. Korovchinsky[6] and V.S. Shchedrov[7].

---

[1]Andreev A. I., Komarov K. L., Karpushchenko N. I. (1997) Iznos relsov i koles podvizhnogo sostava [Wear of Rails and Wheels of the Rrolling Stock]. *Zheleznodorozhnyiy transport* [Railway Transport]. No 10, p.p. 31-36.

[2]Kuznetsov V.D. (1947) *Fizika tverdogo tela* [Rigid Body Physics]. Tomsk. Krasnoe Znamya, 539 p.

[3]Rebinder P.A. (1958) *Fiziko-himicheskaya mehanika – novaya oblast nauki* [Physical and Chemical Mechanics is a New Field of Science]. Moscow. Znanie, 36 p.

[4]Bershadsky L. I. (1977) Trenie kak termomehanicheskiy fenomen [Friction as a Thermomechanical Phenomenon]. *Report of the Ukrainian Academy of Sciences*. No 6, p.p. 186-190.

[5]Chichinadze A.V. (1967) *Raschet i issledovanie vneshnego treniya pri tormozhenii* [Calculation and Study of the External Friction during Braking]. Moskow. Nauka, 231p.

[6]Korovchinsky M. V. (1975) Termo-kontaktnyie protsessy pri kachenii i skolzhenii detaley mashin [Thermo-Contact Processes in Machine Parts Rolling and Sliding. *Mashinovedenie*. No 3, p.p.15.

[7]Shchedrov V. S. (1950) Predvaritelnoe smeschenie na uprugo-vyazkom kontakte [Preliminary Displacement on the Elastic-Viscous Contact]. *Trenie i iznos v mashinah* [Friction and Wear in Machines]. Moscow. Leningrad. AS USSR, 219 p.

The aspects of the material which are within the metal science scope of studies are also taken into account for the structural phase transitions and transformations on contacting surfaces during friction. They are outlined in the works of K. L. Johnson[8], B.I. Kostetskiy[9] and H. Krause[10].

The contemporary ideas on the wheel-rail adhesion are based on an integrated approach to the above-mentioned theories of friction.

2.4. Study of Adhesion Characteristics

For the mathematical modeling of the rail vehicle movement, it is important to use the reliable external characteristics in the contacts of wheels and rails. The adhesion characteristics are commonly determined as the dependence of the adhesion coefficient on the specific sliding speed in the main contact. The presence of the longitudinal sliding of wheels relative to the rails is a necessary condition for the appearance of the adhesive forces in the contacts, in particular the traction force. A large number of studies has been devoted to the study of adhesion characteristics. The authors of [73] proposed to represent the adhesive characteristics in the following form:

$$k_x\left(\varepsilon_x, \varepsilon_y\right), \;\; k_x\left(\varepsilon_x, \varepsilon_y\right), \tag{2.3}$$

where k_x, k_y – the relative coefficients of the adhesion in the contacts, in the longitudinal and the transverse directions, respectively.

$\varepsilon_x, \varepsilon_y$ – the relative sliding in the contacts, in the longitudinal and the transverse directions respectively.

$$k_x = \frac{\psi_x}{\psi_o}; \quad k_y = \frac{\psi_y}{\psi_o}; \quad \varepsilon_x = \frac{V_{sx}}{V_c}; \quad \varepsilon_y = \frac{V_{sy}}{V_c}, \tag{2.4}$$

where ψ_x, ψ_y – the current values of the adhesion coefficients, in the longitudinal and the transverse directions, respectively;

ψ_Q – the physical adhesion coefficient;

V_{sx} , V_{sy} – the velocities of sliding in the center of the contact patch, in the longitudinal and the transverse directions, respectively;

V_c – the comparison speed.

[8]Johnson K. L. (1964) The effect of a Tangential Force upon the Rolling Motion of an Elastic Sphere upon a Plane. *J.Appl.mec*. V.31.No 2, p.p.339-340.

[9]Kostetskiy B.I. (1985) Strukturno-energeticheskaya prisposablivaemost materialov pri trenii [Structural and Energy Adaptability of Materials when Friction]. *Trenie i iznos* [Friction and wear]. Vol. 6. No. 2, p.p. 201-212.

[10]Krause H., Poll G. (1983) *The Influence of Tangential Tractions at the Surface on the Stresses in Contacting Bodies during Rolling-Sliding Contact*. Wear. 250 p.

As a comparison speed, either the speed of the wheel center (V) or the surface speed of wheel tread circle (ωR) can be applied

The presence of the ascending and descending branches of the adhesion characteristics is confirmed by the results of most studies [100–104]. Figure 2.1 shows a typical characteristics of the wheel-rail adhesion. Conditionally, it can be divided into three areas: 1 – proportionality area, in which the dependence is linear; 2 – elastic sliding area; 3 – totally sliding area. Moreover, one can observe here a large range of the numerical values.

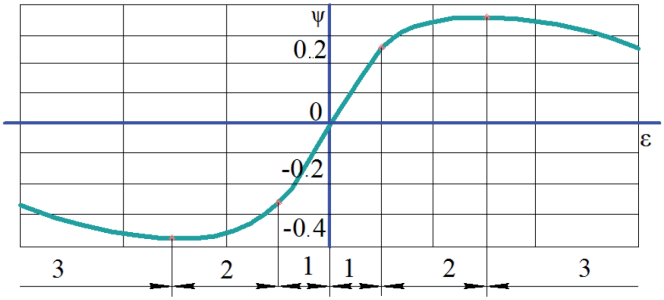

Figure 2.1. Typical Characteristics of Wheel-Rail Adhesion

F. Barwell [100], H. Mariama and T. Ohyama [101] revealed a significant decrease in the adhesion coefficient in the case of high humidity in the air and water penetration into the contact (refer to figure 2.2, 2.3).

J. Chap showed that when a load is variable, the adhesion coefficient is smaller than when the load is constant (refer to 2.4) [102].

The drawback of many experimental studies carried out with real locomotive testing is the dubious accuracy of the experiment due to the apparent inability to omit or to take into account a number of side factors, mainly dynamic ones, associated with the oscillations and the vibrations in the wheel-rail system. Especially this applies to the area of low and medium sliding within adhesion characteristics.

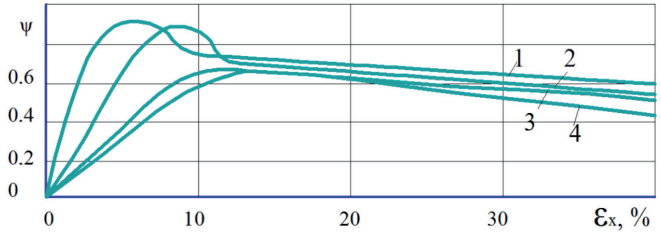

Figure 2.2. Adhesion Characteristics with Different Values of Air Humidity (according to F. Barwell's Data [100]): 1 – 20 %; 2 – 40 %; 3 – 65 %; 4 – 100 %

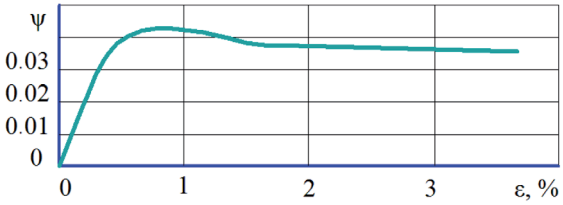

Figure 2.3. Adhesion Characteristics with Water Penetration into the Contact (according to the data by H. Mariama and T. Ohyama [101])

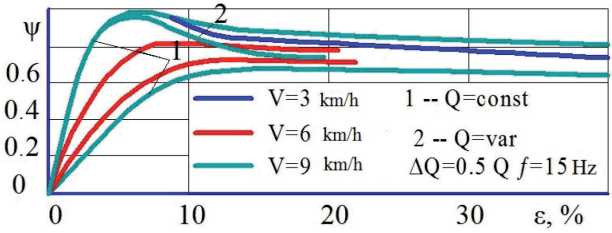

Figure 2.4. Adhesion Characteristics with Dynamic Vertical Load (according to J. Chap's Data [102])

On the other hand, the experiments on simulating units cannot really depict the physical processes in wheel-rail contacts through the practical lack of the reliable criteria of the contact interaction similarity at high normal and tangential stresses.

As the issue of the special interest, we would like to outline the experimental unit for studies of the adhesion characteristics based on the full-size wheel and the full-size rail [103]. The advantage of such experimental unit is the capability of ensuring the conditions most similar to the real contact. This unit takes into account the low values of the resistance to the movement in comparison with the boundary forces of adhesion. The unit allows us to simulate the process of wheel starting and to obtain the characteristics of the wheel-rail adhesion as the dependence of the longitudinal and the transverse adhesion forces on the longitudinal and transverse relative sliding in the contact. The scheme of this unit is shown in Figure 2.5. The main parts of the unit are the unit frame, the drive, the braking system and the control panel. Frame (1) is a rigid welded construction of sectional metal. To increase the rigidity in the plane of the wheel rotation as well as in the transverse vertical plane, there are applied braces (2) on which magnetic-rack brake (3) is suspended. The frame contains two pairs of horn plates, namely, the lower and the upper ones.

Axle boxes (4) carrying the roller spindle are installed in the lower horn plate while axle boxes (5) carrying the wheel axle are in the upper horn plate. The lower horn plates are fixed on the base of frame (6). The upper horn plates are welded to

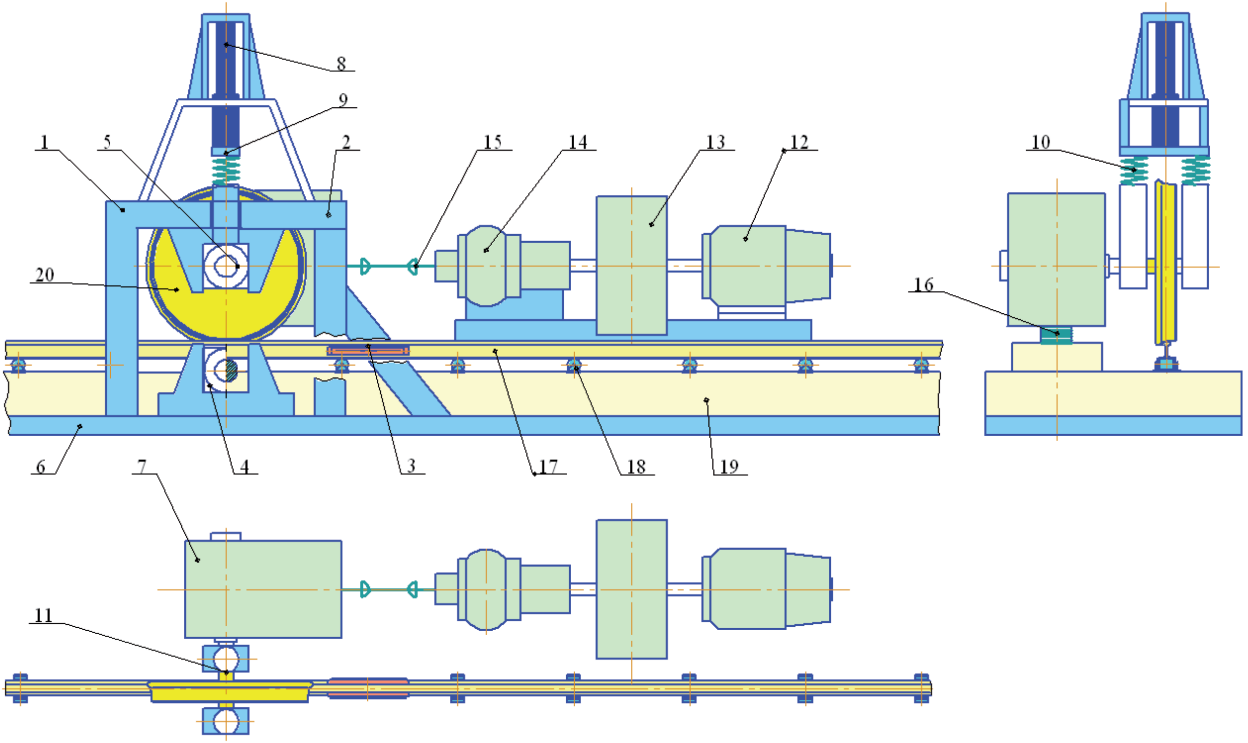

Figure 2.5. The Test Unit for the Experimental Study of the Adhesion Characteristics [103]

frame legs (1). The vertical load is created by hydraulic prop (8), which transfers the stress both through the cross girder (9) and through two complete units of rubber elements (10) to axle boxes (5) of wheel axle (11).

In order to create the oscillations of the vertical load, the chamber of hydraulic prop is installed connected by channel pipe with the plunger, which is activated by the locking piece on the electric motor shaft. The alternating frequency of the electric motor rotation is set by the vertical load.

The plunger travel depends on the configuration of the locking piece and it is constant but the oscillation amplitude of the vertical load is changed by our selection of rubber elements quantity (10). The earth pressure cell is installed on the cross girder (9), whereby the vertical load of the wheel on the rail is measured and registered with the oscillograph. For calibrating the earth pressure cell, the standard pressure gage is applied connected to the chamber of the hydraulic prop.

The drive of the experimental unit comprises starting motor (12), flywheel (13), fluid converter (14) with the charging and discharge system, gimbal drive (15), and traction gear box (16). In the function of starting motor (12), they use the direct current motor with complex excitement.

The motor control is carried out from the driving desk.

Electric motor (12) is connected with a flexible diaphragm coupling equipped with flywheel (13). The speed transformer of Ukrainian ТГМ-23 locomotive is used as the traction gear box, which is favorable in the arrangement of the experimental unit.

As this, the unit has a conic module, it becomes possible to arrange all lines of the drive unit (the electric motor – the flywheel – the fluid converter – the traction gear box) along the base on the guide track.

The speed transformer has two levels with reduction ratio of 1:3.46 and 1:6.93 and a reverse gear on two elastic supports (17).

The adhesion force measurement is conducted with a help of four strain-gage dynamometers installed in the clearance points between the horn plates of a magnetic track brake and the experimental unit frame stops.

The research made with the experimental unit has allowed us to obtain the adhesion characteristics in longitudinal and transversal directions (refer to figure 2.6) [104].

In the function of regression equations k_x and k_y on $\varepsilon_x, \varepsilon_y$ are accepted the following expressions:

$$k_x = \frac{\varepsilon_x}{a_c \cdot \varepsilon_x^2 + b_c \cdot \varepsilon_x + c} \cdot \frac{1}{d_c \cdot \varepsilon_y^2 + 1}; \; k_y = \frac{\varepsilon_y}{f_c \cdot \varepsilon_y^2 + q_c} \cdot \frac{1}{h_c \cdot \varepsilon_x + 1}. \quad (2.5)$$

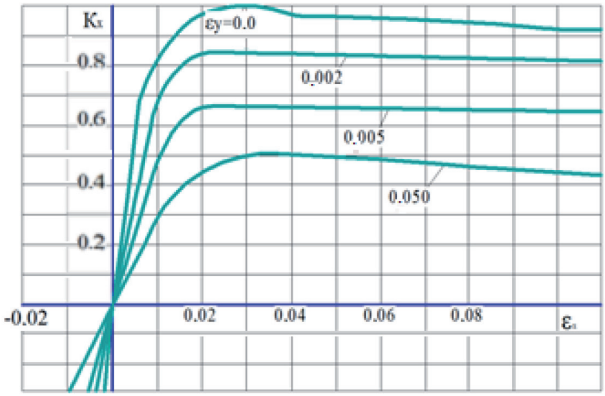

a

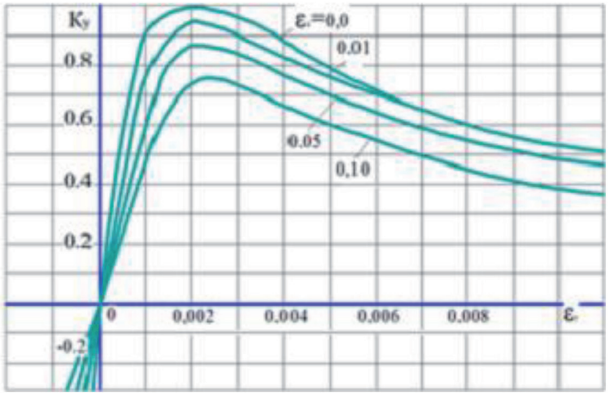

b

Figure 2.6. Experimental Data of Adhesion

2.5. The Guidance of the Carriage by the Railway Track

2.5.1. The Role of Wheel Flange Reactions in the Wheel Pairs Control and the Coefficient of the Derailment Resistance

The derailing of wheel pair is among the leading causes of disasters, emergencies and drastic accidents in the rail sector, they make up to 25%. The first derailing accident in the history of railway happened with *Camden & Am*boy passenger train in the USA in 1833. The train was travelling at speed of 40 km/h

and the accident took away about 100 passengers' lives. Since that first tragic event and until now, there have been thousands of occurrences with train derailing, resulting in dozens of thousands of victims in the history of railway. Over the past few decades, the number of train derailing has significantly decreased, but unfortunately it happens quite frequent [105–109].

The derailing mechanism of the railway vehicles is a complex process being the subject matter of the intensive research throughout the world. The main criterion to judge about the safety of transportation is the safety factor against derailment in the form of the ratio between the transversal force and the vertical load of the wheel on the rail [110]. The Nadal's theory in respect to the safety factor against derailment appears to be very simple, it applies a great number of assumptions and leaves behind many peculiarities of the wheel and rail contact [111, 112]. In particular the Nadal's Formula ignores the influence of the wheel attack angle and the motion mode (traction, stopping, braking) on the safety parameters [113, 114]. Thus, the safety factor against derailment for rail carriages is determined by the formula [110] as below:

$$k_y = \left[\frac{Y}{P}\right] \div \frac{Y}{P} \geq \left[k_y\right] \tag{2.6}$$

where P – the vertical load of the wheel on the rail;
Y – the lateral force in the Grebnov contact;
k_y – the minimum permissible safety factor against derailment;
$\left[\frac{Y}{P}\right]$ – the ratio of lateral force to the vertical load in the flange contact, at which the release of the wheel rolling surface from the rail occurs. According to Nadal's formula we have the following [110]:

$$\left[\frac{Y}{P}\right] = \frac{tg\beta - \mu}{1 + \mu \cdot tg\beta}, \tag{2.7}$$

where β – the flange inclination angle;
μ – the friction coefficient in the wheel and rail contact.

Formula (2.7) is valid only for the case when the attack angle equals zero ($\psi = 0$).

There have been numerous attempts made to improve Nadal's Formula with the objective to enhance the safety level for the new railway vehicles when they are being only developed. More accurate version of Nadal's Formula is Vagner's Formula [115], which takes into account the deviations of the normal load produced by the wheel on the rail from the vertical loading:

$$\left[\frac{Y}{P}\right] = \frac{tg\beta - \mu \cdot \cos\gamma}{(1 + \mu \cdot tg\beta) \cdot \cos\gamma}, \quad (2.8)$$

where γ – the deviation angle of the normal load produced by the wheel on the rail from the vertical one.

Based on Nadal's Formula, publication [116] provides the analysis to show how spin acts in the flange contact and its role. Here, it is claimed that the data obtained are more true to the life than those received by Nadal's Formula. The safety criterion is proposed, it enables less conservative values to be revealed than those of Nadal's Formula.

The another attempt to make Nadal's Formula more accurate is done in publication [117]. This work is grounded on the study on the longitudinal contact force of creeping and the wheel-rail attack angle. The results obtain by this research are slightly different from the Nadal's criterion as they account slipping neither within the main contact nor within the wheel pair operation mode.

In publication [118], the main types of derailing are analyzed. Three of them are related to the rail track features while the other two are stipulated by the shapes of the wheel and the rail. It is proved that the wheel flange inclination angle is the main geometric parameter to influence the probability of derailing. The statistical data of the large-scale accidents in the railway sphere are given and the causes are analyzed in [119]. The necessity to make the researches on the flange contact is outlined as it is the main factor of the safety. Publication [120] developed the equations to assess the load on the wheel with consideration of the centrifugal force, the deviations in the trajectory shape and the deformation in the secondary suspension of the railway vehicles. The method for calculating the critical value of the safety factor has been proposed and it incorporates both the wheel-rail attack angle and equivalent friction coefficient.

The specific character is revealed when the wheel contacts with the rail [121]:

- 3-D reaction distribution within the wheel and rail contact;
- kinematics of the two-point contact;
- redistribution of the forces and kinematic parameters between the contacts when contact dislacement;
- dependence of the flange contact force direction on both the attack angle and the movement mode of the locomotive wheel pairs (traction, stopping or braking);
- the probability for the vertical constituent of the friction force in the flange contact to appear.

Based on the data of the numerical simulation for the railway vehicles, research [122] addresses the problem of the track with its side and vertical roughness. The roughness is of occasional character. The safety level is estimated by the

relation between the transversal and the vertical forces at the point where the wheel contacts the rail. The level of comfort is assessed by the values of the lateral acceleration and the vertical acceleration.

The common opinion prompts that the railway wheel flange dangerous gradient is the main reason of the accidents in the sphere of the railway transportations. Authors [123] estimate the friction coefficient within the wheel flange and rail contact on the accident probability. It is found that the friction coefficient varies considerably due to various factors, namely: the quality of the wheel and the rail surfaces, weather conditions and the speed of train running. The derailing danger is evaluated here by Nadal's criterion with different friction coefficients. The results allowed the conclusion that the measures to decrease the friction coefficient are effective even in the cases when the safety factor against derailment shows the values higher that the Nadal's criterion boundary ones.

The method to ensure safety against derailing is proposed in [124], grounded on the wheel unloading factor. The method permits an estimation of the railway transport safety by means of the study if the railway wheel unloading is within the safety zone. The dynamic testing has been carried out, they apply the methods of the indirect measurement for the railway wheel pressing the subway rail track. It has been revealed that the data on the safety level are beyond the normal ones when hunting while at the stable run they are within the safety norm.

The main dynamic parameter of three different truck types are compared in [125]: the vertical and horizontal dynamic factors, the safety factor against derailment.

Unfortunately, rail vehicle derailment also takes place at low speeds in the curved sections of tracks. Publication [126] is devoted to this problem and studies the mechanism of the wheel flange lift for the quantitative assessment on the factors causing railway transport derailing. The results of the tests with the real time derailing of the passenger trains have been analyzed and the verification with the tests on the experimental roller unit has been also applied. The study resulted in the new method for assessment of the safety level against derailment in the curved sections of the rail track.

Publication [127] describes the derailing mechanism and the method of continuous monitoring for the forces between the wheel and the rail, the research results in the new criterion of the dangerous situation assessment.

3-D nonlinear dynamic model of the wheel pair system and suspension is presented in [128]. The influence of the friction coefficient and the speed of the train movement on the derailment phenomenon is studied together with the various ways to paint the rails and their impact on derailment. The specific character of the two-point wheel-rail contact is not left behind in this publication and the recommendations how to enhance the safety against derailment have been developed.

A brief review of the distinct problems of the railway transport dynamics is provided by [129], including the analysis on the derailment mechanism. The authors state that none of the existing safety criteria are able to determine the derailment probability completely. They propose to apply several safety criteria simultaneously. In the analysis on the derailment mechanism [130], the role of the attack angle is shown. However, the authors do not go further out of the description and do not write about any calculated dependencies revealed. The procedure to calculate the longitudinal location of the wheel flange contact, in particular the eccentricity, is calculated with Vang's method [131] and submitted in 3-D grid. The results of the simulation have been compared with the results where the calculations for the arrangement were conventional. The researches have come to the conclusion that the more accurate arrangement of the contact point found by Vang's method permits having the less of the flange inclination. However, the influence of the longitudinal location of the contact point bear the slightest effect on both the flange inclination (less than 40 degrees) and the attack angle (less than 1 degree) when train movement.

Mathematical models with the wheel and the rail spacious configurations were applied to study the characteristics of derailment [133, 134]. The authors note that the detailed characteristics of the wheel-rail contact geometry is crucial for the accuracy of the dynamic analysis of the rail vehicles.

The following issues are considered:

- the study of the contact geometry to determine the location point of the main and the flange contacts;
- surfacing for the contacting bodies;
- calculation of the relative speed in the contact points;
- determination of contact forces.

In articles [135, 136], the requirements to the contemporary rolling stock are given with the detailed analysis on the dedicated characteristics for the freight wagons. However, the research omits the potential and the way how to improve the dynamic features of the rolling stock. It would be interesting to regard in this aspect the safety parameters with the movement of various wagons or carriages.

The improved carrying system for the rolling stock is reported in [137] due to the better methods applied to study its strength in statics. At this, the dynamics with the safety factor was out of the research focus.

The existing methods of assessment against derailment are analyzed in [138]. It has been revealed that the reserve of the factor acting against the wheel flange rolling into the rail top is an integral indicator of the movement safety. This indicator is defined employing the information as follows: 1) the vertical loading, 2) the lateral force, 3) the friction force acting in the wheel flange-rail contact and 4) the wheel pair geometry.

Despite of the numerous researches on the safety factor against derailment [105–138], the dynamic factors have not been regarded in this context. In particular, the accumulated effects of the wheel-rail attack angle and the influence of the retract forces of the passing wheel on the wheel pair derailment are not sufficiently studied. Both from the operational standpoint and from the theoretical one, the assessment of the safety factor through the lateral effort in the wheel flange contact is unsuitable and inaccurate. The analysis of the horizontal flange effort even within one wheel pair is difficult as this kind of effort is influenced at a great extent by the friction force generated in the contact of the other wheel of the pair.

2.5.2. The Kinematics of the Wheel Pairs Contact with Rails

The motion of a wheel pair in the rail track with attack angle (ψ) is shown in the skewed position. Figure 2.7 shows the velocity diagram as blue vectors and the diagram of forces as red vectors in the contact points of the wheel pair with rails. Climbing wheel (2) has a two-point contact with the rail in point K_{21} (the main contact) and point K_{22} (flange contact). The passing wheel (1) in this case has one-point contact in point K_{11}. Let us consider the instance when the climbing wheel is in the derailing condition. The loading being equal to zero in the climbing wheel main contact is assumed to be the derailing condition.

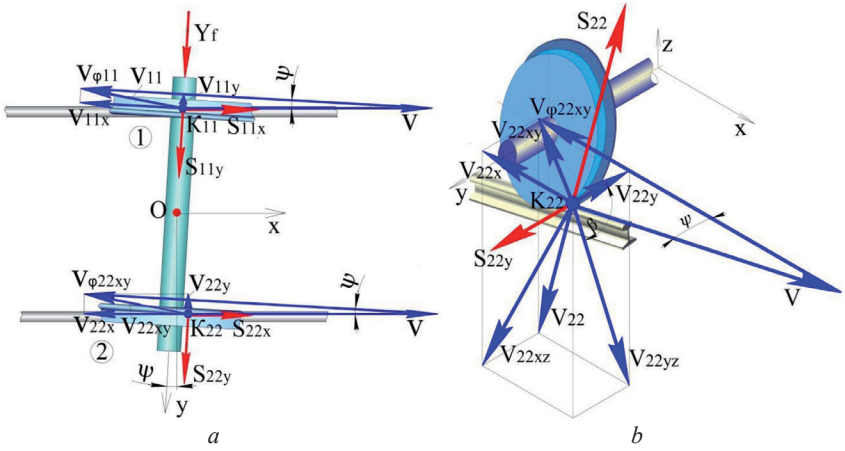

Figure 2.7. The Velocity Vectors Diagram (Blue Color) and the Diagram of Forces (Red Color) in the Wheel Pair and Rails Contacts:
***a* – velocities and forces projections in the wheel pair and rails contacts on horizontal plane *Oxy*; *b* – spatial pattern of speeds and forces in the climbing wheel flange contact**

When simulating the kinematic characteristics of the wheel pair and the rails, the following parameters of their signs were considered:

V – the wheel pair velocity of motion along the track axis;

$V_{\varphi 11}$ – the wheel surface velocity in contact point K_{11}, associated with the wheel pair rotation relative to its axis;

V_{11} – the velocity of the wheel slipping along the rail in contact point K_{11};

V_{11x}, V_{11y} – the projections of velocity V_{11}, on axes Ox and Oy, respectively;

$V_{\varphi 22xy}$ – the wheel surface velocity projection in contact point K_{22} on horizontal plane Oxy;

V_{22xy} – the wheel slipping velocity projection along the rail in contact point K_{22} on horizontal plane Oxy;

V_{22x}, V_{22y} – the projections of velocity V_{22} on Ox and Oy respectively;

V_{22xz} – V_{22} velocity projection on longitudinal vertical plane Oxz;

Y_f – axial response in the axle box assembly influencing the wheel pair – frame force;

S_{11y}, S_{22y} – friction forces projections S_{22} in contacts K_{11} and K_{22} on Oy axis;

S_{22xz}, S_{22x}, S_{22z} – friction forces projections S_{22} in contact K_{22} longitudinally and vertically on plane Oxz, respectively; Ox and Oz axes;

β – the flange inclination angle.

The vector equations of slipping speeds in contacts K_{11} and K_{22} obtained by superposition principle as the constituents of the relative displacement of the wheels rolling surfaces and rails:

$$\overline{V}_{22xy} = \overline{V} + \overline{V}_{\varphi 22xy}\,;\ \overline{V}_{22xy} = \overline{V} + \overline{V}_{\varphi 22xy}\,. \tag{2.9}$$

$$\overline{V}_{22} = \overline{V}_{22xy} + \overline{V}_{22xz} + \overline{V}_{22yz}\,. \tag{2.10}$$

Figure 2.8 shows the contact forces diagram in the flange contact in the projections on longitudinal vertical plane Oxz and transversal vertical plane Oyz.

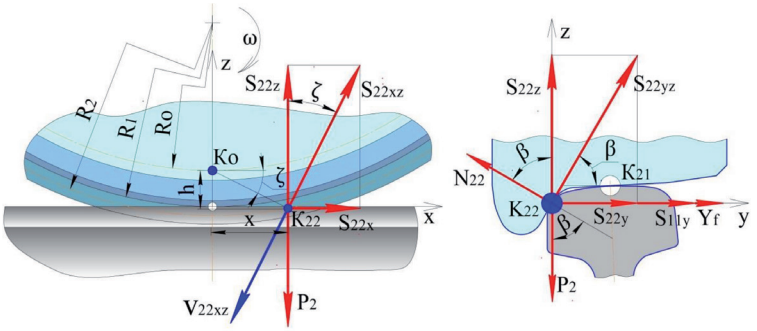

Figure 2.8. Diagram of Forces Projections in the Flange Contact; a – Projections on Longitudinal Vertical Plane *Oxz; b* – Projections on Transversal Vertical Plane *Oyz*

In Figure 2.8, the following signs are accepted:

ζ – the angle that determines the position of vector S_{22xz} relatively to the vertical axis;

ω – the angular velocity of the wheel pair rotation around its own axis;

N_{22} – the normal load in flange contact K_{22};

K_0 – the instantaneous center of the wheel rotation;

R_0 – the distance from the wheel center to the instantaneous center of wheel rotation K_0;

R_1, R_2 – the wheel radiuses in the main and the flange contacts respectively;

P_2 – the vertical load in flange contact K_{22}.

2.5.3. Power Interaction of the Wheel Flanges and the Rail

The total horizontal lateral loading in flange contact *Y* equals to the sum of the frame force *Yf* and retract forces S_{11y} and S_{22y} in contacts K_{11} and K_{22}:

$$Y = Y_f + S_{11y} + S_{22y}. \tag{2.11}$$

Frictional contact forces S_{11y} and S_{22y} in contacts K_{11} and K_{22} are called retract forces in the wheeled vehicles control theory. Retract forces S_{11y} and S_{22y} are the forces of friction directed opposite to sliding velocities vectors V_{11y} and V_{22y}. Forces S_{11y} and S_{22y} can approximately be determined with formulas of Coulomb's law. In this case, the most hazardous instance of derailing is at angle $\zeta = 0$.

$$S_{11y} = P_1 \cdot \mu;\ S_{22y} = N_{22} \cdot \mu \cdot \cos\beta, \tag{2.12}$$

where P_1 – the vertical load in contact K_{11};

μ – the sliding friction coefficient in the wheel and rail contacts.

Then

$$Y = \mu\left(P_1 + N_{22} \cdot \cos\beta\right) + Y_f. \tag{2.13}$$

The equilibrium equation of the contact forces are represented as a sum of the projections on axes *Oy* and *Oz* (refer to figure 2.9 b):

$$\begin{cases} \sum F_y = 0: \\ \sum F_z = 0: \end{cases} \quad \begin{cases} Y - N_{22} \cdot \sin\beta = 0; \\ N_{22} \cdot \mu \cdot \sin\beta + N_{22} \cdot \cos\beta - P_2 = 0. \end{cases} \tag{2.14}$$

From the other equation (2.14) we obtain as written:

$$N_{22} = \frac{P_2}{\mu \cdot \sin\beta + \cos\beta}. \tag{2.15}$$

Taking into account the fact that the first wheel has no flange contact, and the other wheel main contact is completely unloaded, we can assume that $P_1 = P_2 = P$, then we obtain from the first equation (2.14) as expressed below:

$$\mu \cdot P \cdot \left(1 + \frac{\cos\beta}{\mu \cdot \sin\beta + \cos\beta}\right) + Y_f - P\frac{\sin\beta}{\mu \cdot \sin\beta + \cos\beta} = 0 . \qquad (2.16)$$

2.5.4. The Criterion of the Derailment Prevention

The critical ratio between the frame force and the vertical load, at which the main contact complete unloading occurs, can be found by using the formula below:

$$\left[\frac{Y_f}{P}\right] = \frac{tg\beta\left(1-\mu^2\right) - 2\mu}{\mu \cdot tg\beta + 1} . \qquad (2.17)$$

In Figure 2.9, we show the comparative dependences of critical ratio $[Y_f / P]$ on flange inclination angle β and friction coefficient μ, calculated as per classical Nadal's formula (2.7) and improved formula (2.17).

For many decades, Nadal's formula has been the main criterion of rail carriages assessment of derailing preventing stability [110]. However, many researches [111–114] have noted that this formula is primitive and neglects many factors that influence railroad vehicles movement safety. There have been numerous attempts known to correct Nadal's formula with the aim to make it more

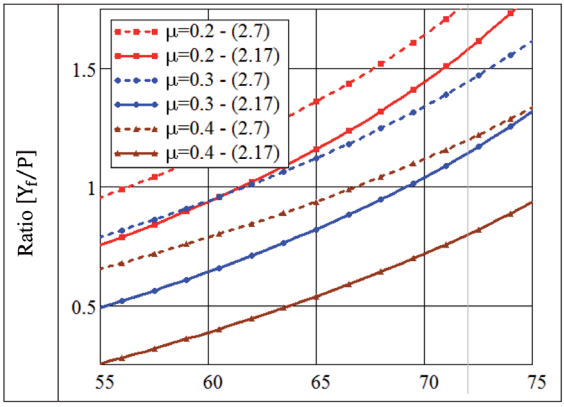

Figure 2.9. Critical Ratio Comparative Dependences $[Y_f / P]$ on the Flange Inclination Angle β and Friction Coefficient μ, Calculated as per Classical Nadal's Formula (2.7) and Improved Formula (2.17)

accurate [115–128]. In spite of the efforts made, the derailing of locomotives and carriages are still taking place regularly enough [129].

The results presented in this section are one more attempt to do this job with the safety criterion preventing derailing based on Nadal's theory.

The idea of the research is based on hypothesis which includes the following baselines of wheel pairs contacting with rails:

• slipping that takes place in the flange contact of the climbing wheel can create the friction force and the vertical constituent of the latter decreases the vertical load force on the rail in the main contact. In this case, the horizontal component increases the lateral load in the flange contact;

• slipping in the climbing wheel main contact creates the friction forces which increase the total horizontal transversal load on the climbing wheel flange.

The combination of these factors and their influence on the safety criterion against derailing has not been studied in the famous research works. The corrected formula for the safety coefficient to prevent derailing is as follows:

$$k_y = \frac{P}{Y_f} \div \frac{\mu \cdot tg\beta + 1}{tg\beta\left(1-\mu^2\right) - 2\mu} \geq [k_y], \tag{2.18}$$

where $[k_y]$ – the minimal permissible standard coefficient of the safety reserve preventing derailing.

As it could be seen from Figure 2.17, the values of ratio $[Y_f / P]$ obtained with corrected formula (2.17) are by 10–50 % lower (depending on the flange inclination angle β and friction coefficient μ) than the values calculated according to classical Nadal's formula (2.7). Thus, it became obvious that the Nadal's safety criterion required improvement. The techniques based on the specific features of frictional interaction of the wheel pair and the rail have been proposed to do this. However, the following issues have not been regarded in the dedicated studies:

• the dependence of the friction force vertical component in the climbing wheel flange contact on the attack angle;

• the influence of friction force in the climbing wheel pair flange contact on the increase in the lateral load on the flange;

• the influence of the friction force acting in the passing wheel-rail contact on the increase in the lateral load acting on the flange of the climbing wheel.

Unlike the traditional approach, the assessment of the safety factor to prevent derailing applies the frame force as the main factor instead of the lateral load on the flange as it has been used before. The cumulative effect of these factors on the derailing conditions has not been considered earlier. Dependence (2.18) is able to increase the accuracy of the safety coefficient, which allows enhancing the vehicles safety level at both during their engineering stage and during their operation.

3 THEORETICAL STUDY ON RESISTANCE TO THE MOVEMENT ASSOCIATED WITH THE CONTROL OF THE CARRIAGE BY THE RAILWAY TRACK

3.1. The Choice on the Calculation Schemes for Modeling the Carriages Control by the Railway Track

3.1.1. The System of Coordinates and the Simulation Features for the Rail Carriages

The interaction of the rolling stock and the railway track is associated with three functions of the wheel pairs: resistance, guidance and movement. Through using coordinate system of XYZΘΦΨ (fig. 3.1) for each function one can distinguish the kinematic links, their function applies to the relative displacement of the rolling stock and the track on the dedicated coordinates.

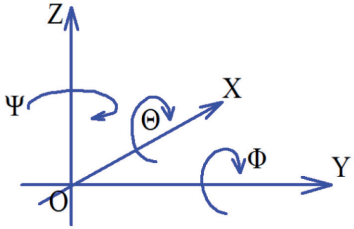

Figure 3.1. Coordinate System of the Rolling Stock and the Track Relative Displacement

The resistance function is associated with the necessity to compensate gravitational forces, and it imposes some constraints on movement on the following coordinates: *Z* (bouncing vertical linear displacement – *z*), Φ (pitching angular – φ) and Θ (angular displacement of lateral hunting – θ).

The guidance function is shown on coordinates Y (lateral linear displacement – y) and Ψ (angular rotating displacement in horizontal plane – ψ).

The rolling stock movement along the track axis is done by wheel pairs as a mover, which controls the jerking displacements (x).

The functions of the mover and the guidance are related with two directions within the problem of the rolling stock and track frictional interaction, i.e. the study of the horizontal dynamics of train and the locomotive traction features. Despite of the relative independence of these two directions, they are studied in interaction, as they are united by the common problem of the wheel-track adhesion.

Moreover, the simulation of the "rolling stock-track" mechanical system reveals the own peculiarities if compared against the simulation techniques of the other systems. First, it is the presence of the conventional track, which possesses the own features and boundaries. The rail base simulation is the main target in some theoretical studies and within the definite movement mode range due to the fact that it is able to define the truthfulness of the entire "rolling stock-track" system model. In most of the problems that dynamics deals with, the rolling stock may be considered as a system of absolutely rigid bodies connected with spring-dissipative links. The exception is the closed subsystems with high stiffness when the own elasticity of the elements is necessary to take into account. As an example of such subsystem we can regard the system of torque transmission from the engine to the wheels, i.e. a drive system. In many studies, torque stiffness of wheel pair axes is considered in this aspect.

One of the specific features of "rolling stock-track" system is the presence of the several positions for the static balance allowed due to the non-positional elements connection, for instance, frictional ones:

- wheels and rails;
- wheel pair axes and axle boxes, if there is the clearance in axial thrusts;
- bodies and trucks that are connected with guide blocks;
- bodies and trucks connected through side bearings.

Therefore, the partial derivatives of the gravitation force potential energy corresponding general coordinates are very often included into the movement equation.

When studying the motion with constant speed (V), which occurs most often, it is possible to exclude longitudinal coordinate (X) as a cyclical one from the consideration in order to work with the motion in a five-dimensional coordinate system. In this case, we admit that the rolling stock mass center moves at speed V.

In theoretical studies of rolling stock controllability, two main methods of mathematical modelling were used:

- the quasi-static method, which applies stationary models for calculation of the controllability factors;

• the time area study method or defined method, which uses nonlinear systems of differential equations.

The results obtained with fixed models are oriented toward a special case of stabilized motion without consideration of any dynamic processes.

The solutions made with the defined models are related to speed-displacement dependencies in the time mode, they correspond to the general coordinates. Moreover, according to calculation results, the dependencies of controllability and movement parameters on geometric and speed parameters of the rolling stock have been developed.

The problems of the temporary area are the most labour consuming ones in terms of integration, however, they allow more detailed understanding of the real processes, because the solutions are obtained commonly from the time dependencies, and the modelling itself is a «numerical experiment».

The model function has been taken into account for comparing the theoretical and experimental data, as well as for selecting the mathematical model correctness criteria. In this case, the most significant variables that reflect the essence of the process under study, i.e. so called main initial data, have been selected for the estimation.

The intermediate values that can be easily checked at adjusting models and computational programs are included into selected variables as the additional initial data, namely, they are the movement trajectory parameters associated with track limits: motion, speed, acceleration and hunting frequency.

The correctness of the simulation has been significantly enhanced due to the introducing the true external functions into the mathematical models: adherence experimental characteristics [104], contacting parameters with precise description of working surface geometries of rails an wheels, contact point coordinates and effective conicities.

The selection of the criteria for rolling stock track guidance modelling is based on the assumption that the resistance increases at track curved sections compared to straight ones, and under other equal conditions it is mediated with the kinematic resistance to the movement. The kinematic resistance to the movement is accepted as the main criterion of the correctness as it may be assessed by the experimental characteristics as a difference between the motion resistance on a curved section and the motion resistance on a straight section, or as additional motion resistance on a curve. If the calculated data of the kinematic resistance on curved sections sufficiently coincide with the experimental data, the mathematical model is considered to be correct, and it may be used for obtaining the numerical dependencies for the straight track sections.

The second truthfulness criterion applied is the resistance to the wheel pair rolling. In this case, the theoretical results have been compared with the experimental results of known studies.

3.1.2. The Calculation Models of the Carriages under the Study

The choice of a computational pattern for mathematical modelling is associated with the choice of model truthfulness criteria and detalization rational degree. As the majority of the researches devoted to the rolling stock horizontal dynamics, we use plane coordinate system XУΨ with generalized coordinates for mathematical models:

x, y – the longitudinal and transversal displacements of the mass centers of the bodies included in the system;

ψ – the body angular displacements in the plain view;

φ – the additional coordinate (turning angles of wheel pairs around the transversal symmetry axis).

Coordinate φ is added to the generalized coordinates, because it may not be considered as a cyclic one even at constant speed of movement.

When composing the differential equations of the rolling stock movement, the following general indexes of the values are used:

i – the wheel numbers of the wheel pair (*i*=1, 2);

j – the wheel pair numbers (for two axle trucks *j*=1, 2; for three axle trucks *j*=1, 2, 3);

k – the truck numbers (*k*=1, 2).

Tables 3.1–3.3 show the systems of generalized coordinates for each computation pattern considered.

Furthermore, the following designations for the geometric parameters are adopted here:

2*B* – the distance between the thread circles of a wheel pair;

2*A* – the distance between the points of the longitudinal force transmission from the wheel pair axis to the axle box and further from the axle box to the truck frame;

C_{jk} – the distance from *k*-th truck pivot to *j*-th wheel pair axis;

D_k – the distance from the body lateral axis to *k*-th truck pivot;

E – the distance between pivots of the intermediate beams.

Values C_{jk}, D_k, *E* are positive, if the force torque is positive, the arm they compose is also positive.

In Figure 3.2, the general pattern of the adopted designations of the geometrical parameters is shown.

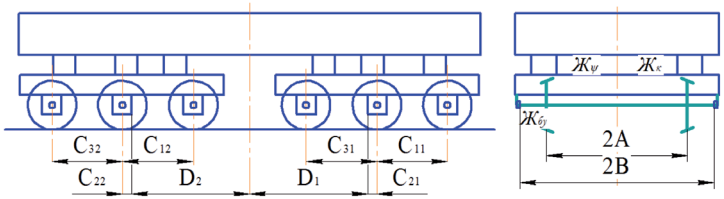

Figure 3.2. Diagram of Rolling Stock Geometric Parameter Designations

Table 3.1

Generalized Coordinates and Quantity of Motion Differential Equations for Computational Patterns for the Rolling Stocks without Intermediate Beams in Trucks

Number of the Pattern	Rolling Stock Type	Body		Truck frame			Wheel pairs				Equation Quantity
		y_c	ψ_c	#	$y_т$	$\psi_т$	#	y	ψ	φ	
1	FD 1-5O-1 Steam Locomotive	y_c	ψ_c	1	$y_{т1}$	$\psi_{т1}$	1	y_1	ψ_1	φ_1	34
							2	y_2	ψ_2	φ_2	
							3	y_3	ψ_3	φ_3	
							4	y_4	ψ_4	φ_4	
							5	y_5	ψ_5	φ_5	
							6	y_6	ψ_6	φ_6	
				2	$y_{т2}$	$\psi_{т2}$	7	y_7	ψ_7	φ_7	
2	EM50 Steam Locomotive	y_c	ψ_c				1	y_1	ψ_1	φ_1	22
							2	y_2	ψ_2	φ_2	
							3	y_3	ψ_3	φ_3	
							4	y_4	ψ_4	φ_4	
							5	y_5	ψ_5	φ_5	
3	Diesel Locomotive EEL 2-5O-1	y_c	ψ_c	1			1	y_1	ψ_1	φ_1	36
							2	y_2	ψ_2	φ_2	
							3	y_3	ψ_3	φ_3	
							4	y_4	ψ_4	φ_4	
							5	y_5	ψ_5	φ_5	
							6	y_6	ψ_6	φ_6	
							7	y_7	ψ_7	φ_7	
				2	$y_{т2}$	$\psi_{т2}$	8	y_8	ψ_8	φ_8	
4	VL19 VL22 VL22M VL23 Electric Locomotive	y_c	ψ_c	1		$\psi_{т1}$	11			φ_{11}	13
							21	y_{21}	ψ_{21}	φ_{21}	
					y		31			φ_{31}	
				2		$\psi_{т2}$	12			φ_{12}	
							22	y_{22}	ψ_{22}	φ_{22}	
							32			φ_{32}	
5	VL8 Electric Locomotive	y_c	ψ_c	1		$\psi_{т1}$	11		ψ_{11}	φ_{11}	21
							21		ψ_{21}	φ_{21}	
				2			12		ψ_{12}	φ_{12}	
							22		ψ_{22}	φ_{22}	
				3			13		ψ_{13}	φ_{13}	
							23		ψ_{23}	φ_{23}	
				4			14		ψ_{14}	φ_{14}	
							24		ψ_{24}	φ_{24}	
6	ChS2 Electric Locomotive	y_c	ψ_c	1	$y_{т1}$	$\psi_{т1}$	11	y_{11}	ψ_{11}	φ_{11}	24
							21	y_{21}	ψ_{21}	φ_{21}	
							31	y_{31}	ψ_{31}	φ_{31}	
				2	$y_{т2}$	$\psi_{т2}$	12	y_{12}	ψ_{12}	φ_{12}	
							22	y_{22}	ψ_{22}	φ_{22}	
							32	y_{32}	ψ_{32}	φ_{32}	

Number of the Pattern	Rolling Stock Type	Body		Truck frame			Wheel pairs				Equation Quantity
		y_c	ψ_c	#	$y_т$	$\psi_т$	#	y	ψ	φ	
7	Re2/2 Electric Locomotive	y_c	ψ_c	1	$y_{т1}$	$\psi_{т1}$	11			φ_{11}	12
							21			φ_{21}	
				2	$y_{т2}$	$\psi_{т2}$	12			φ_{12}	
							22			φ_{22}	
				3	$y_{т3}$	$\psi_{т3}$	13			φ_{13}	
							23			φ_{23}	
8	TE3 TE10 TE10L M62 Diesel Locomotives	y_c	ψ_c	1		$\psi_{т1}$	11		ψ_{11}	φ_{11}	18
							21	y_{12}	ψ_{21}	φ_{21}	
							31		ψ_{31}	φ_{31}	
				2		$\psi_{т2}$	12		ψ_{12}	φ_{12}	
							22	y_{22}	ψ_{22}	φ_{22}	
							32		ψ_{32}	φ_{32}	
9	2TE116 2TE10V 2TE10M TE109 Diesel Locomotives	y_c	ψ_c	1	$y_{т1}$	$\psi_{т1}$	11	y_{11}	ψ_{11}	φ_{11}	30
							21	y_{21}	ψ_{21}	φ_{21}	
							31	y_{31}	ψ_{31}	φ_{31}	
				2	$y_{т2}$	$\psi_{т2}$	12	y_{12}	ψ_{12}	φ_{12}	
							22	y_{22}	ψ_{22}	φ_{22}	
							32	y_{32}	ψ_{32}	φ_{32}	
10	2TE121 Diesel Locomotive	y_c	ψ_c	1	$y_{т1}$	$\psi_{т1}$	11	y_{11}	ψ_{11}	φ_{11}	30
							21	y_{21}	ψ_{21}	φ_{21}	
							31	y_{31}	ψ_{31}	φ_{31}	
				2	$y_{т2}$	$\psi_{т2}$	12	y_{12}	ψ_{12}	φ_{12}	
							22	y_{22}	ψ_{22}	φ_{22}	
							32	y_{32}	ψ_{32}	φ_{32}	

Table 3.2

Generalized Coordinates and Quantity of Motion Differential Equations for Computational Patterns for the Rolling Stocks with an Intermediate Beam in Trucks

Number of Pattern	Rolling Stock Type	Body		Intermediate Beam		Truck Frame			Wheel Pairs				Equation Quantity
		y_c	ψ_c	$y_Б$	$\psi_Б$	#	$y_т$	$\psi_т$	#	y	ψ	φ	
11	VL60 Electric Locomotive, TEP60 Diesel Locomotive	y_c	ψ_c			1	$y_{т1}$	$\psi_{т1}$	11	y_{11}	ψ_{11}	φ_{11}	30
									21	y_{21}	ψ_{21}	φ_{21}	
									31	y_{31}	ψ_{31}	φ_{31}	
						2	$y_{т2}$	$\psi_{т2}$	12	y_{12}	ψ_{12}	φ_{12}	
									22	y_{22}	ψ_{22}	φ_{22}	
									32	y_{32}	ψ_{32}	φ_{32}	
12	VL80, VL10 Electric Locomotives	y_c	ψ_c			1	$y_{т1}$	$\psi_{т1}$	11	y_{11}	ψ_{11}	φ_{11}	18
									21	y_{21}	ψ_{21}	φ_{21}	
						2	$y_{т2}$	$\psi_{т2}$	12	y_{12}	ψ_{12}	φ_{12}	
									22	y_{22}	ψ_{22}	φ_{22}	

Number of Pattern	Rolling Stock Type	Body		Intermediate Beam		Truck Frame			Wheel Pairs				Equation Quantity
		y_c	ψ_c	$y_Б$	$\psi_Б$	#	$y_т$	$\psi_т$	#	y	ψ	φ	
13	VL15, VL85 Electric Locomotive	y_c	ψ_c			1	$y_{т1}$	$\psi_{т1}$	11	y_{11}	ψ_{11}	φ_{11}	26
									12	y_{21}	ψ_{21}	φ_{21}	
						2	$y_{т2}$	$\psi_{т2}$	21	y_{12}	ψ_{12}	φ_{12}	
									22	y_{22}	ψ_{22}	φ_{22}	
						3	$y_{т3}$	$\psi_{т3}$	31	y_{13}	ψ_{13}	φ_{13}	
									32	y_{23}	ψ_{23}	φ_{23}	
14	TE136 Diesel Locomotive					1			11	y_{11}	ψ_{11}	φ_{11}	24
									21	y_{21}	ψ_{21}	φ_{21}	
						2			12	y_{12}	ψ_{12}	φ_{12}	
									22	y_{22}	ψ_{22}	φ_{22}	
						3			13	y_{13}	ψ_{13}	φ_{13}	
									23	y_{23}	ψ_{23}	φ_{23}	
						4			14	y_{14}	ψ_{14}	φ_{14}	
									24	y_{24}	ψ_{24}	φ_{24}	
15	TEM7 Diesel Locomotive	y_c	ψ_c	$y_{Б1}$	$\psi_{Б1}$	1	$y_{т1}$	$\psi_{т1}$	11	y_{11}	ψ_{11}	φ_{11}	36
									21	y_{21}	ψ_{21}	φ_{21}	
						2	$y_{т2}$	$\psi_{т2}$	12	y_{12}	ψ_{12}	φ_{12}	
									22	y_{22}	ψ_{22}	φ_{22}	
				$y_{Б2}$	$\psi_{Б2}$	3	$y_{т3}$	$\psi_{т3}$	13	y_{13}	ψ_{13}	φ_{13}	
									23	y_{23}	ψ_{23}	φ_{23}	
						4	$y_{т4}$	$\psi_{т4}$	14	y_{14}	ψ_{14}	φ_{14}	
									24	y_{24}	ψ_{24}	φ_{24}	
16	ER200, Passen ger Wagons	y_c	ψ_c			1	$y_{т1}$	$\psi_{т1}$	11	y_{11}	ψ_{11}	φ_{11}	18
									21	y_{21}	ψ_{21}	φ_{21}	
						2	$y_{т2}$	$\psi_{т2}$	12	y_{12}	ψ_{12}	φ_{12}	
									22	y_{22}	ψ_{22}	φ_{22}	

Table 3.3

Generalized Coordinates and Quantity of Motion Differential Equations for Computational Patterns for the Rolling Stocks with Longitudinal and Lateral Beams in Trucks

Number of Pattern	Wagon Type	Body		Longitudinal Bolster Beams		Lateral Bolster Beams		Truck Sides			Wheel Pairs			Equation Quantity
		y_c	ψ_c	$y_П$	$\psi_П$	$y_Ш$	$\psi_Ш$	$x_Б$	$y_Б$	$\psi_Б$	y	ψ	φ	
17	4-Axle Wagons on Trucks 18-100	y_c	ψ_c			$y_{Ш1}$	$\psi_{Ш1}$	$x_{Б11}$	$y_{Б11}$	$\psi_{Б11}$	y_{11}	ψ_{11}	φ_{11}	30
								$x_{Б21}$	$y_{Б21}$	$\psi_{Б21}$	y_{21}	ψ_{21}	φ_{21}	
						$y_{Ш2}$	$\psi_{Ш2}$	$x_{Б12}$	$y_{Б12}$	$\psi_{Б12}$	y_{12}	ψ_{12}	φ_{12}	
								$x_{Б22}$	$y_{Б22}$	$\psi_{Б22}$	y_{22}	ψ_{22}	φ_{22}	

Number of Pattern	Wagon Type	Body		Longitudinal Bolster Beams		Lateral Bolster Beams		Truck Sides			Wheel Pairs			Equation Quantity
		y_c	ψ_c	$y_П$	$\psi_П$	$y_Ш$	$\psi_Ш$	$x_Б$	$y_Б$	$\psi_Б$	y	ψ	φ	
18	8-Axle Wagons on Trucks 18-101	y_c	ψ_c	$y_{П1}$	$\psi_{П1}$	$y_{Ш1}$	$\psi_{Ш1}$	$x_{Б11}$	$y_{Б11}$	$\psi_{Б11}$	y_{11}	ψ_{11}	φ_{11}	62
								$x_{Б21}$	$y_{Б12}$	$\psi_{Б21}$	y_{21}	ψ_{21}	φ_{21}	
						$y_{Ш2}$	$\psi_{Ш2}$	$x_{Б12}$	$y_{Б12}$	$\psi_{Б12}$	y_{12}	ψ_{12}	φ_{12}	
								$x_{Б22}$	$y_{Б22}$	$\psi_{Б22}$	y_{22}	ψ_{22}	φ_{22}	
				$y_{П2}$	$\psi_{П2}$	$y_{Ш3}$	$\psi_{Ш3}$	$x_{Б13}$	$y_{Б13}$	$\psi_{Б13}$	y_{13}	ψ_{13}	φ_{13}	
								$x_{Б23}$	$y_{Б23}$	$\psi_{Б23}$	y_{23}	ψ_{23}	φ_{23}	
						$y_{Ш4}$	$\psi_{Ш4}$	$x_{Б14}$	$y_{Б14}$	$\psi_{Б14}$	y_{14}	ψ_{14}	φ_{14}	
								$x_{Б24}$	$y_{Б24}$	$\psi_{Б24}$	y_{24}	ψ_{24}	φ_{24}	
19	6-Axle Wagons on Trucks 18-102	y_c	ψ_c			$y_{Ш1}$	$\psi_{Ш1}$	$x_{Б11}$	$y_{Б11}$	$\psi_{Б11}$	y_{11}	ψ_{11}	φ_{11}	36
								$x_{Б21}$	$y_{Б21}$	$\psi_{Б21}$	y_{21}	ψ_{21}	φ_{21}	
											y_{31}	ψ_{31}	φ_{31}	
						$y_{Ш2}$	$\psi_{Ш2}$	$x_{Б12}$	$y_{Б12}$	$\psi_{Б12}$	y_{12}	ψ_{12}	φ_{12}	
								x_{22}	y_{22}	$\psi_{Б22}$	y_{22}	ψ_{22}	φ_{22}	
											y_{32}	ψ_{32}	φ_{32}	

3.2. Differential Equations of the Carriage Movement

The equation systems for each rolling stock type are to contain several subsystems of the same type:

- a wheel pair (with axle box cases);
- a truck frame (with brakes equipment, axle box and body shock absorber suspension);
- body.

3.2.1. Equations of the Wheel Pairs Movement

The generalized coordinates are as follows: y_{jk}, ψ_{jk}, φ_{jk}. We illustrate the generalized forces in Figure 3.1 and the following is to be taken into account:

$S_{x\,ijk}$, $S_{y\,ijk}$ – the longitudinal and the lateral reactions at wheel-rail contacts;

$F_{bx\,ijk}$, $F_{by\,jk}$ – the longitudinal and the lateral reactions in the axle box units.

Thus, the motion equation on the generalized coordinates of y_{jk}, ψ_{jk}, φ_{jk} is as written:

$$\ddot{y}_{jk} = \frac{1}{m}\left(\sum_{i=1}^{2} S_{y\,ijk} - F_{by\,jk}\right);$$

$$\ddot{\psi}_{jk} = \frac{1}{I_z}\left[\left(S^*_{x1jk} - S^*_{x2jk}\right)A - \left(F_{bx1jk} - F_{bx2jk}\right)B\right]; \qquad (3.1)$$

$$\ddot{\varphi}_{jk} = -\frac{1}{I_y}\sum_{i=1}^{2}\left(S_{xijk}R_{ijk}\right);$$

$$F_{bxijk} = F_{bx}\left(\Delta_{bxijk}\right);\ F_{byijk} = F_{by}\left(\Delta_{byijk}\right),$$

where S_{xijk}, S_{yijk} – the longitudinal and the lateral components of the adhesion forces at wheel-rail contacts in the moving coordinate system of the railway track;

S^*_{xijk}, S^*_{yijk} – the longitudinal and the lateral components of the adhesion forces at wheel-rail contacts in the moving coordinate system of the wheel pair;

$F_{bx}\left(\Delta_{bxijk}\right)$, $F_{by}\left(\Delta_{byijk}\right)$ – the features of the axle box connection in the longitudinal and the lateral directions;

Δ_{bxijk}, Δ_{byijk} – the longitudinal and the lateral displacements in the axle box units.

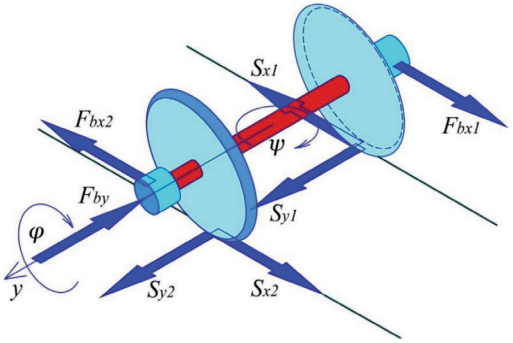

Figure 3.3. Diagram of Forces and Torques: Influence on a Wheel Pair Shown in Generalized Coordinates of y_{jk}, ψ_{jk}, φ_{jk}

The values of Δ_{bxijk} i Δ_{byijk} depend on generalized coordinates of y_{jk}, ψ_{jk}, y_{mk}, ψ_{mk} and are conditioned by the design features of a certain rolling stock, then we obtain:

$$\Delta_{b1ijk} = B\left(\psi_{mk} - \psi_c\right);$$

$$\Delta_{b2ijk} = B\left(\psi_c - \psi_{mk}\right); \qquad (3.2)$$

$$\Delta_{byijk} = y_{mk} - y_{jk}.$$

When simulating the rolling stocks with wheel pairs that rotate independently, coordinate φ_{jk} is substituted with coordinates φ_{ijk} (i=1,2).

3.2.2. Equations of the Truck Frame Movement

In this case we choose the generalized coordinates of y_{mk}, ψ_{mk}. The generalized forces are shown in Figure 3.4 and the following is to be taken into account:

$F_{bx\,ijk}$, $F_{by\,jk}$ – the axle box reactions;

F_{mk}, M_{mk} – the reacting force and the reaction torque at the connections of the trucks with the body (the pivot node and supporting-and-counter device).

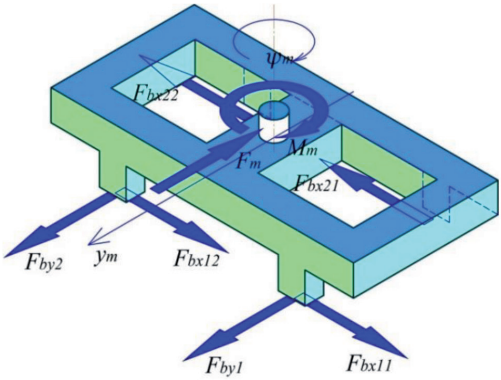

Figure 3.4. Diagram of Forces and Torques. Influence on Two-Axle Truck Frame in Generalized Coordinates of y_{mk}, ψ_{mk}

The motion equation for N-axle trucks is as follows:

$$\ddot{y}_k = \frac{1}{m_m}\left(\sum_{j=1}^{N} F_{by\,jk} - F_{mk}\right)$$

$$\ddot{\psi}_k = \frac{1}{I_{mz}}\left[B\sum_{j=1}^{N}\left(F_{bx1\,jk} - F_{bx2\,jk}\right) + \sum_{j=1}^{N}\left(F_{by\,jk} - M_{mk}\right)\right]; \qquad (3.3)$$

$$F_{mk} = F_m\left(\Delta_{my\,k}\right);\ M_{mk} = M_m\left(\Delta_{m\psi\,k}\right),$$

where $F_m\left(\Delta_{my\,k}\right)$, $M_m\left(\Delta_{m\psi\,k}\right)$ – the characteristics of the counter device in the body-truck contact;

$\Delta_{my\,k}$, $\Delta_{m\psi\,k}$ –relative longitudinal and angular displacement of the body and the truck as the dependence on the generalized coordinates y_{mk}, ψ_{mk}, y_c, ψ_c:

$$\Delta_{my\,k} = y_{mk} - y_c;$$
$$\Delta_{m\psi\,k} = \psi_{mk} - \psi_c. \qquad (3.4)$$

These dependencies in the forms of the equations complete the differential equation system.

3.2.3. Equations of the Body Movement

The generalized coordinates for this type of equations is y_c, ψ_c, while the generalized forces are F_{mk}, M_{mk}.

The motion equation for the body of L-truck train is expressed as follows:

$$\ddot{y}_c = \frac{1}{m_c}\sum_{k=1}^{L} F_{mk}\ ;\ \ddot{\psi}_c = \frac{1}{J_c}\sum_{k=1}^{L}\left(F_{mk}D_k + M_{mk}\right). \tag{3.5}$$

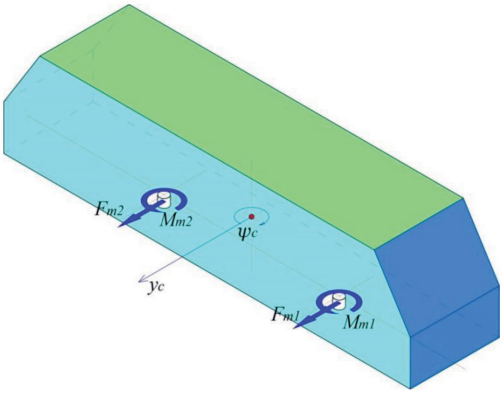

Figure 3.5. Diagram of Forces and Torques: Influence on Two-Axle Truck Frame in Generalized Coordinates of y_c, ψ_c

3.3. Mathematical Models of Locomotives

When choosing the rolling stocks as the objects of the theoretical study, the authors pursued the targets as described below.

Firstly, we needed to outline the features of kinematic movement resistance for the most widely applied train types in the same way as it was performed for the main movement resistance, for instance, in *Rules of Traction Calculations for Train Operation* [29].

Secondly, based on the obtained features to conclude on the advantages of some truck arrangement in terms of the kinematic movement resistance.

Thirdly, to determine the most rational schemes of the rolling stock controlled guidance on tracks.

Due to this, the attempt to cover the most of the rolling stock types, including the contemporary and the old designs that have not been studied in the perspective of the kinematic resistance to the movement.

Since the time of the railway transport appeared, the rolling stock mechanical part has not changed its principles but has evolved a lot. The especially vast variety can be found in truck arrangements of the hauling units. The latter are the locomotive truck arrangement, which enhancement is associated with the difficulties of combining the contradictory functions of wheel pairs: support, guidance and movement.

The transition from a truck arrangement frame design to the design with the truck has added to the problems be solved. One complex solution to be found has been substituted with some minor ones.

Among the multitudinous studies done on locomotive rolling stock dynamics all over the world, the most important are those that aim at decreasing the movement resistance and wheel-rail wear, especially at track curved sections.

There are known some directions how to solve the outlined problems:

- optimization of wheel rolling surface profiles;
- optimization of wheel-rail material mechanical properties;
- lubricating the wheel flange and rail contact;
- radial positioning of wheel pairs in curves;
- using the wheel pairs with independently rolling wheels;
- control over the body inclination in curves, etc.

3.3.1. Mathematical Models of Frame Locomotives

The train of the frame design is the train which possesses the axes installed in one rigid body frame. However, very often such rolling stocks contain turable wheel pairs or trucks. They are able to incline, i.e. one or two axle wheels that either guide or support. Such design is specific to steam locomotives, first electric and diesel locomotives. There is a number of axle configuration variants of locomotives, including ones with steering axles.

The movement simulation of the frame design locomotive has been performed based on the example of FD steam locomotives with 1-50-1 axle configuration and EM five axle steam locomotive.

The Motion Equation FD Steam Locomotive is composed of interconnected body subsystems, leading trucks, main and leading wheel pairs.

The motion equation for the body is written as below:

$$\ddot{y}_c = \frac{1}{m_c}\left(\sum_{j=1}^{5} F_{by\,j} + \sum_{k=1}^{2} F_{mk}\right), \tag{3.6}$$

$$\ddot{\psi}_c = \frac{1}{J_c}\left[\sum_{k=1}^{2}\left(F_{mk}D_k + M_{mk}\right) + \sum_{j=1}^{5} F_{by\,j}C_j + A\sum_{j=1}^{5}\left(F_{bx\,1j} - F_{bx2\,j}\right)\right].$$

The equation of hunting and lateral deviation of leading trucks (k=1, 2) is expressed as here:

$$\ddot{y}_{mk} = \frac{1}{m_m}\left(F_{by\,k} - F_{mk}\right), \tag{3.7}$$

$$\ddot{\psi}_{mk} = \frac{1}{J_m^*}\left[F_{by\,k}C_k + \left(F_{bx1k} - F_{bx2k}\right)B^* - M_{mk}\right].$$

The main wheel pair motion equation (j=1,...,5) is as follows:

$$\ddot{y}_j = \frac{1}{m_j}\left[\sum_{i=1}^{2} S_{y\,ij} - F_{by\,j}\right],$$

$$\ddot{\psi}_j = \frac{1}{J_{zj}}\left[\left(S^*_{x\,1j} - S^*_{x2j}\right)A - \left(F_{x\,1j} - F_{x\,2j}\right)B\right], \tag{3.8}$$

$$\ddot{\varphi}_j = \frac{1}{J_{yj}}\sum_{i=1}^{2}\left(S_{x\,ij}R_{ij}\right).$$

The equation for the leading wheel pair (k=1, 2) is as given:

$$\ddot{y}_k = \frac{1}{m}\left(\sum_{i=1}^{2} F_{y\,ik} - F_{y\,mk}\right),$$

$$\ddot{\psi}_k = \frac{1}{J_z}\left[\left(S^*_{x\,1k} - S^*_{x2k}\right)A - \left(F_{bx1k} - F_{bx2k}\right)B\right], \tag{3.9}$$

$$\ddot{\varphi}_k = -\frac{1}{J_y}\sum_{i=1}^{2}\left(S_{x\,ik}R_{ik}\right).$$

The design features of the FD steam locomotive influence dependencies of the relative displacements in the nodes. The external characteristics are introduced for them and are described by the following equations of the links.

The deformation in the axle box connections of the main wheel pairs with the body:

$$\begin{aligned}
\Delta_{bx1j} &= B\left(\psi_c - \psi_{1j}\right);\\
\Delta_{bx2j} &= B\left(\psi_{2j} - \psi_c\right);\\
\Delta_{by} &= y_j - y_c - C_j\psi_c;
\end{aligned} \tag{3.10}$$

The displacement in the axle box connections of the leading wheel pairs with truck-rods is absent.

The relative displacement in the counter devices of the leading trucks can be expressed as below:

$$\begin{aligned}
\Delta_{myk} &= y_k - C_k\psi_k - y_c - D_k\psi_c;\\
\Delta_{m\psi k} &= \psi_k - \psi_c.
\end{aligned} \tag{3.11}$$

The motion equation of EM steam locomotive is much simpler due to the absence of the leading trucks.

The wheel pair motion equation (j=1,...,5) can be written as follows:

$$\ddot{y}_c = \frac{1}{m_c}\sum_{j=1}^{5} F_{by\,j}\ , \tag{3.12}$$

$$\ddot{\psi}_c = \frac{1}{J_c}\sum_{j=1}^{5}\left[F_{by\,j}C_j + A\left(F_{bx\,1j} - F_{bx\,2j}\right)\right].$$

The motion equation for the wheel pair (j=1,...,5) is as shown below:

$$\ddot{x}_j = \frac{1}{m_j}\sum_{i=1}^{2}\left(S_{x\,ij} - F_{bx\,j}\right),$$

$$\ddot{y}_j = \frac{1}{m_j}\left[\sum_{i=1}^{2}\left(S_{y\,ij} + H_{ij}\right) - F_{by\,j}\right], \tag{3.13}$$

$$\ddot{\psi}_j = \frac{1}{J_{z\,j}}\left[\left(S^*_{x\,1j} - S^*_{x\,2j}\right)A - \left(F_{bx\,1j} - F_{bx\,2j}\right)B\right];$$

$$\ddot{\varphi}_j = -\frac{1}{J_{y\,j}}\sum_{i=1}^{2}\left(S_{x\,ij}R_{ij}\right).$$

The equations for the links describe the dependencies of the relative displacements in the axle box connections of the wheel pairs and the body for EM steam locomotive. They express the relation with the independent variables as follows:

$$\begin{aligned}\Delta_{bx1j} &= B\left(\psi_j - \psi_c\right);\\ \Delta_{bx2j} &= B\left(\psi_c - \psi_j\right);\\ \Delta_{by\,j} &= y_j - y_c - C_j\psi_c\ .\end{aligned} \tag{3.14}$$

3.3.2. Locomotives with Linked Carriages

The first electric locomotives of the truck design were produced with joint trucks. It was necessary to transmit the traction force through them, since the coupling devices were installed on trucks at that time. *General Elektric* initially applied this principle with their electric locomotives.

Two joint 3-axle trucks were the characteristic feature for certain trains. This design has been used further in electric locomotives of VL19, VL22m and VL8.

There is a number of rolling stock designs based on truck joining, they are with force transmission through the body and partially joined spring elements, as the instance can serve electric locomotives of ChS-2, Re 2/2 or Hitachi.

The motion equations for electric locomotives with joint trucks of VL19, VL22m and VL23 types. If we assume that there is no clearance in truck connection ball joints, then the structural configuration of this type of rolling stocks may be described by the following relations:

$$y_{m1} = y - D\psi_{m1};\ y_{m2} = y + D\psi_{m2};$$
$$y_c = y - \frac{D}{2}\left(\psi_{m1} - \psi_{m2}\right); \tag{3.15}$$
$$\psi_c = \frac{\psi_{m1} - \psi_{m2}}{2},$$

where y_{m1}, y_{m2}, ψ_{m1}, ψ_{m2} – the transversal displacements and the rotation angles in relation to the trucks;

y – the transversal displacements of the truck connection ball joint center;

y_c, ψ_c – the transversal displacement and the rotation angle in respect to the body.

The oscillations of the train transversal dissipation and hunting take into account equations (3.15) and can be described by three equations in respect to the variables of y, ψ_{m1}, ψ_{m2} as here:

$$A \times \ddot{\vec{y}} = \vec{F}; \tag{3.16}$$

$$A = \begin{bmatrix} 2a & -a & a \\ -a & b & 0 \\ a & 0 & b \end{bmatrix};\ \ddot{\vec{y}} = \begin{bmatrix} \ddot{y} \\ \ddot{\psi}_{m1} \\ \ddot{\psi}_2 \end{bmatrix};\ \vec{\mathrm{F}} = \begin{bmatrix} F_y \\ F_1 \\ F_2 \end{bmatrix}; \tag{3.17}$$

$$a = \left(\frac{m_c}{2} + m_m\right)D;\ b = m_c\frac{D^2}{4} + m_m D^2 + \frac{J_c}{2} + J_m; \tag{3.18}$$

$$F_y = \sum_{i=1}^{2}\sum_{j=1,3}\sum_{k=1}^{2}\left(S_{y\,ijk} + H_{ijk}\right) + \sum_{k=1}^{2} F_{by2k}; \tag{3.19}$$

$$F_{m(k=1,2)} = \sum_{j=1,3}\left(S_{ijk} + H_{ijk}\right)C_{jk} + F_{by2k}C_{2k} + \sum_{i=1}^{2}\left(S_{x\,1jk} - S_{x2\,jk}\right)A - M_{ck},$$

where M_{ck} – the torque in the supporting-and-counter devices that depend on the angles of the relative turn of the body and the truck ($\Delta\psi_k$). Then we obtain:

$$\Delta_{\psi 1} = \frac{\psi_{m1} - \psi_{m2}}{2};\ \Delta_{\psi 2} = \frac{\psi_{m2} - \psi_{m1}}{2}. \tag{3.20}$$

The equations of the lateral dissipation of the middle wheel pairs on the trucks are written as below:

$$\ddot{y}_{2k} = \frac{1}{m}\left(S_{y\,i2k} + H_{i2k}\right). \tag{3.21}$$

The equations of wheel pair angular velocity oscillations:

$$\ddot{\varphi}_{jk} = -\frac{1}{J_y}\sum_{i=1}^{2}\left(S_{x\,ijk} R_{ijk}\right). \tag{3.22}$$

The motion equation for eight-axle locomotive of VL8 type. Four 2-axle trucks are joint with four ball joints on VL8 electric locomotives.

Considering the design features of VL8 series electric locomotives, it can be assumed that there are no transversal clearances in the axle box nodes, whereas the axle box longitudinal position in relation to the truck frame depended on the directions of the axle box reactions ($F_{bx\,ijk}$) and the clearances in the truck frame horn plates (Δ_{bxijk}).

The clearance-free ball joints of the trucks are described by the following constraint equations:

$$y_{m1} = y - D\left(2\psi_{m2} - \psi_{m1}\right);\ y_{m2} = y - D\psi_{m2};$$

$$y_{m3} = y + D\psi_{m3};\ y_{m4} = y + D\left(2\psi_{m3} + \psi_{m4}\right);$$

$$y_{c1} = y - \frac{D}{2}\left(\psi_{m1} + 3\psi_{m2}\right); \tag{3.23}$$

$$y_{c1} = y - \frac{D}{2}\left(\psi_{m1} + 3\psi_{m2}\right);$$

$$y_{c2} = y + \frac{D}{2}\left(3\psi_{m3} + \psi_{m4}\right);$$

$$\psi_{c1} = \frac{\psi_{m1} - \psi_{m2}}{2};\ \psi_{c2} = \frac{\psi_{m3} + \psi_{m4}}{2}.$$

In (3.23), the following should be understood as given:

$y_{c1}, y_{c2}, \psi_{c1}, \psi_{c2}$ – the displacements of the bodies in the first and the second sections;

y – the lateral displacement of the second (middle) inter-truck ball joint;

$y_{m1}, y_{m2}, y_{m3}, y_{m4}, \psi_{m1}, \psi_{m2}, \psi_{m3}, \psi_{m4}$ – the lateral and angular displacements of the trucks, respectively

The oscillation equations of the locomotive lateral dissipation and hunting:

$$\begin{bmatrix} a_{11} & a_{12} & a_{13} & a_{14} & a_{15} \\ a_{21} & a_{22} & a_{23} & a_{24} & a_{25} \\ a_{31} & a_{32} & a_{33} & a_{34} & a_{35} \\ a_{41} & a_{42} & a_{43} & a_{44} & a_{45} \\ a_{51} & a_{52} & a_{53} & a_{54} & a_{55} \end{bmatrix} \times \begin{bmatrix} y \\ \psi_{m1} \\ \psi_{m2} \\ \psi_{m3} \\ \psi_{m4} \end{bmatrix} = \begin{bmatrix} F_y \\ M_{m1} \\ M_{m2} \\ M_{m3} \\ M_{m4} \end{bmatrix}, \qquad (3.24)$$

where

$a_{11} = 4m_1$	$a_{12} = -Dm_1$	$a_{13} = -3Dm_1$	$a_{14} = 3Dm_1$	$a_{15} = Dm_1$
$a_{21} = -Dm_1$	$a_{22} = D^2m_2 + J_m$	$a_{23} = D^2m_3$	$a_{24} = 0$	$a_{25} = 0$
$a_{31} = -3Dm_1$	$a_{32} = D^2m_3$	$a_{33} = D^2m_4 + J_m$	$a_{34} = 0$	$a_{35} = 0$
$a_{41} = 3Dm_1$	$a_{42} = 0$	$a_{43} = 0$	$a_{44} = D^2m_4 + J_m$	$a_{45} = D^2m_3$
$a_{51} = Dm_1$	$a_{52} = 0$	$a_{53} = 0$	$a_{54} = D^2m_3$	$a_{55} = D^2m_2 + J_m$

$$m_1 = m_m + \frac{m_c}{2};\ m_2 = m_m + \frac{m_c}{4};\ m_3 = 2m_m + \frac{3}{4}m_c; \qquad (3.25)$$

$$m_4 = 5m_m + \frac{9}{4}m_c;\ F_y = \sum_{j=1}^{2}\sum_{k=1}^{4} F_{by\,jk},$$

$$M_{mk} = \sum_{i=1}^{2}\left(S_{y\,i2k} - S_{y\,i1k} - H_{i1k} + H_{i2k}\right)C_{jk} + \sum_{j=1}^{2}\left(S_{x\,1jk} - S_{x\,2jk}\right)A.$$

The equation of wheel pair rotation and hunting is as follows:

$$\ddot{\varphi}_{jk} = -\frac{1}{J_y}\sum_{i=1}^{2}\left(S_{x\,ijk}R_{ijk}\right), \qquad (3.26)$$

$$\ddot{\psi}_{jk(j=1\ldots2;k=1\ldots4)} = \frac{1}{J_z}\left[\left(S_{x\,1jk} - S_{x\,2jk}\right)A - \left(F_{bx\,1jk} - F_{bx\,2jk}\right)B\right].$$

The motion equation for a six-axle two-truck locomotive with spring inter-truck connection of ChS2 type. Schematically, the locomotive underframes of Skoda ChS2 and ChS2T passenger electric locomotives are different from the other locomotives as the former have the spring transversal inter-truck connection and spring transversal connection of the body with the truck. The elastic mass distribution in the transversal and the angular directions allows obtaining the differential equation simple system for the rolling stock movement.

The equation for the body horizontal oscillation is as given:

$$\ddot{y}_c = \frac{1}{m_c}\sum_{k=1}^{2}F_{ck};\ \ddot{\psi}_c = \frac{1}{J_\kappa}\sum_{k=1}^{2}M_{c\,k}. \qquad (3.27)$$

The equation for the truck horizontal oscillation is as follows:

$$\ddot{y}_{mk} = \frac{1}{m_m}\left(\sum_{j=1}^{2} F_{by\,jk} - F_{pk} - F_{ck}\right), \tag{3.28}$$

$$\ddot{\psi}_{mk} = \frac{1}{J_m}\left\{\sum_{j=1}^{3}\left[F_{by\,jk}C_{jk} + \left(F_{bx\,1jk} - F_{bx\,2jk}\right)B\right] - F_{p\,k}D - M_{ck}\right\}. \tag{3.29}$$

where F_{pk} – the reactions in the spring inter-truck connection, they depend on the deformation of the counter spring, then we obtain:

$$\Delta_p = y_{m1} - y_{m2} + D\left(\psi_{m1} + \psi_{m2}\right), \tag{3.30}$$

F_{ck}, M_{ck} – the reactions within the truck supporting-and-counter devices that depend on the dedicated transversal and angular displacements of the trucks and the body, then as written:

$$\Delta_{yk} = y_{mk} - y_c + \psi_c D_k\,;\ \Delta_{\psi k} = \psi_c - \psi_{mk}\,. \tag{3.31}$$

The oscillation equations of lateral dissipation, hunting and wheel pairs rolling are as follows:

$$\ddot{y}_{jk} = \frac{1}{}\left(\sum_{i=1}^{2} S_{y\,ijk} - F_{by\,jk}\right),$$

$$\psi_{jk} = \frac{1}{J}\left[\left(S_{x\,1jk} - S_{x\,2jk}\right)A - \left(F_{bx\,1jk} - F_{bx\,2jk}\right)B\right], \tag{3.32}$$

$$\ddot{\varphi}_{jk} = -\frac{1}{J_y}\sum_{i=1}^{2}\left(S_{x\,ijk}R_{ijk}\right).$$

The motion equation for a six-axle three-truck rolling stock with joined end trucks (Re 2/2). The end truck joining through a lever-torsional system of the same type as in Re 2/2 electric locomotive allows the middle truck to deflect in the lateral direction with respect to the body independently from the other trucks. It significantly enhances the features of train guiding in curved track sections. The equations to relate the displacements of the end trucks and the body are the following:

$$y_c = \frac{y_{m1} + y_{m3}}{2}\,;\ \psi_c = \frac{y_{m3} - y_{m1}}{4D}. \tag{3.33}$$

The equations of the truck lateral oscillations are written as given:

$$\ddot{y}_{m1} = \frac{F_{m1}a_1 - F_{m3}a_2}{a_1^2 - a_2^2}\,;$$

$$\ddot{y}_{m2} = \frac{1}{m_m}\left[\sum_{i=1}^{2}\sum_{j=1}^{2}\left(S_{y\,ij2} + H_{\,ij2}\right) - F_c\right]; \tag{3.34}$$

$$\ddot{y}_{m3} = \frac{F_{m1}a_2 - F_{m3}a_1}{a_2^2 - a_1^2},$$

where

$$a_1 = \frac{m_c}{2} + \frac{J_c}{16D^2} + m_m;$$

$$F_{m1} = \sum_{i=1}^{2}\sum_{j=1}^{2}\left(S_{yij1} + H_{\,ij1}\right) - F_p; \tag{3.35}$$

$$a_2 = -\frac{J_c}{16D^2};\ F_{m3} = \sum_{i=1}^{2}\sum_{j=1}^{2}\left(S_{y\,ij3} + H_{ij3}\right) + F_p.$$

The wheel pair rotation equations to describe angular velocity oscillations in the coordinates of φ_{jk}:

$$\ddot{\varphi}_{jk} = \frac{1}{J_y}\left[M_O - \sum_{i=1}^{2}\left(S_{xijk}R_{ijk}\right)\right]. \tag{3.36}$$

3.3.3. Six-Axle Carriages with the Axial Formula of 3o-3o

Among the locomotives produced all over the world, 3o – 3o axle configuration is the most numerous. Independently from the peculiarities of the rolling stock design version, their mathematical models differ between the deferent types of trains. The simplest truck arrangement is with the trucks of TEZ type (i.e. diesel locomotives of TE10, 2TE10L, TE40, M62, etc).

The truck motion equations that take into account the presence of the longitudinal clearance in the axle box nodes are as given:

$$\ddot{y}_{m1} = m_v\left[F_{m1}\left(\frac{m_c}{4} + \frac{J_c}{4D^2} + m_m\right) - F_{m2}\left(\frac{m_c}{4} - \frac{J_c}{4D^2}\right)\right];$$

$$\ddot{y}_{m2} = m_v\left[F_{m1}\left(\frac{m_c}{4} - \frac{J_c}{4D^2}\right) - F_{m2}\left(\frac{m_c}{4} + \frac{J_c}{4D^2} + m_m\right)\right]; \tag{3.37}$$

$$\ddot{\psi}_{mk} = \frac{1}{J_m}\left[B\sum_{j=1}^{3}\left(F_{bx1\,jk} - F_{bx2\,jk}\right) + \sum_{j=1,3}C_{jk}\sum_{i=1}^{2}\left(S_{yijk} + H_{ijk}\right) + F_{by2k}C_{2k} - M_{ck}\right];$$

where

$$m_v = \frac{4D^2}{4D^2 m_m^2 + m_c J_c + 2D^2 m_m m_c + 2m_m J_c}; \tag{3.38}$$

$$F_{mk} = \sum_{i=1}^{2} \left(S_{y\ ijk} + H_{\ ijk} \right) + F_{by\ 2k}\ .$$

The equations of the lateral dissipation for middle wheel pairs of the trucks to possess the clearances with respect to the axle boxes:

$$y_{2k} = \frac{1}{m} \left(\sum_{i=1}^{2} S_{y\ i2k} - F_{by\ 2k} \right). \tag{3.39}$$

The equations of wheel pair hunting and rotation are as below:

$$\ddot{\psi}_{jk} = \frac{1}{J_z} \left[\left(S^*_{x1\,jk} - S^*_{x2\,jk} \right) A - \left(F_{bx1\,jk} - F_{bx\ 2\,jk} \right) B \right], \tag{3.40}$$

$$\ddot{\varphi}_{jk} = -\frac{1}{J_y} \sum_{i=1}^{2} \left(S_{xijk} R_{ijk} \right). \tag{3.41}$$

Six-axle sections with modernized trucks. The trucks within diesel locomotives of TE10V, TE10M, 2TE116, TE109, TE120, V300, TE114 and others have evolved a lot compared with TEZ trucks though the same axial configuration remained in them. Their main features are horn plate-free axle-box connection of Alstrom type, but with spring links in the transversal and the longitudinal directions. Moreover, such diesel locomotives are equipped with shock absorber suspension at the body-truck connection, which is spring in the transversal direction.

The trucks of 2TE121 diesel locomotives have horn plates and are equipped with balanced spring suspension, including coil springs, spring balance, and supporting-and-framing traction drive. In the secondary suspension, they apply four supports with rubber-metal elements, the same idea as in 2TE116 diesel locomotive.

Inspired by the designer ideas of the French electric locomotives of F, FP, SS7100-series, trucks for VL60 electric locomotive, TEP60 diesel locomotives and TEP75 diesel locomotives were created. VL60 electric locomotive has the transversal spring connection between the body and the truck through the rubber-metal pendulum supports.

In case of the transversal masses distribution of the body and the trucks, as well as in the longitudinal spring and the transversal spring connection of the wheel pairs with the truck frame, which is specific to many locomotives, for

instance, 2TE10V, 2TE10M, 2TE116, TE109, TE130, V300, TEP60, TEP70, 2TE121 and others, the oscillation system configuration may be described by the following equations:

The body oscillation equations:

$$\ddot{y}_c = \frac{1}{m_c}\left(F_{yc1} + F_{yc2}\right);$$

$$\ddot{\psi}_c = \frac{1}{J_c}\sum_{k=1}^{2}\left(2D_k F_{yc\,k} + M_{c\,k}\right);$$

$$\ddot{y}_{mk(k=1...2)} = \frac{1}{m_m}\sum_{j=1}^{3}\left(F_{by\,jk} - F_{yc\,k}\right);$$

$$\ddot{\psi}_{m\,k(k=1...2)} = \frac{1}{J_m}\sum_{j=1}^{3}\left[B\left(F_{bx\,1jk} - F_{bx\,2jk}\right) + C_{jk}F_{by\,jk} - M_{c\,k}\right]; \quad (3.42)$$

$$\ddot{x}_{jk(j=1...3,k=1...2)} = \frac{1}{m}\sum_{i=1}^{2}\left(S_{x\,ijk} - F_{bx\,ijk}\right);$$

$$\ddot{y}_{jk(j=1...3,k=1...2)} = \frac{1}{m}\sum_{i=1}^{2}\left(S_{y\,ijk} + H_{ijk} - F_{by\,jk}\right);$$

$$\ddot{\psi}_{jk(j=1...3,k=1...2)} = \frac{1}{J_z}\left[\left(S^*_{x\,1jk} - S^*_{x\,2jk}\right)A - \left(F_{bx\,1jk} - F_{bx\,2jk}\right)B\right];$$

$$\ddot{\varphi}_{jk(j=1...3,k=1...2)} = -\frac{1}{J_y}\sum_{i=1}^{2}\left(F_{зч\,ijk\,x}R_{ijk}\right).$$

The reactions in the truck spring-dissipative links:

$$F_{bx\,ijk} = \varkappa_{bx}\Delta_{bx\,ijk} + \beta_{bx}\dot{\Delta}_{bx\,ijk};$$

$$\Delta_{bx\,ijk} = \left(\psi_{jk} - \psi_{m\,k}\right)B_i;$$

$$\dot{\Delta}_{bx\,ijk} = \left(\dot{\psi}_{jk} - \dot{\psi}_{m\,k}\right)B_i;$$

$$F_{by\,jk(j=1,3;k=1...2)} = \varkappa_{by}\,\Delta_{by\,jk} + \beta_{by}\,\dot{\Delta}_{by\,jk};$$

$$\Delta_{by\,jk(j=1,3;k=1...2)} = y_{mk} - y_c - \psi_{mk}C_{jk} + \psi_c\left(D_k + C_{jk}\right); \quad (3.43)$$

$$\dot{\Delta}_{by\,jk(j=1,3;k=1...2)} = \dot{y}_{mk} - y_c - \dot{\psi}_{mk}C_{jk} + \dot{\psi}_c\left(D_k + C_{jk}\right);$$

$$F_{c(k=1...2)} = \varkappa_{cy}\,\Delta_{cy\,k} + \beta_{cy}\,\dot{\Delta}_{cy\,k};$$

$$\Delta_{cy\,k} = y_{mk} - y_c - \psi_c D_k;$$

$$\dot{\Delta}_{cy\,k} = \dot{y}_{mk} - \dot{y}_c - \dot{\psi}_c D_k.$$

3.3.4. Multiaxial Locomotives Based on Two-Axle Carriages

Using the two axle module trucks allows obtaining a line of many-axle locomotives: four axle in one section as VL10, VL80; six axle locomotives as VL15, VL85; eight axle ones as TE13b and TEM7.

Motion equation for eight axle locomotives of VL80 Type. VL10, VL80 eight-axle electric locomotives are equipped with four-axle sections on unified 2-axle trucks. The traction force and the braking are transmitted through pivot devices equipped with ball joints and the horn-plate-free axle box nodes.

The first stage suspension is combined with the springs and has the transversal spring connection of the body with the trucks.

The equations of the body lateral oscillations can be expressed as written:

$$m_c\ddot{y}_c + \beta_{cy}\left(2\dot{y}_c - \dot{y}_{m1} - \dot{y}_{m2}\right) + \varkappa_{cy}\left(2y_c - y_{m1} - y_{m2}\right) = 0\,; \quad (3.44)$$

$$J_c\ddot{\psi}_c + \beta_{cy}\left(2\dot{y}_c - \dot{y}_{m1} - \dot{y}_{m2}\right)D^2 + \varkappa_{cy}\left(2y_c - y_{m1} - y_{m2}\right)D^2 +$$

$$+\beta_{c\psi}\left(2\dot{\psi}_c - \dot{\psi}_{m1} - \dot{\psi}_{m2}\right) + \varkappa_{c\psi}\left(2\psi_c - \psi_{m1} - \psi_{m2}\right) = 0\,,$$

where $\varkappa_{cy}$, β_{cy}, $\varkappa_{c\psi}$, $\beta_{c\psi}$ – the transversal and angular stiffness, the damping coefficient of the supporting-and-counter device for the body-truck connection, respectively.

The equations of truck lateral oscillations (k=1,2):

$$m_m y_{mk} + \beta_{cy}\left(\dot{y}_{mk} - \dot{y}_c + \dot{\psi}_c D\right) + \varkappa_{cy}\left(y_{mk} - y_c + \psi_c D\right) +$$

$$+\beta_{by}\left(y_{mk} - \sum_{j=1}^{2}\dot{y}_{jk}\right) + \varkappa_{by}\left(y_{mk} - \sum_{j=1}^{2} y_{jk}\right) = 0; \quad (3.45)$$

$$J_m\ddot{\psi}_{mk} + \beta_{c\psi}\left(\dot{\psi}_{mk} - \dot{\psi}_c\right) + 2B^2\beta_{bx}\left(2\dot{\psi}_{mk} - \sum_{j=1}^{2}\dot{\psi}_{jk}\right) +$$

$$+\beta_{by}\left[2C^2\dot{\psi}_m + C\left(\dot{y}_{1k} - \dot{y}_{2k}\right)\right] + \varkappa_{c\psi}\left(\psi_{mk} - \psi_k\right) +$$

$$+2B^2\varkappa_{bx}\left(2\psi_{mk} - \sum_{j=1}^{2}\psi_{jk}\right) - \varkappa_{by}\left[2C^2\psi_m + C\left(y_{1k} - y_{jk}\right)\right] = 0;$$

where $\varkappa_{bx}$, β_{bx}, $\varkappa_{by}$, β_{by} – the longitudinal and the transversal stiffnesses, the damping coefficients in the axle box and truck frame connections, respectively;

$\varkappa_{cy}$, β_{cy}, $\varkappa_{c\psi}$, $\beta_{c\psi}$ – stiffnesses and damping coefficients in the transversal and the angular directions, respectively.

The equation of hunting, the transversal dissipation and rotation of the wheel pairs (j=1,2; k=1,2) can be described as below:

$$\begin{gathered} m\ddot{y}_{jk} + \beta_{by}\left(\dot{y}_{jk} - \dot{y}_{m\,k} - C\dot{\psi}_{m\,k}\right) + \\ + \varkappa_{by}\left(y_{jk} - y_{m\,k} - C\psi_{m\,k}\right) = \sum_{i=1}^{2}\left(S_{y\,ijk} + H_{ijk}\right) \\ J\ddot{\psi}_{jk} + 2B^2\beta_{bx}\left(\dot{\psi}_{jk} - \dot{\psi}_{mk}\right) + 2B^2\varkappa_{bx}\left(\psi_{jk} - \psi_{mk}\right) = \left(S_{x1\,jk} - S_{x2\,jk}\right)A; \\ J_y\ddot{\varphi}_{jk} = M_{djk} - \sum_{i=1}^{2} S_{xkx}R_{ijk}. \end{gathered} \tag{3.46}$$

The motion equation for twelve axle locomotives of VL85 type. The truck arrangement for VL15 and VL85 electric locomotives (12-axles, 2 sections) is made of 2-axle trucks: three trucks in each body section. The inclined rods that balance loading on wheel pairs in case of applying traction force and braking are used for longitudinal connection of the body and the trucks. To enhance guiding in curves, the possibility of large transversal displacements of the middle truck in respect to the body is stipulated. The end trucks are equipped with cradle suspension, which is similar to the suspension of VL80 electric locomotives. The stiffness values and the coefficients of damping for the horizontal connection between the ends truck and the body as well as the middle trucks with the body are different and designated respectively as: $\varkappa_c$, β_c, $\varkappa_\psi$, β_ψ, $\varkappa_c^*, \beta_c^*$, $\varkappa_\psi^*, \beta_\psi^*$.

The equations of the body transversal oscillations are expressed as follows:

$$\begin{gathered} m_c\ddot{y}_c + \left(2\beta_c + \beta_c^*\right)\dot{y}_c - \beta_c\left(\dot{y}_{m1} + \dot{y}_{m3}\right) - \beta_c^*\dot{y}_{m2} + \\ + \left(2\varkappa_c + \varkappa_c^*\right)y_c - \varkappa_c\left(y_{m1} + y_{m3}\right) - \varkappa_c^* y_{m2} = 0; \\ J_c\ddot{\psi}_c + \left(2\beta_c D^2 + 2\beta_\psi + \beta_\psi^*\right)\dot{\psi}_c - \beta_\psi\left(\dot{\psi}_{m1} + \dot{\psi}_{m2}\right) - \beta_\psi^*\psi_{m2} + \\ + \left(2\varkappa_c D^2 + 2\varkappa_\psi + \varkappa_\psi^*\right)\psi_c - \varkappa_\psi\left(\psi_{m1} + \psi_{m3}\right) - \varkappa_\psi^*\psi_{m2} = 0. \end{gathered} \tag{3.47}$$

The equations of truck oscillations can be written as given below:

$$\begin{gathered} m_m\ddot{y}_{m1} - \beta_\kappa\dot{y}_\kappa + \left(\beta_\kappa + 2\beta_{by}\right)\dot{y}_{m1} + \beta_c D\dot{\psi}_c - \beta_{by}\left(\dot{y}_{11} + \dot{y}_{21}\right) - \\ - \varkappa_c y_c + \left(\varkappa_c + 2\varkappa_{by}\right)y_{m1} + \varkappa_c D\psi_c - \varkappa_{by}\left(y_{11} + y_{21}\right) = 0; \\ m_m\ddot{y}_{m2} - \beta_c^*\dot{y}_c + \left(\beta_c^* + 2\beta_{by}\right)\dot{y}_{m2} - \beta_{by}\left(y_{12} + y_{22}\right) - \\ - \varkappa_c^* y_c + \left(\varkappa_c^* + 2\varkappa_{by}\right)y_{m2} - \varkappa_{by}\left(y_{12} + y_{22}\right) = 0; \\ m_m\ddot{y}_{m3} - \beta_c\dot{y}_c + \left(\beta_c + 2\beta_{by}\right)y_{m3} - \beta_c D\dot{\psi}_c - \beta_{by}\left(\dot{y}_{13} + \dot{y}_{23}\right) - \\ - \varkappa_c yc + \left(\varkappa_c + 2\varkappa_{by}\right)y_{m3} - \varkappa_c D\psi_c - \varkappa_{by}\left(y_{13} + y_{23}\right) = 0. \end{gathered} \tag{3.48}$$

$$J_m\ddot{\psi}_{m1}+\left(\beta_\psi+4\beta_{bx}B^2+2\beta_{by}C^2\right)\dot{\psi}_{m1}-\beta_\psi\dot{\psi}_c-2\beta_{bx}B^2\left(\dot{\psi}_{11}+\dot{\psi}_{21}\right)-$$
$$-\beta_{by}C\left(\dot{y}_{11}-\dot{y}_{21}\right)+\left(\varkappa_\psi+4\varkappa_{bx}B^2+2\varkappa_{by}C^2\right)\psi_{m1}-\varkappa_\psi\psi_c-$$
$$-2\varkappa_{bx}B^2\left(\psi_{11}+\psi_{21}\right)-\varkappa_{by}C\left(y_{11}-y_{21}\right)=0;$$
$$J_m\ddot{\psi}_{m2}+\left(\beta_\psi^*+4\beta_{bx}B^2+2\beta_bC^2\right)\dot{\psi}_{m2}-\beta_\psi^*\dot{\psi}_c-2\beta_{bx}B^2\left(\dot{\psi}_{12}+\dot{\psi}_{22}\right)-$$
$$-\beta_{by}C\left(\dot{y}_{12}-\dot{y}_{22}\right)+\left(\varkappa_\psi^*+4\varkappa_{by}B^2+2\varkappa_{by}C^2\right)\psi_{m2}-\varkappa_\psi^*\psi_c-$$
$$-2\varkappa_{bx}C^2\left(\psi_{12}+\psi_{22}\right)-\varkappa_{by}C\left(y_{12}-y_{22}\right)=0;$$

The spring rods are used in the axle box nodes. They distribute the masses of the wheel-motor assemblies and trucks into the direction of the coordinates under consideration. The equations of wheel pair oscillation (j=1...2; k=1...3) are as below:

$$m\ddot{y}_{jk}-\beta_{by}\dot{y}_{mk}-\beta_{by}C\dot{\psi}_{mk}-\varkappa_{by}y_{mk}-\varkappa_{by}C\psi_{mk}=\sum_{i=1}^{2}\left(S_{ijky}+H_{ijk}\right);\quad(3.49)$$
$$J\ddot{\psi}_{jk}+2\beta_{bx}B^2\dot{\psi}_{jk}-2\beta_{bx}B^2\dot{\psi}_{mk}+\varkappa_{bx}B^2\psi_{jk}-2\varkappa_{bx}B^2\psi_{mk}=$$
$$=\left(S_{1jkx}-S_{2jkx}\right)A;$$
$$J_y\ddot{\varphi}_{jk}=\sum_{i=1}^{2}S_{ijkx}R_{ijk}.$$

Eight-axle sections with four-axle trucks of TE136 type. The truck arrangement of TE136 diesel locomotive contains two four-axle trucks composed of two-axle trucks with opposed arrangement of motors on each axle. The two-axle trucks are joined with each other through a low mounted balancing beam with a seat for the pivot node.

The eight-axle truck design is described by the following constraint equations:

$$y_{mk}=\frac{1}{2}\sum_{j=1}^{2}y_{jk}\ ;\ \psi_{mk}=\frac{1}{2C}\left(y_{2k}-y_{1k}\right);$$
$$y_{з1}=\frac{1}{4}\sum_{j=1}^{2}\sum_{k=1}^{2}y_{jk}\ ;\ y_{з2}=\frac{1}{4}\sum_{j=1}^{2}\sum_{k=3}^{4}y_{jk}\ ;\quad(3.50)$$
$$\psi_{з1}=\frac{1}{4E}\sum_{j=1}^{2}\left(y_{j2}-y_{j1}\right);\ \psi_{з2}=\frac{1}{4E}\sum_{j=1}^{2}\left(y_{j4}-y_{j3}\right);$$
$$y_c=\frac{1}{8}\sum_{j=1}^{2}\sum_{k=1}^{4}y_{jk}\ ;\ \psi_c=\frac{1}{8D}\left(\sum_{j=1}^{2}\sum_{k=3}^{4}y_{jk}-\sum_{j=1}^{2}\sum_{k=1}^{2}y_{jk}\right).$$

The motion equation system is composed of 24 differential equations of the second order:

$$A \times \ddot{\vec{y}} = \vec{Q}\,; \tag{3.51}$$

$$A = \left[\begin{array}{c|c|c} A_1(8\times 8) & 0 & 0 \\ \hline 0 & A_2(8\times 8) & 0 \\ \hline 0 & 0 & A_3(8\times 8) \end{array}\right], \tag{3.52}$$

$$A_1 = \begin{bmatrix} m_{np} & m_1 & m_2 & m_2 & m_3 & m_3 & m_3 & m_3 \\ m_1 & m_{np} & m_2 & m_2 & m_3 & m_3 & m_3 & m_3 \\ m_2 & m_2 & m_{np} & m_1 & m_3 & m_3 & m_3 & m_3 \\ m_2 & m_2 & m_1 & m_{np} & m_3 & m_3 & m_3 & m_3 \\ m_3 & m_3 & m_3 & m_3 & m_{np} & m_1 & m_2 & m_2 \\ m_3 & m_3 & m_3 & m_3 & m_1 & m_{np} & m_2 & m_2 \\ m_3 & m_3 & m_3 & m_3 & m_2 & m_2 & m_{np} & m_1 \\ m_3 & m_3 & m_3 & m_3 & m_2 & m_2 & m_1 & m_{np} \end{bmatrix}, \tag{3.53}$$

$$A_2 = \begin{vmatrix} J_z & 0 & \ldots & 0 \\ 0 & J_z & \ldots & 0 \\ \ldots & \ldots & \ldots & \ldots \\ 0 & 0 & \ldots & J_z \end{vmatrix};\ A_3 = \begin{vmatrix} J_y & 0 & \ldots & 0 \\ 0 & J_y & \ldots & 0 \\ \ldots & \ldots & \ldots & \ldots \\ 0 & 0 & \ldots & J_y \end{vmatrix};$$

$$m_{np} = \frac{m_c}{64} + \frac{m_Б}{16} + \frac{m_m}{4} + \frac{J_c}{64D^2} + \frac{J_Б}{16E^2} - \frac{J_m}{4C^2} + m\,;$$

$$m_1 = \frac{m_c}{64} + \frac{m_Б}{16} + \frac{m_m}{4} + \frac{J_c}{64D^2} + \frac{J_Б}{16E^2} - \frac{J_m}{4C^2}\,; \tag{3.54}$$

$$m_2 = \frac{m_c}{64} + \frac{m_Б}{16} + \frac{J_c}{64D^2} - \frac{J_Б}{16E^2}\,;$$

$$m_3 = \frac{1}{64}\left(m_c - \frac{J_c}{D^2}\right).$$

$$\ddot{\vec{y}} = \begin{bmatrix} \ddot{y}_{11} \\ \dots \\ \ddot{y}_{24} \\ \ddot{\psi}_{11} \\ \dots \\ \ddot{\psi}_{24} \\ \ddot{\varphi}_{11} \\ \dots \\ \ddot{\varphi}_{24} \end{bmatrix}; \quad \vec{Q} = \begin{bmatrix} F_{y11} \\ \dots \\ F_{y24} \\ M_{\psi 11} \\ \dots \\ M_{\psi 24} \\ M_{\varphi 11} \\ \dots \\ M_{\varphi 24} \end{bmatrix}; \quad \begin{array}{l} F_{y(j=1\dots2;k=1\dots4)} = \sum_{i=1}^{2} \left(S_{yk} + H_{ijk} \right) + F_{by\,jk}; \\ M_{\psi(j=1\dots2;k=1\dots4)} = \left(S_{x1\,jk} - S_{x2\,jk} \right) A - \\ \quad - \left(F_{bx1\,jk} - F_{bx2\,jk} \right) B; \\ M_{\varphi(j=1\dots2;k=1\dots4)} = M_{\partial j} - \sum_{i=1}^{2} S_{xik} R_{ijk}. \end{array} \tag{3.55}$$

In (3.55), $F_{by\,jk}$ – the cumulative box reactions caused by supporting-and-counter devices at the connection of the body with balancers and the balancers with the trucks.

Here, the following designations are adopted:

M_{c1}, M_{c2} – the reciprocal moments in the body-balancing device connections;

M_{m1}, M_{m2}, M_{m3}, M_{m4} – the reciprocal moments in the connections of balancing devices with truck frames.

The values of the indicated moments depend on relative displacements and speeds of the joined elements as written:

$$M_{cj\ (j=1\dots2)} = M_c \left(\Delta_{\psi cj}, \dot{\Delta}_{\psi cj} \right); \quad M_{mj(j=1\dots4)} = M_m \left(\Delta_{\psi mj}, \dot{\Delta}_{\psi mj} \right);$$

$$\Delta_{\psi cl} = \psi_{Bl} - \psi_c; \quad \dot{\Delta}_{\psi cl} = \dot{\psi}_{Bl} - \dot{\psi}_c;$$

$$\Delta_{\psi mk} = \psi_{mk} - \psi_{Bl}; \quad \dot{\Delta}_{\psi k} = \dot{\psi}_{mk} - \dot{\psi}_{Bl};$$

$$\psi_{B1} = \frac{1}{4E}\left(y_{12} + y_{22} - y_{11} - y_{21} \right); \tag{3.56}$$

$$\psi_{B2} = \frac{1}{4E}\left(y_{14} + y_{24} - y_{13} - y_{23} \right);$$

$$\psi_c = \frac{1}{8D}\left(y_{13} + y_{23} + y_{14} + y_{24} - y_{11} - y_{21} - y_{12} - y_{22} \right);$$

$$\psi_{mk(k=1\dots4)} = \frac{1}{2C}\left(y_{2k} - y_{1k} \right); \quad \dot{\psi}_{mk} = \frac{1}{2C}\left(\dot{y}_{2k} - \dot{y}_{1k} \right);$$

$$\dot{\psi}_{B1} = \frac{1}{4E}\left(\dot{y}_{12} + \dot{y}_{22} - \dot{y}_{11} - \dot{y}_{21} \right); \quad \dot{\psi}_{B2} = \frac{1}{4E}\left(\dot{y}_{14} + \dot{y}_{24} - \dot{y}_{13} - \dot{y}_{23} \right); \tag{3.57}$$

$$\dot{\psi}_c = \frac{1}{8D}\left(\dot{y}_{13} + \dot{y}_{23} + \dot{y}_{14} + \dot{y}_{24} - \dot{y}_{11} - \dot{y}_{21} - \dot{y}_{12} - \dot{y}_{22} \right);$$

$$F_{by11} = F_{m1} + \frac{F_{c1}}{2} - \frac{F_{Б1}}{2} - \frac{F_c}{4} - F_{b1};$$

$$F_{by21} = -F_{m1} + \frac{F_{c1}}{2} - \frac{F_{Б1}}{2} - \frac{F_c}{4} + F_{b1};$$

$$F_{by12} = F_{m2} - \frac{F_{c1}}{2} + \frac{F_{Б1}}{2} - \frac{F_c}{4} - F_{b2}; \qquad (3.58)$$

$$F_{by22} = -F_{m2} - \frac{F_{c1}}{2} + \frac{F_{Б1}}{2} - \frac{F_c}{4} + F_{b2};$$

$$F_{by13} = F_{m3} + \frac{F_{c2}}{2} - \frac{F_{Б2}}{2} + \frac{F_c}{4} - F_{b3};$$

$$F_{by23} = -F_{m3} + \frac{F_{c2}}{2} - \frac{F_{Б2}}{2} + \frac{F_c}{4} + F_{b3};$$

$$F_{by14} = F_{m4} - \frac{F_{c2}}{2} + \frac{F_{Б2}}{2} + \frac{F_c}{4} - F_{b4};$$

$$F_{by24} = -F_{m4} - \frac{F_{c2}}{2} + \frac{F_{Б2}}{2} + \frac{F_c}{4} + F_{b4}; \qquad (3.59)$$

$$F_{k(k=1...4)} = \frac{M_{mk}}{C};\ F_{cl\ (l=1...2)} = \frac{M_{cl}}{E};\ F_c = \frac{M_{c1} + M_{c2}}{D};$$

$$F_{Б1} = \frac{M_{m1} + M_{m2}}{E};\ F_{Б2} = \frac{M_{m3} + M_{m4}}{E};$$

$$F_{bk\ (k=1...4)} = \frac{B}{2C}\left(F_{bx11k} + F_{bx12k} - F_{bx21k} - F_{bx22k}\right).$$

TEM7 type locomotive with trucks and intermediate frames. TEM7 diesel locomotive is a switcher and carrier, its two four-axle trucks are composed of two-axle trucks which are free from horn plates and joined with intermediate frames by pendulum suspensions. The traction forces generated by the two-axle trucks are transmitted to the intermediate frames through the traction link-and-lever mechanism that include horizontal and inclined rods. The locomotive is characterized by a very small value of the minimal radius of sheering into curves – 80 m.

The displacement of the body and the truck intermediate frames are constrained by the following relations:

$$y_c = \frac{y_{Б1} + y_{Б2}}{2};\ \psi_c = \frac{y_{Б2} - y_{Б1}}{2E}. \qquad (3.60)$$

The equations for the intermediate beams are as follows:

$$\left(\frac{m_c}{4}+m_Б+\frac{J_c}{4E^2}\right)\ddot{y}_{Б1}+\left(\frac{m_c}{4}-\frac{J_c}{4E^2}\right)y_{Б2}=F_{c1}-F_{m1}-F_{m2}\,; \quad (3.61)$$

$$\left(\frac{m_c}{4}+m_Б+\frac{J_к}{4E^2}\right)\ddot{y}_{Б2}+\left(\frac{m_c}{4}-\frac{J_c}{4E^2}\right)y_{Б1}=F_{c2}-F_{m3}-F_{m4}\,.$$

The reactions in the contacts of the body with the intermediate beams are marked as F_{c1}, F_{c2} while those of the beams with the trucks are F_{m1}... F_{m4}. These reactions depend on the mutual displacements and speeds of the joined elements, as well as the features of the related joints.

The truck motion equations (k=1...4) are as written:

$$m_m y_{mk}=F_{mk}-\sum_{j=1}^{2}F_{by\,jk}\,; \quad (3.62)$$

$$J_m\ddot{\psi}_{mk}=M_{mk}+\left(F_{by1k}-F_{by2k}\right)C+\left(F_{bx1\,jk}-F_{bx2\,jk}\right)A\,.$$

The wheel pair motion equations are expressed as below:

$$m\ddot{y}_{jk}=\sum_{i=1}^{2}\left(S_{yijk}+H_{ijk}\right)-F_{byjk}\,;$$

$$J_y\ddot{\psi}_{jk}=\left(S_{x1\,jk}-S_{x2\,jk}\right)-\left(F_{bx1\,jk}-F_{bx2\,jk}\right)A; \quad (3.63)$$

$$J_y\ddot{\varphi}_{jk}=\sum_{i=1}^{2}S_{xijk}R_{ijk}\,.$$

3.4. Models of Electric Trains, Diesel Trains, Passenger Carriages, Trams and Underground Carriages

On the one hand, railway wagon track arrangements are much simpler due to absence of axle motors, but, on the other hand, there are more enhancement possibilities to improve the dynamic features of the rolling stock at the stage of its design. As the example can serve this situation: at one and the same time, a radially installed wheel pair is a far future perspective for the locomotives but a conventional design for the railway wagons in many countries. Electric trains and electric-diesel trains occupy an intermediate place in this sense.

Actually, almost all passenger wagons, electric trains and electric-diesel trains are equipped with two-axle trucks within their truck arrangements.

In Ukraine, only two versions of the suburban trains have been used: DR1 diesel trains and ER electric trains.

A number of sophisticated and interesting engineering solutions are implemented in DR1 truck arrangement. For instance, the springs of the body spring suspension are used as elastic elements for not only the body-truck vertical connection but also for their transversal one. The truck frame is lowered below the axle box assemblies of a lever type.

ER electric trains of various modifications are very similar to each other by their truck arrangements. The spring suspension is a two stage suspension with the friction shock absorbers in the axle box stage and with hydraulic shock absorber in the body stage. The connections of the body with the trucks are by the cradle mechanisms. However, ER200 electric train trucks are more perfect.

The development of the passenger transport at the territories out of the post-Soviet Union influence has always aimed at improvement of the electric trains and the increase in maximal travelling speeds. In many countries (France, Japan, Germany) electric train speeds with up to 200-300 km/h are called just conventional. The achievements of the regular service at such speeds are the results of the extended studies of the truck and the spring suspension. Additionally, it should be noted that in the indicated geographic area, the same attention was paid to the track design, the track quality and the maintenance. As a rule, special railway lines are built for the high-speed passenger traffic. Achieving the high speed movement without complex solving of rolling stock problems is very difficult.

The designs of the trucks for the above mentioned high-speed electric trains are not much different by the principle scheme but possess the number of the individual properties.

The two-axle motor truck of a TGC electric train (France) is characterized by installing the traction electric motors and gear boxes on the body, while the torque is transmitted to the axles through Tripod couplings famous for their operation reliability. A *TGV* electric train holds the record for railway high speed of 574.8 km/h, set in 2007 on Paris-Lion way. The previous record has been also set by French TGV of Alstom Company.

L-GSG4 trucks of similar structure are used in German electric trains (BD4, RBDe4). The second stage of the spring suspension is coil springs, rubber-metal elements, one-link axle boxes, support-and-frame suspension of traction motors with axle gear boxes.

The suburban electric trains of Switzerland apply *L-GA2T* trucks.

The modified *L-AK-M* trucks are also installed at Holland suburban electric trains.

ICM long distance electric trains in Holland are equipped with *L-GA2* trucks, whereas *DH2* diesel trains apply *L-S2G4* trucks.

High-speed passenger railway lines of France and Finland operate railway wagons with *L-GSG2* trucks.

The truck arrangement of the majority of the passenger railway wagons has two two-axle trucks.

The railway wagons being operated in Ukraine mainly have *KVZ-TsNII* trucks that are unified for all passenger railway wagons of long distance service and inter-regional destinations, as well as for suburban electric trains. The trucks are equipped with two-stage spring suspension. The central suspension has a cradle structure. The axle-box suspensions are made of coil springs and wedge type dampers. This suspension stage not only functions as a first suspension, but it provides a spring joint of a wheel pair with the truck frame in horizontal plane.

The passenger railway wagon truck designs are vary greatly in the countries of Europe, Asia and America, and they differ in the wagon or the train class.

Minden-Deutz is a German truck. It served as a prototype of a typical truck of the conventional long distance trains of Western Europe. It has doubled suspension. In the box stage free from horn plates, the box connection with the frame is performed through flat spring of axle box links. The developed truck structures are unified for passenger railway wagons and trailing wagons of diesel trains with speeds of up to 200 km/h.

The truck of *DT-200* model designed for travelling at 250 km/h is the most commonly used in Japan. In the axle box node, the link structure as the connection with the truck frame is implemented. The stiffness of the air suspension in the first stage is 1.1 kN/mm; the stiffness of the central suspension in the vertical direction is 0.45 kN/mm, whereas in the lateral direction it is 0.36 kN/mm. The weight of the truck with the traction motors is 10 t; the base – 2.5 m; the track – 1.435 m.

The worldwide practice has two more examples of the conventional trucks with air suspension: *Pioneer* (USA) for suburban railway wagons and *R28* for long distance railways of France and Germany.

One of perspective designs of trucks for passenger wagons is *TSK-1* truck for RT-200 train and speed of up to 250 km/h. The air suspension and the improved longitudinal connection of the wheel pairs with the truck frame are their main differences from the conventional designs.

The truck structure similar to *MSZhD* is used in subway wagons of *E* (*Em*, *Ema*, *Emkh*, *Ezh*, *Ezhz*) and *I*.

Almost all trams or street trains used worldwide are equipped with two axle trucks. Sometimes they are installed on 6-axle joined wagons, for instance, Austrian *E6* and *C6* trams, or German *2000* Tram, but more often they are 4-axle wagons, for instance, *CLRV* type (Canada), *Bt* or *Be 8/8*.

In spite of the variety in the design solutions for the truck arrangements with axle configuration of 20-20 or 2-2, the computational patterns for almost all passenger railway wagons and electric-diesel trains are similar, and they may be described by the same motion equations.

The body lateral oscillation equation:

$$m_c \ddot{y}_c = F_{c1} + F_{c2};$$

$$J_c \ddot{y}_c = \left(F_{c2} - F_{c1}\right) D + \sum_{k=1}^{2} M_{ck}. \tag{3.64}$$

The values of the reaction within the body-truck connection depend on the relative displacements and speeds of the body and the trucks, as well as the connection features within the transversal and angular directions.

Thus, the equations of the truck lateral oscillations (k=1,2) are in the form as given:

$$m_m \ddot{y}_{mk} = \sum_{j=1}^{2} F_{byjk} - F_{ck}; \tag{3.65}$$

$$J_m \ddot{\psi}_{mk} = \left(F_{by2k} - F_{by1k}\right) C - M_{ck}.$$

The equations of hunting, transversal dissipation and rotation of the wheel pairs (j=1,2; k=1,2) are shown below:

$$\begin{gathered} m\ddot{y}_{jk} = \sum_{i=1}^{2} \left(S_{yk} + H_{ijk}\right) - F_{byjk}; \\ J\ddot{\psi}_{jk} = \left(S_{x1jk} - S_{x2jk}\right) A - \left(F_{bx1jk} - F_{bx2jk}\right) B; \\ J_y \ddot{\varphi}_{jk} = \sum_{i=1}^{2} S_{x\,ijk} R_{ijk}. \end{gathered} \tag{3.66}$$

3.5. Mathematical Models of Freight Carriages

The railways of Ukraine, Russia and CIS countries mainly operate freight wagons with two axle trucks of 18-100 model (TsNII-KhZ-0). These trucks are used in all four-axle wagons for long distance, as well as in four axle trucks of eight-axle open wagons and tanks wagons.

The model of a four axle wagon with 18-100 type trucks is composed of 11 masses: the wagon body, two body bolsters, four side frames and four wheel pairs.

In the truck, two spring sets are applied. Each of them is composed of seven double coil springs.

The body horizontal oscillation equation is as follows:

$$m_c \ddot{y}_c = \sum_{k=1}^{2} F_{ck} \; ; \tag{3.67}$$

$$J_c \ddot{\psi}_c = \left(F_{c2} - F_{c1}\right) D + \sum_{k=1}^{2} M_{ck} \; .$$

The equations of the horizontal oscillations of the truck body bolsters (k=1,2) are as below:

$$m_{Ш} \ddot{y}_{Ш} = -F_{ck} + \sum_{l=1}^{2} F_{Блky} \; ; \tag{3.68}$$

$$J_{Ш} \ddot{\psi}_{Шk} = -M_{ck} + \left(F_{Б1kx} - F_{Б2kx}\right) L + \sum_{l=1}^{2} M_{Блk} \; .$$

Truck joint frames of the trucks have comparably low parallelogram stiffness and, as a result, low resistance to the longitudinal relative movement of side frames. At the same time, they have high inter-axle stiffness at relative rotation of wheel pairs.

The equations of truck side frame oscillations (l=1.2; k=1.2) are as written:

$$m_{Б} \ddot{y}_{Блk} = -F_{Блky} + \sum_{j=1}^{2} F_{by\,jk} \; ;$$

$$m_{Б} \ddot{x}_{Бl\,k} = -F_{Бl\,kx} + \sum_{j=1}^{2} F_{bx\,ljk} \; ; \tag{3.69}$$

$$J_{Б} \ddot{\psi}_{Бl\,k} = -M_{Блk} + \sum_{j=1}^{2} \sum_{i=1}^{2} M_{bijk} + \left(F_{by2k} - F_{by1k}\right) C \; .$$

The equations of the wheel pair horizontal oscillations (k=1,2; j=1,2) are as below:

$$m \ddot{y}_{jk} = F_{by\,jk} + \sum_{i=1}^{2} \left(S_{y\,ijk} + H_{ijk}\right);$$

$$J \ddot{\psi}_{jk} = -M_{bijk} + \left(S_{x1\,jk} - S_{x2\,jk}\right) A - \left(F_{bx\,1jk} - F_{bx2\,jk}\right) B \; ; \tag{3.70}$$

$$J_y \ddot{\varphi}_{jk} = \sum_{i=1}^{2} S_{xijk} R_{ijk} \, .$$

Three-axle trucks of 18-102 type are produced for six-axle freight wagons. These trucks have two side semi-frames of joined type, which provides even load transmission over all three-wheel pairs.

The semi-frame on each side rests with its one end directly on the axle box case of the outermost wheel pair, and with the other end on the balance outermost end, the balance, in its turn, rests on the axle box body of the middle wheel pair.

The body horizontal oscillation equations for a six-axle freight wagon are as follows:

$$m_c \ddot{y}_c = \sum_{k=1}^{2} F_{ck} \; ; \tag{3.71}$$

$$J_c \ddot{\psi}_c = \left(F_{c2} - F_{c1}\right) D + \sum_{k=1}^{2} M_{ck} \; .$$

The equations of the horizontal oscillations of truck body bolsters (k=1,2) are as below:

$$m_{Ш} \ddot{y}_{Шk} = -F_{ck} + \sum_{l=1}^{4} F_{Блky} \; ; \tag{3.72}$$

$$J_{Ш} \ddot{\psi}_{Шk} = -M_{ck} + \left(F_{Б1kx} + F_{Б3kx} - F_{Б2kx} - F_{Б4kx}\right) L +$$

$$+ \left(F_{Б4k} + F_{Б4k} - F_{Б1k} - F_{Б2k}\right) E + \sum_{l=1}^{4} M_{Блk} .$$

The frames of 18-102 and 18-100 trucks have movable side frames that provide low parallelogram stiffness, but high inter-axle stiffness, when the wheel pairs turn. The equations for the horizontal oscillations of the truck side frame (l=1,2; k=1,2) may be expressed as below:

$$m_{Б} \ddot{y}_{Блk} = -F_{Блky} + \sum_{j=1}^{3} F_{by\,jk} \; ;$$

$$m_{Б} \ddot{x}_{Блk} = -F_{Блkx} + \sum_{j=1}^{3} F_{bx\,ljk} \; ; \tag{3.73}$$

$$J_{Б} \ddot{\psi}_{Блk} = -M_{Блk} + \sum_{j=1}^{3} \sum_{i=1}^{2} M_{b\,ijk} + \left(F_{by3k} - F_{by\,1k}\right) C \; .$$

The equations of wheel pair horizontal oscillations (k=1.2; j=1.3) are written as:

$$m \ddot{y}_{jk} = -F_{by\,jk} + \sum_{i=1}^{2} \left(S_{y\,ijk} + H_{ijk}\right) ;$$

$$J \ddot{\psi}_{jk} = -M_{b\,ijk} + \left(S_{x\,1jk} - S_{x\,2jk}\right) A - \left(F_{bx1\,jk} - F_{bx2\,jk}\right) B \; ; \tag{3.74}$$

$$J_y \ddot{\varphi}_{jk} = \sum_{i=1}^{2} S_{x\,ijk} R_{ijk} .$$

Eight-axle freight wagons are equipped with four-axle trucks of 18-101 type. The trucks are composed by two 18-100 trucks and longitudinal binder.

The body horizontal oscillation equations can be expressed as given:

$$m_c \ddot{y}_c = \sum_{k=1}^{2} F_{ck} \ ; \tag{3.75}$$

$$J_c \ddot{\psi}_c = \left(F_{c\,2} - F_{c\,1}\right) D + \sum_{k=1}^{2} M_{c\,k} \ .$$

The equations for the horizontal oscillations of the truck longitudinal beams are as follows:

$$m_{П} \ddot{y}_{П1} = -F_{c1} + \sum_{k=1}^{2} F_{Шky} \ ;$$

$$m_{П} \ddot{y}_{П2} = -F_{c2} + \sum_{k=3}^{4} F_{Шky} \ ; \tag{3.76}$$

$$J_{П} \ddot{\psi}_{П1} = -M_{c1} + \left(F_{Ш2y} - F_{Ш1y}\right) E + \sum_{k=1}^{2} M_{Шk} \ ;$$

$$J_{П} \ddot{\psi}_{П2} = -M_{c2} + \left(F_{Ш4y} - F_{Ш3y}\right) E + \sum_{k=3}^{4} M_{Шk} \ .$$

The equations for the horizontal oscillations of the truck transversal bolsters (k=1,4) are to be written as below:

$$m_{Ш} \ddot{y}_{Шk} = -F_{Шky} + \sum_{l=1}^{2} F_{Бlky} \ ; \tag{3.77}$$

$$J_{Ш} \ddot{\psi}_{Ш\,k} = -M_{ck} + \left(F_{Б1kx} - F_{Б2kx}\right) L + \sum_{l=1}^{2} M_{Блk} .$$

The equations of the horizontal oscillations of the truck side frame (l=1,2; k=1,4) are to be expressed in the form as the written below:

$$m_{Б} \ddot{y}_{Блk} = -F_{Блky} + \sum_{j=1}^{2} F_{by\,jk} \ ;$$

$$m_{Б} \ddot{x}_{Блk} = -F_{Блkx} + \sum_{j=1}^{2} F_{bx\,ljk} \ ; \tag{3.78}$$

$$J_{Б} \ddot{\psi}_{Блk} = -M_{Блk} + \sum_{j=1}^{2} \sum_{i=1}^{2} M_{bijk} + \left(F_{by2k} - F_{by1k}\right) C \ .$$

The equations of wheel pair horizontal oscillations (k=1,4; j=1,2) are obtained as below:

$$m\ddot{y}_{jk} = -F_{by\,jk} + \sum_{i=1}^{2}\left(S_{y\,jk} + H_{ijk}\right);$$

$$J\ddot{\psi}_{jk} = -M_{b\,ijk} + \left(S_{x\,1jk} - S_{x2\,jk}\right)A - \left(F_{bx1\,jk} - F_{bx2\,jk}\right)B; \quad (3.79)$$

$$J_y\ddot{\varphi}_{jk} = \sum_{i=1}^{2} S_{x\,ijk}R_{ijk}.$$

Four-axle wagons prevail in the freight wagon fleets of Western European countries. *R25C* model in some versions is the main truck type in European Unit countries.

The truck frames have closed and stiff structure, which is composed of two longitudinal beams, one bolster and two end transversal beams.

The railways of USA and Canada mostly use the trucks which are similar to *TsNII-Kh-O* truck pattern.

3.6. Simulation of the Contacting Parts of the Carriage

According to the mathematical description principle for the connections between the separate rolling stock elements, they may be divided into two groups.

To the first group we attribute the connections that have linear characteristics included into Lagrange equation as the constant coefficients at partial derivative.

The longitudinal and the transversal connections in axle box link nodes that do not have transversal play are considered as linear connections. These connections are represented by the stiffness with the coefficient of $Ж_{bx}$, $Ж_{by}$ while damping coefficients – β_{bx}, β_{by}.

The parameters of the other connections, as a rule, are non-linear. According to the adopted coordinate system, let us consider only the transversal and the angular connections in terms of the connections of the body with the trucks.

The transversal connection of the body with the trucks could be built in two variants, i.e. rigid or spring. The rigid connection is typically applied for the body resting on the trucks through a flat cylindrical or spherical heel, or if a rigid bolster is present.

The spring connection is provided by various devices, and it possesses a wide range of features. The following design variants are known:

- pendulum supports with a spring counter mechanism;
- cradle suspension;
- bolster beam with spring transversal displacement;

- Flexy-Coil suspension;
- air or rubber-and-metal spring suspensions.

The connection with pendulum supports is implemented for locomotives of SS7100, VV1650, F, FP, VL60 and TEP60. It has features related to the precompression of the counter springs. The stiffness of one pendulum support in the transversal direction can be determined by the formula as given:

$$\mathcal{Ж}_y = \frac{F_0}{y} + \frac{\mathcal{Ж}_{pp}}{2} - \frac{P}{2\sqrt{l^2 - y^2}}, \tag{3.80}$$

where F_0, $\mathcal{Ж}_{pp}$ – the force of precompression and the stiffness of the counter device spring;

l – the pendulum support height;

P – the body weight.

The angular stiffness of the pendulum mechanism at two supports installed at distance C from each other may be expressed as below:

$$\mathcal{Ж}_\psi = 0,5\mathcal{Ж}_y C^2 . \tag{3.81}$$

It should be admitted that the classical pendulum suspension with its original feature of simplicity has undergone signification modifications mainly due to the weak damping of hunting oscillations, and it has been enhanced by installing additional supports with bearers.

The structural combination of the bolster node with the spring counter device towards the transversal direction is typical for a large group of locomotives: VL10, VL80, TE10B, TE10M, TE116, TE109, TE120, TE132.

The spring counter device can function in parallel with the rubber-and-metal supports that possess high visco-elastic resistance, or with bearers applying dry friction resistance. The back moment can be also created by roller supports with profiled plates.

In ER1 electric trains and subway wagons of G, D, E series, the body rests on the intermediate cradle beam through the central spherical support, while the intermediate cradle beam, in its turn, rests on the cradle through the spring elements of the second stage spring suspension. The quasi-spring counter forces of the cradle mechanism have the gravitational origin. The cradle suspension is insufficient for damping hunting oscillations. Due to this, a number of enhanced structures of the cradle suspension have been developed. In particular, they are used in electric trains of ER2, ER9, ER22.

The most simple engineering solution for the support-and-counter device is recognized Flexicoil spring suspension, where the springs act both in the vertical and the transversal directions. Such suspension is used in electric locomotives of E151 and E120, TGV electric train, diesel trains of DR1, DR2, TG16, TEP70.

As it has been mentioned above, the characteristics of the wheel pair connection with the truck frame at axle box node links are close to the linear ones, therefore during simulation it is possible to consider them as the constant coefficients in Lagrange's partial differential equations. Let us consider the non-linear characteristics for a pedestal box in the case of installing the wheel pair in the axle boxes with axial clearance (transversal play).

Though both the manufacturers and the operators try to decrease the longitudinal clearance to approach zero in the horn plate of the axle box node, in practice it always achieves the values of 0.5...2.5 mm, which significantly influences the wheel pair hunting.

If we assume the total longitudinal clearance in an axle box assembly as $2\Delta xo$, then the characteristics of the longitudinal connection between a wheel pair and axle boxes is as follows:

$$\begin{aligned} &\text{at} \quad \Delta x < -\Delta xo, && \text{then } F_{bx} = Ж_{bx}(\Delta x + \Delta xo); \\ &\text{if} \quad -\Delta xo < \Delta x < \Delta xo, && \text{then } Fbx = 0; \\ &\text{if} \quad \Delta x > \Delta xo, && \text{then } F_{bx} = Ж_{bx}(\Delta x - \Delta xo), \end{aligned} \tag{3.82}$$

where $Ж_{bx}$ – the stiffness of the contact between the axle box and the horn plate guides;

Δx – the longitudinal displacement of the wheel pair neck middle section in relation to the axle box horn plates.

If between the wheel pair and the axle box there is the axial clearance, the following designations are to be introduced:

δ_o – the one side free axial clearance (play) in the axle box node;

F_{mp} – the friction force, which prevents the axial displacement of the wheel pair axle neck in respect to the axle box case;

F_n – the precompression of axial thrust springs;

$Ж_{by}$ – the stiffness in the axial thrust in the axle box connection.

Finally, the reactions in the axle boxes may be described by the following relations:

where: $\Delta y < -\Delta yo$; $F_{by} = -(\Delta y + \delta_o)Ж_{by} - F_n - F_{mp}\,\text{sign}(\dot{\Delta}_y)$;

$$\Delta y_o < \Delta y < \Delta yo;\ F_{by} = -F_{mp}\,\text{sign}(\dot{\Delta}_y); \tag{3.83}$$

$$\Delta y > \Delta yo;\ F_{by} = (\Delta y + \delta o)Ж_{by} + F_n - F_{mp}\,\text{sign}(\dot{\Delta}_y).$$

4 SIMULATING THE EXTERNAL CONTROL ACTION

4.1. Generalized Contact and Axle Equipment Reactions

The force interaction between the wheel and the track is difficult for description, but at the same time, it is very important for the studies of the dynamic issues of frictional interaction between the rolling stock and the track, as well as the phenomenon of the rolling stock guiding with the track. In a general case, wheel-track contacting takes place in two contact areas: on the rolling surface and on the wheel flange. More simply, the contact can be considered as a two-point contact. In this case, the principle vector of the contact interaction between *i*-*n* wheel (*i*=1 –for the left wheel, *i*=2 –for the right wheel), of *j*-*n* wheel pair, *k*-*n* truck has the following structure:

$$\vec{F}_{ijk} = \vec{N}_{ijkI} + \vec{N}_{ijkII} + \vec{S}_{ijkI} + \vec{S}_{ijkII} \ , \tag{4.1}$$

where $\vec{N}_{ijkI}$, $\vec{N}_{ijkII}$, $\vec{S}_{ijkI}$, $\vec{S}_{ijkII}$ –the principle vectors of the normal reactions and the adhesion forces of the first or main contact and the second or wheel flange contact, then as written:

$$\vec{N}_{ijkI} = \vec{P}_{ijkI} + \vec{H}_{ijkI}; \quad \vec{N}_{ijkII} = \vec{P}_{ijkII} + \vec{H}_{ijkII} \ ,$$

where $\vec{P}_{ijkI}$, $\vec{H}_{ijkI}$, $\vec{P}_{ijkII}$, $\vec{H}_{ijkII}$ –the vertical and the horizontal transversal components of the normal contact reactions, while the following should be considered:

$$H_{ijkI} = P_{ijkI} \cdot g_{ijkI}; \quad H_{ijkII} = P_{ijkII} \cdot g_{ijkII} \ , \tag{4.2}$$

where $g_{ijkI} = tg\left(\gamma_{ijkI}\right), g_{ijkII} = tg\left(\gamma_{ijkII}\right)$ – the conditional conicities of the wheel profiles at the dedicated contact points;

$\gamma_{ijkI}, \gamma_{ijkII}$ –the inclination angles of the common tangents towards the horizon in the dedicated contact centers of the wheel-rail profiles.

At the static vertical loading on wheel P_0, we obtain as follows:

$$P_0 = P_{ijkI} + P_{ijkII} . \tag{4.3}$$

Total gravitational component H_{ijk} from two contacts is defined as a sum of two reactions $\vec{H}_{ijkI}$ and $\vec{H}_{ijkII}$, on condition that:

$$H_{ijk} = P_0\left[k_{ijk}g_{ijkI} + \left(1-k_{ijk}\right)g_{ijkII}\right]. \tag{4.4}$$

where k_{ijk} –the coefficient to incorporate the vertical load distribution between contact I and contact II with values within 0 to 1. According to the linear law, the load changes from P_{ijkI} to P_{ijkII} with two-point contacting $dy_I \le dy_{jk} \le dy_{II}$, we obtain:

$$P_{ijkI} = P_0 k_{ijk}; \quad P_{ijkII} = P_0\left(k_{ijk} - 1\right), \tag{4.5}$$

where $k_{ijk} = \dfrac{dy_{jk} - dy_I}{dy_{II} - dy_I}$;

d_{yjk} –the instantaneous transversal displacement of the wheel profile in respect to the rail;

d_{yI}, d_{yII} –the transversal displacements of the wheel profile in respect to the rail at points of entering into and exiting from the two-point contact.

Values of d_{yI} and d_{yII} that depend on certain profiles of rolling surfaces of the wheel and the rail.

The adhesion contact forces have a spacious structure, then as written:

$$\begin{aligned}\vec{S}_{ijkI} &= \vec{S}_{xijkI} + \vec{S}_{yijkI} + \vec{S}_{zijkI};\\ \vec{S}_{ijkII} &= \vec{S}_{xijkII} + \vec{S}_{yijkII} + \vec{S}_{zijkII},\end{aligned} \tag{4.6}$$

where $\vec{S}_{xijk}$, $\vec{S}_{yijk}$, $\vec{S}_{zijk}$ – the longitudinal component, transversal component, vertical component at the dedicated contact points.

We can ignore the reaction of $\vec{S}_{zijkI}$, since its value is associated with the touch prevention and for the contact it is insignificant.

The values of the other components are determined by the following equations:

$$S_{xijkII} = N_{ijkII}\psi_o K_x\left(\varepsilon_{xijkII}, \varepsilon_{yijkII}\right);\ S_{xijkII} = N_{ijkII}\psi_o K_x\left(\varepsilon_{xijkII}, \varepsilon_{yijkII}\right);$$

$$S_{yijkI} = N_{ijkI}\psi_o K_y\left(\varepsilon_{xijkI}, \varepsilon_{yijkI}\right);\ S_{yijkII} = N_{ijkII}\psi_o K_y\left(\varepsilon_{xijkII}, \varepsilon_{yijkII}\right); \tag{4.7}$$

$$S_{ziykII} = N_{ijkII}\psi_o K_z\left(\varepsilon_{zijkII}\right),$$

where ε_{xijkI}, ε_{yijkI}, ε_{xijkII}, ε_{yijkII}, ε_{zijIII} –the longitudinal component, the transversal component, the vertical component of relative slipping in the dedicated contacts;

N_{ijkI}, N_{ijkII} –the normal reactions in contact I and contact II;

ψ_o –the cuoff adhesion coefficient (physical);

$K_x(\varepsilon_{xijkx}, \varepsilon_{yijk})$, $K_y(\varepsilon_{xijk}, \varepsilon_{yijk})$, $K_z(\varepsilon_{zijk})$ –the experimental adhesion characteristics.

The adhesion features are introduced as the external functions. The method and the results of the studies on the experimental characteristics are described in [104].

The relative slipping in contacts (longitudinal, transversal and vertical) is determined by the following formulas:

$$\varepsilon_{xijkI} = \frac{V^*_{sxijkI}}{\dot{\varphi}_{jk} R_{ijkI}};\ \varepsilon_{yijkI} = \frac{V^*_{syijkI}}{\dot{\varphi}_{jk} R_{ijkI}};\ \varepsilon_{xijkII} = \frac{V^*_{sxijkII}}{\dot{\varphi}_{jk} R_{ijkII}};$$
$$\varepsilon_{yijkII} = \frac{V^*_{syijkII}}{\dot{\varphi}_{jk} R_{ijkII}};\ \varepsilon_{zijkII} = \frac{V^*_{szijkII}}{\dot{\varphi}_{jk} R_{ijkII}}, \tag{4.8}$$

where $\dot{\varphi}_{jk}$ –the angular speed of wheel pair rotation.

For the equations derived from relative sliding, the following designations are adopted:

V_{sijkI}, V_{sijkII} –the total velocities of sliding in the contacts;

V_{sxijkI}, $V_{sxijkII}$, V_{syijkI}, $V_{syijkII}$, $V_{szijkII}$ –the longitudinal component, the transversal component, the vertical component of sliding velocities in the dedicated contacts of fixed coordinate system XOY, linked to the track;

V^*_{sxijkI} , $V^*_{sxijkII}$, V^*_{syijkI} , $V^*_{syijkII}$, $V^*_{szijkII}$ –the longitudinal component, the transversal component, the vertical component of sliding velocities in the dedicated contacts of moving coordinate system X_jOY_j linked to the wheels;

V_{jk} –absolute velocity of wheel pair geometrical center.

The positive direction of the sliding velocity is assumed as the direction corresponding to the positive value of the dedicated adhesion force.

$$\overline{V}_{sijkI} = \overline{V}^*_{sxijkxI} + \overline{V}^*_{syijkyI};$$
$$V^*_{sx1jkI} = \dot{\varphi}_{jk} R_{1jkI} - \dot{x}_{jk} - \left(\dot{y}_{jk} - \dot{y}_{p1jk}\right)\psi_{jk} - A\dot{\psi}_{jk};$$
$$V^*_{sx2jkI} = \dot{\varphi}_{jk} R_{2jkI} - \dot{x}_{jk} - \left(\dot{y}_{jk} - \dot{y}_{p2jk}\right)\psi_{jk} + A\dot{\psi}_{jk};$$
$$V^*_{sy1jkI} = \dot{x}_{jk}\sin\psi_{jk} - \dot{y}_{jk} + \dot{y}_{p1jk};$$
$$V^*_{sy2jkI} = \dot{x}_{jk}\sin\psi_{jk} - \dot{y}_{jk} + \dot{y}_{p2jk},$$
$$\overline{V}_{sijkII} = \overline{V}^*_{sxijkII} + \overline{V}^*_{syijkII} + \overline{V}^*_{szijkII}; \tag{4.9}$$
$$V^*_{sx1jkII} = \dot{\varphi}_{jk} R^*_{jk1II}\cos\chi_{1jk} - \dot{x}_{jk} - \left(\dot{y}_{jk} - \dot{y}_{p1jk}\right)\psi_{jk} - A\dot{\psi}_{jk};$$
$$V^*_{sx2jkII} = \dot{\varphi}_{jk} R^*_{2jkII}\cos\chi_{2jk} - \dot{x}_{jk} - \left(\dot{y}_{jk} - \dot{y}_{p2jk}\right)\psi_{jk} + A\dot{\psi}_{jk};$$
$$V^*_{sy1jkII} = \dot{x}_{jk}\psi_{jk} - \dot{y}_{jk} + \dot{y}_{p1jk};$$
$$V^*_{sy2jkII} = \dot{x}_{jk}\psi_{jk} - \dot{y}_{jk} + \dot{y}_{p2jk};$$

$$V^*_{sz1\,jkII} = \dot{\varphi} R^*_{1\,jkII} \sin\chi_{1\,jk};$$

$$V^*_{sz2\,jkII} = \dot{\varphi} R^*_{2\,jkII} \sin\chi_{2\,jk},$$

where R_{1jkI}, R_{2jkI} –the radiuses of the rolling surfaces of the first and the second wheels in contacts I;

R^*_{ijkII} – the equivalent radiuses of contacts II;

χ_{ijkII} –the angles of the previous contact (Figure 4.1.);

ψ_{jk} –the attack angle of the wheel pair;

$\dot{x}_{jk}$, $\dot{y}_{jk}$ –the projection of the absolute velocity of the wheel pair center on axis *X-Y* in fixed coordinate system *XOY*;

$\dot{y}_{pijk}$ –the velocities of the transversal displacements of the rail sections that contact with the dedicated wheels

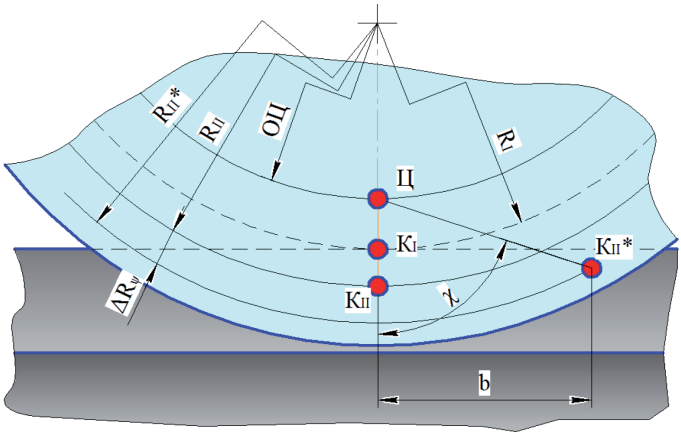

Figure 4.1. Position of Contact Centers in Case of Two Point Contacting and Wheel Climbing on the Rail

Values R^*_{ijkII} and χ_{ijkII} can be obtained from the equations below:

$$R^*_{ijkII} = \sqrt{b^2_{ijk} + \left(R_{ijkII} - \Delta R_{\psi ijk}\right)^2};$$

$$tg\chi_{ijkII} = \frac{b_{ijk}}{R_{ijkII} - \Delta R_{\psi ijk}}, \qquad (4.10)$$

where R_{ijkII} –the radiuses of the wheels rolling surfaces in contacts II when the attack angle is absent;

b_{ijk}, $\Delta R_{\psi ijk}$ –the previous contact and the radiuses increase at expenses of the wheel pair attack angles, then we write:

$$\Delta R_{\psi ijk} = 1.235 \frac{\psi_{jk}^2}{g_{II}^{1,82}};\ b_{ijk} = \frac{\psi_{jk}}{0.15\psi_{jk}^2 + 3.6 \cdot 10^{-4} g_{II}}. \qquad (4.11)$$

The normal loads in the contacts can be determined according to the formulas below:

$$N_{ijkI} = \frac{P_{ijkI}}{\cos\left(arctg\left(g_I\right)\right)};\quad N_{ijkII} = \frac{P_{ijkII}}{\cos\left(arctg\left(g_{II}\right)\right)}. \qquad (4.12)$$

The longitudinal and the transversal axle-box reactions in general view depend on the clearances or deformations in the axle-box nodes:

$$F_{bxijk} = F_{bx}\ \left(\Delta_{bxijk}\right);\quad F_{byijk} = F_{by}\ \left(\Delta_{byijk}\right). \qquad (4.13)$$

The reactions in the axle box nodes can be described by the following relations: the longitudinal reactions in the axle boxes: $F_{mx\ ijk} = -F_{bx\ ijk}$;

$$\text{if}\begin{cases} \delta_{ox} \geq \Delta_{bxijk} \geq -\delta_{ox}; \\ \Delta_{bxijk} > \delta_{ox}; \\ \Delta_{bxijk} < -\delta_{ox}; \end{cases} \quad \begin{cases} F_{bxijk} = 0; \\ F_{bxijk} = (\Delta_{bxijk} - \delta_{ox}) Ж_{bx}; \\ F_{bxijk} = (\Delta_{bxijk} + \delta_{ox}) Ж_{bx}; \end{cases} \qquad (4.14)$$

the transversal reactions in the axle boxes: $F_{my\ ijk} = -F_{by\ ijk}$

$$\text{if}\begin{cases} \delta_o \geq \Delta_{by\ jk} \geq -\delta_{oy}; \\ \Delta_{byjk} > \delta_{oy}; \\ \Delta_{byjk} < -\delta_{oy}; \end{cases} \quad \begin{cases} F_{byjk} = 0; \quad F_{my\ jk} = 0; \\ F_{by\ jk} = (\Delta_{byjk} - \delta_{oy}) Ж_{by} - F_n; \\ F_{by\ jk} = (\Delta_{byjk} + \delta_{oy}) Ж_{by} - F_n; \end{cases} \qquad (4.15)$$

$$\Delta_{bx\ ijk} = x_{b\ ijk} - x_{ijk};\ \Delta_{by\ jky} = y_{bjk} - y_{jk},$$

where $x_{bijk}, y_{bjk}, x_{ijk}, y_{jk}$ –the longitudinal and the transversal displacements of the truck and the wheels pair elements in the axle box connections;

δ_{ox}, δ_{oy} –the longitudinal and the transversal one-sided clearances in the axle box connection;

$Ж_{bx}, Ж_{by}$ –the longitudinal stiffness and the transversal stiffness of the axle box connection;

$F_{bx\ ijk}, F_{mx\ ijk}, F_{by\ jk}, F_{my\ jk}$ –the reactions in the axle box connection applied in the longitudinal direction towards the axle box case; applied in the transversal direction towards the axle end of the wheel pair; applied in both directions towards the truck frame;

F_n –the preliminary compression of the spring element engaged in the axial stop.

4.2. Analysis on the Control of Power Factors

The power factors operating in the 'rolling stock-track' system can be divided into guiding factors and resistance factors within the process of rail track guidance. The sign of the guiding factor is the positive direction of the moment that creates the considered factor in relation to the motion direction. The feature of the resistance factor is its negative value.

However, this division is conditional, because the forces or the moments of the same origin may be of the guiding or the resisting nature in different motion modes or even in different wheel pairs.

4.2.1. Structure of the Power Factors Affecting Wheel Pairs

The main vectors of the transversal external forces that influence the wheel pairs in the absolute coordinates system *XOY* may be expressed as given:

$$F_{yjk} = \sum_{i=1}^{2}\left(S_{xijkI} + S_{xijkII}\right)\cdot\sin\left(\psi_{jk} - \psi_{mk}\right) + \\ + \sum_{i=1}^{2}\left(S_{yijkI} + S_{yijkII}\right)\cdot\cos\left(\psi_{jk} - \psi_{mk}\right) + \sum_{i=1}^{2}\left(H_{ijkI} + H_{ijkII}\right) - F_{byjk}; \tag{4.16}$$

The main moments of the external forces that influence the wheel pairs are as described below:

$$M_{jk} = S_{x\,1\,jkI}\,A_{I1} - S_{x2\,jkI}\,A_{I2} + S_{x1\,jkII}\,A_{II1} - \\ - S_{x2\,jkII}\,A_{II2} + \left(F_{bx2\,jk} - F_{bx1\,jk}\right)B\ . \tag{4.17}$$

In equations (4.16)-(4.17), it should be interpreted as follows:

ψ_{jk}, ψ_{mk} –turning angles with respect to the wheel pairs and trucks in the absolute coordinates system of *XOY*, where $\psi_{jk} = \psi_{rjk} + \psi'_{jk}$;

ψ_{rjk} –the angular position of the radial straight line that passes through the wheel pair gravity center;

A_{Ii}, A_{IIi} –the distance from wheel pair center to the relevant contact centers;

i –the wheel number in the wheel pair;

j –the wheel pair number;

k –the truck number.

The equilibrium equation for N-axial trucks can be expressed as written:

$$F_{mk} = \sum_{j=1}^{N} F_{byjk} - F_{cyk} + \frac{M_{ck}}{D_k} = 0\,; \tag{4.18}$$

$$M_{mk} = \sum_{j=1}^{N} \left(F_{bx1\,jk} - F_{bx2\,jk} \right) B - \sum_{j=1}^{N} F_{by\,jk} C_{jk} - M_{ck} = 0\,.$$

The equilibrium equation of L-truck rolling stock is as follows:

$$F_c = \sum_{k=1}^{L} F_{ck} = 0\,;\; M_c = \sum_{k=1}^{L} M_{ck} = 0\,. \tag{4.19}$$

Equations (4.16)-(4.19) describe the stationary models for trains entering into the curves of the tracks.

As it was noted before, the power factors under consideration cannot be unambiguously classified only as the guiding factors, or only as the resistance factors. The specific values and the directions of the forces and the moments depend on the position, which the wheel pairs take in the rail track.

4.2.2. Power Factors for Rolling Stocks Control when Interaction between Wheel Pairs and Tracks

The components of the longitudinal adhesion forces create a directing moment, which acts on the wheel pair. The moment's positive value is to increase in case of the lateral displacement of the wheel pair to the outer side of the curve. The partial longitudinal sliding in the wheel-rail contacts caused by these displacements depends on the profiles of the wheels rolling surfaces, the wheel pairs transversal displacement with respect to track axis δ_{jk} and curve radius ρ:

$$\begin{aligned} \varepsilon_{1\,jkxI} &= 1 - \frac{R_0}{R_{1\,jkI}} \left(1 + \frac{s}{\rho} \right); \qquad \varepsilon_{2\,jkxI} = 1 - \frac{R_0}{R_{2\,jkI}} \left(1 - \frac{s}{\rho} \right); \\ \varepsilon_{1\,jkxII} &= 1 - \frac{R_0}{R_{1\,jkII}} \left(1 + \frac{s}{\rho} \right); \qquad \varepsilon_{2\,jkxII} = 1 - \frac{R_0}{R_{2\,jkII}} \left(1 - \frac{s}{\rho} \right), \end{aligned} \tag{4.20}$$

where $2s$ –the track width;

R_0, R_{ijkI}, R_{ijkII} –the mean radius of the wheel rolling surface and the radiuses in contact I and contact II, respectively.

When conicity of the rolling surface is 1:20, the maximum slip values, that correspond to the motion in straight lines without touching a flange, reach not more than 0.1%. In the curves with the radius less than 1,000 m, the components of the longitudinal adhesion forces act as a resistance factor. Thus, the mentioned components behave as a force factor for the guiding function only in the straight

lines and curves with the radius more than 1,000 m. In the mid-size and small curves, the components of the longitudinal adhesion forces are the forces of the motion resistance.

The components of the transversal adhesion forces are determined by the transversal sliding (4.8), which depends on wheel pairs attack angles with rails ψ_{jk}.

Depending on the wheel pairs installation, the values of maximal, middle and minimal sliding can be determined according to the equations given below:

$$\varepsilon_{y\,jk}^{\max} = \sin\left[\frac{\pi}{2} - 2\frac{\rho\delta_{jk} + C_k^2}{C_k^2\left(\rho + \delta_{jk}\right)}\right];$$

$$\varepsilon_{y\,jky}^{mid} = \frac{C_k}{\rho + \delta_{jk}}; \qquad (4.21)$$

$$\varepsilon_{y\,jk}^{\min} = \sin\left[\frac{\pi}{2} - 2\frac{\rho\delta_{jk} - C_k^2}{C_k\left(\rho - \delta_{jk}\right)\rho - \delta_{jk}}\right].$$

In Figure 4.2, the dependences of maximal and minimal relative sliding of the outer wheel pair ε_{yjk} on truck wheelbase C_k and the curve radius are shown as profile maps ρ.

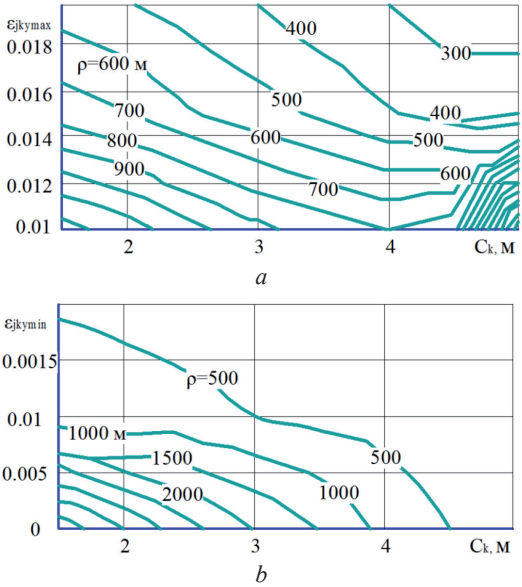

Figure 4.2. Dependences of Maximal (*a*) and Minimal (b) Relative Sliding of the Outer Wheel Pair Climbing (ε_{yjk}) on Truck Wheelbase (C_k) and the Curve Radius (ρ)

The analysis of the shown relations indicates that the components of the transversal adhesion forces can play the role of the guiding factors only provided that the installation of the truck is skewed and the first wheel pair climbing takes place on the inner rail.

In the case of other installation patterns, the factor under the study resists train inversion into the curve. The resistance moments are characterized by high values, because the transversal sliding values are at the critical and the overcritical boundaries.

Moreover, the nature of the resistance moment, which depends on the attack angle or, in other words the increase in the resistance moment with the attack angle increase, introduces certain instability into the process of entering into the curve.

This is particularly evident for the leading wheel pairs mounted on the front of the truck.

The experimental data obtained with 2TE126 diesel locomotive have revealed that in order to eliminate the one-sided installation even on the straight track sections, the greater moment in the support-and-counter device is required.

The gravitational components of the normal reactions are equal to each other, though opposite directional under condition of equal effective conicities of wheels rolling surfaces of the same wheel pair with respect to equations (4.3) and (4.4).

In case of transversal displacement of the wheel pair prior to the flange touching the rail head, conicity difference is rather small for the majority of profiles which virtually does not affect the process of insertion into the curve.

In case of the flange contacting the guiding role of the gravitation components can be rather large depending on normal loads redistribution between contact I and contact II of the two-point wheel-rail contact.

For instance, the flange gravitational component at the wheel vertical loading of 115 kN can reach 196 kN for the flange cone $\gamma = 60^{o}$, while for $\gamma = 70^{o}$ –325 kN.

The dependences between the gravitational components of the adhesion forces on the truck type TE116 position in the rail track are shown in Figure 4.3.

The reverse moment in the body connection with the trucks is an internal moment, which readily create the motion resistance indirectly due to the above force factors.

It is commonly recognized that the reverse moment should be minimal, or even negative in the track's curved segments, this would enable us to improve the guidance characteristics due to forcible trucks installation relating to the track axis.

Figure 4.4 shows the profile maps to describe the dependence of the main vector $\bar{F}$ and main moment $\bar{M}$ of the external forces on the trucks installation.

In Figure 4.5, the dependence of the trucks equilibrium position on the curve radius and the limitations regarding derailing are shown in the form of the blocking circuit.

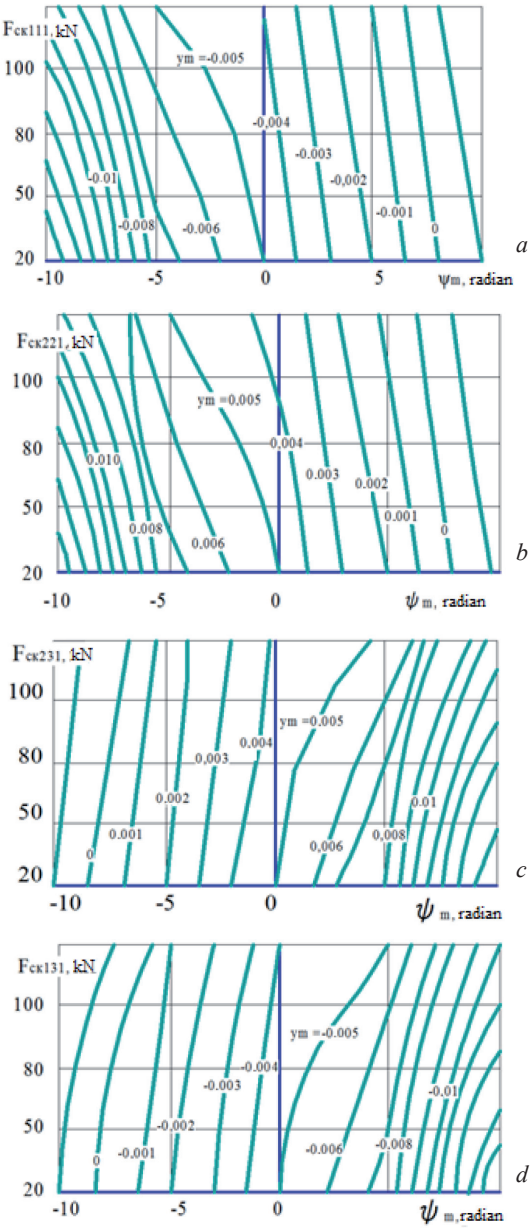

Figure 4.3. Dependences for the Gravitational Components of the Normal Loads in Wheel-Rail Contacts. TE116 Truck Installation in the Curve with the Radius of 900 m

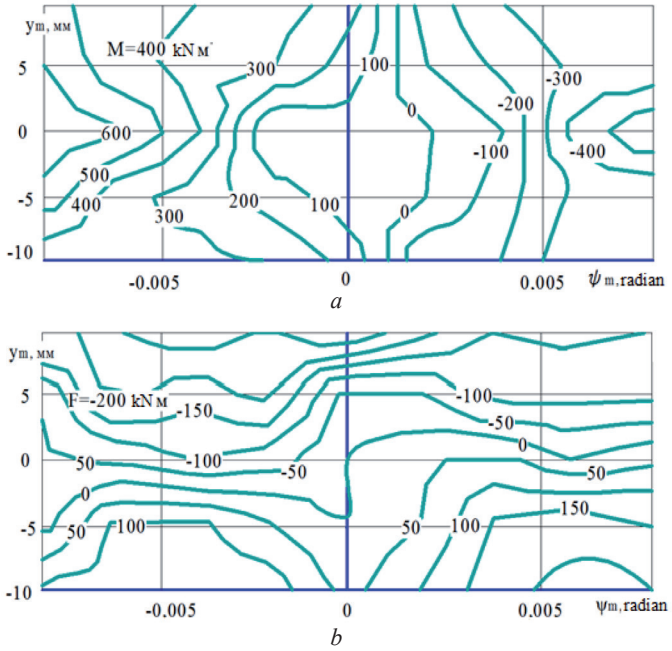

Figure 4.4. Dependence of the Main Vector (*a*) and the Main Moment (b) of the Lateral Contact Forces on 2TE116 Diesel Locomotive Truck Position in the Curve with the Radius of 900 m

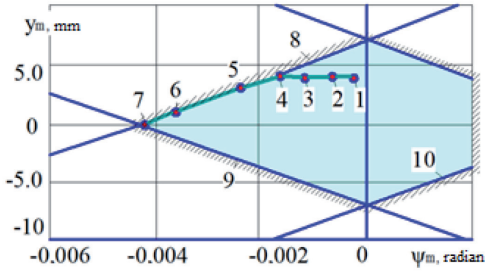

Figure 4.5. Blocking Circuit for 2TE116 Diesel Locomotive Truck Position in Curves of Different Radius: 1– 4,000 m; 2 –2,000 m; 3 –900 m; 4 –700 m; 5 –500 m; 6 –400 m; 7 –250 m

The calculations evidence that the trucks are installed with negative skewness for any curve radius. The kinematic insertion into the curve is possible in the curves with radius exceeding 900 m. If the curves radiuses are within the range of 900–470 m, one-sided flange contact of the first wheel pair occurs with the outer rail. In the curves with the radius less than 470 m, two-sided flange contact always takes place: the first wheel pair and the outer rail, the third wheel pair –the inner rail. The longitudinal and the transversal sliding effects of both the climbing wheel and the free wheel pairs cause the motion resistance and are suppressed by the guiding efforts.

5 MODELING THE KINEMATIC RESISTANCE TO THE MOVEMENT

This section provides the principle provisions of the research methods for the rail rolling stocks kinematic resistance to the movement, based on the closed power circuits. The theory explains some phenomena associated with the kinematics and dynamics of the frictional interaction between the rolling stock and the track, the guidance of the wheel pairs with the rail track and the motion resistance, of both the individual wheel pair and a group of wheel pairs interconnected with the common drive.

5.1. The Nature of the Resistance to the Movement Associated with the Control of the Wheel Pairs by the Railway Track

For many decades, the motion resistance characteristics have not been analyzed at the stage of new rolling stock types design. The improvements on truck arrangements of locomotives and wagons often resulted in worsening in the motion resistance characteristics. The indirect evidence of this is the actual data on the increased wear in the wheel rolling surfaces when operating the new types of multi-axle locomotives. It is worth noting that the intensive flange undercut and the lateral wear of the rail tops are the result of the work produced by the forces of the resistance to the movement and it deserves the special analysis.

The nature of the resistance to the movement is associated with rolling stocks guidance with the track. One of the reasons for the increased wearing of the wheels and the rails is insufficiently exploration maturity of the resistance to the movement associated with the rolling stocks guidance with the track or the kinematic resistance to the movement. The closed power circuits in the system of rail rolling stock guidance are the source of kinematic resistance to the movement, which emerges due to parasitic sliding in the nodes of the closed power circuits. With reference to the theory of closed power circuits, the wheel-rail contacts are nothing but decoupling node points of the frictional type.

The rolling stock kinematic resistance to the movement is caused by the kinematic non-conformity of the geometrical parameters of wheel rolling surfaces and the kinematic parameters of the movement. This becomes the reason of the parasitic sliding.

There are two components in the kinematic resistance phenomenon:

- differential ($w_д$)
- circulatory ($w_ц$).

The first one manifests itself when each wheel contacts separately with the rail through the spatial geometry of the contact.

The other one is a result of the group interaction of the wheel systems or wheel pairs group with the rail track during a guided motion in the rail track due to the circulation of the parasitic power within the limits of one wheel pair, or a group of the wheel pairs connected with the truck frame. The value of this resistance depends on the distribution of relative sliding velocities in the wheel-rail contacts, which are influenced by both, the rolling stock structural parameters, and the rolling stock motion mode. The energy losses due to suppressing the frictional effects of differential sliding and circulatory sliding, determine the kinematic resistance to the movement.

As it is demonstrated in [75], the flange contact between the wheel and rail is characterized by the emergence of the additional differential sliding which leads to the increase in the resistance to the rolling. The picture of differential sliding depends on the wheel attack angle to the rail. When the wheel pair is installed vertically to the track axis, the two wheel contact points are located in the axial plane of the wheel pair in case of the two-point contact, while the flange contact is displaced forward by the value of the touching prevention (b) and upwards by the value of $\Delta R_ψ$, when the phenomenon of the attack angle takes place [75].

The nature of the resistance under the study is associated with the parasitic sliding in the closed power circuits that are created in the wheel pair guidance system by the rail track. The research is based on the energy hypothesis according to which the mechanical energy to suppress the parasitic sliding frictions is the energy of the resistance to the movement.

We suggest that the component of the resistance to the movement to be associated with wheel pairs guidance by the rail track should be termed as the kinematic resistance to the movement. According to the accepted classification, the kinematic resistance to the movement has signs of both, the main resistance and the additional resistance. That is why, in case of the movement on the track straight segments, it should be regarded as a part of the main resistance to the movement, whereas in case of the curved segments, it should be classified as the additional resistance to the movement.

Within the system of truck guiding for the train, there could be distinguished several closed power circuits.

When the two point wheel-rail contact, the closed power circuit is created with two points in the main contact and the flange contacts. The differential slipping emerges in this circuit which can be the reason for the additional kinematic resistance to the movement through the increase in the rolling resistance.

As an example, figure 5.1 shows the distribution diagram of possible normal reactions (N_1, N_2) and adhesion forces (S_1, S_2) in the two-points flange contact of the wheel and the rail.

F_t – the external longitudinal reaction of the truck to the wheel. F_t reaction is the resistance to the movement force which should be suppressed in order to ensure the wheel rolling.

The distribution between normal reactions (N_1, N_2) depends on many factors:

- the motion speed
- the curve radius
- the outer rail lift
- the wheel pair location in the track
- the truck design
- profile of the wheel rolling surface, etc.

Based on Figure 5.1, one can write the following system of the equilibrium equations:

$$\begin{cases} \sum M = S_1 R_1 - S_2 R_2 = 0; \\ \sum F = S_2 - S_1 + F_1 = 0. \end{cases} \tag{5.1}$$

Based on equations (5.1), the value of the kinematic resistance to the movement (W_k) can be obtained:

$$W_k = F_t = S_1 \left(1 - \frac{R_1}{R_2}\right). \tag{5.2}$$

Based on (5.2), the important conclusion can be drawn: the force of the resistance to the movement is $W_k = F_t$ and in any case cannot be equal to zero, when there is the wheel flange contact with the rail.

Under different conditions, the difference between the radiuses of the main contact and the flange contacts reaches 15-30 mm. Therefore, the kinematic resistance to the movement can reach up to 6 % of the adhesion force S_1.

The wheel pairs together with the rail track also create the closed power circuits. The absence of the longitudinal sliding in the wheel-rail contact is only possible in the ideal case. This ideal case is assumed as the case, when a single wheel pair is rolling freely without the flange touching the rails. However, under real conditions of the wheel pair motion within the truck, slipping regularly happens in wheel pairs contacts with rails. This slipping is parasitic and create

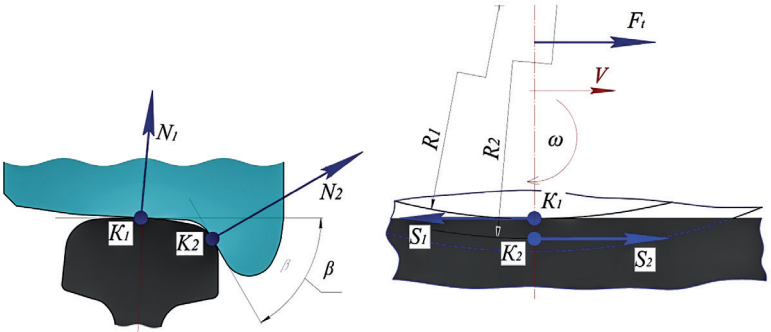

Figure 5.1. Distribution Diagram of Normal Reactions (N_1, N) and Adhesion Forces (S_1, S_2) in the Two-Points Flange Contact of the Wheel and the Rail. K_1, K_2 – the main and the flange contact, respectively; R_1, R_2 – the rolling radiuses in the main contact and the flange contact

the additional kinematic resistance to the movement in both, straight and curved track segments.

Figure 5.2 shows the simplified diagram of adhesion forces (S_{k1}, S_{k2}) and axle box reactions (F_{b1}, F_{b2}), which affect the wheel pair. A case is being modeled when the wheel pair is installed with transversal displacement (Δy) relatively to the track axis and is forcibly rolled on the direct line in the rails. At this, truck hunting is restrained with axle box reactions F_{b1}, F_{b2}.

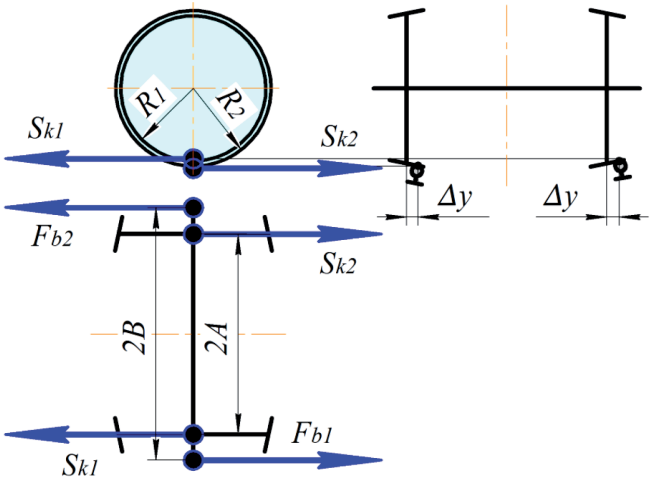

Figure 5.2. Simplified Diagram of Adhesion Forces (S_{k1}, S_{k2}) and Axle Box Reactions (F_{b1}, F_{b2}). Influence on the Wheel Pair

Using Figure 5.2 the following equilibrium equations can be developed:

$$\begin{cases} \left(S_{k1}+S_{k2}\right)A-\left(F_{b1}+F_{b2}\right)B=0; \\ S_{k1}R_1-S_{k2}R_2=0; \\ F_{b1}-F_{b2}-S_{k1}+S_{k2}=0. \end{cases} \tag{5.3}$$

The value of the kinematic resistance to the movement can be obtained from equations (5.3):

$$W_k=S_{b1}-S_{b2}=S_{k1}\left(1-\frac{R_1}{R_2}\right). \tag{5.4}$$

Equations (5.2) and (5.4) reveal the nature of the origin for the emerging kinematic resistance to the movement. The kinematic resistance to the movement appears due to the parasitic slipping in the nodes of the closed power circuits when the wheel pair is guided with the rail track. Such nodes are wheel-rail contacts.

5.2. Mathematical Modeling for Carriages Control by Rails in the Curve

5.2.1. Calculation Scheme of Truck Guiding into the Curve of the Track

Here, we address the wagon two-axle truck steady motion in the circular curve when there is no external influence except the rail track.

In figure 5.3, we illustrate the computational model of the wagon two-axle truck steering provided at its free arrangement in the track. The following designations are applied:

δ – the complete clearance of the wheel pair in the rail track;

δ_{jk} – the clearances in the flange contacts of relevant wheels (j=1, 2) of wheel pairs (k=1, 2);

α – the angle between the truck transversal symmetry axis and the radius of the curve that passes through the truck center pivot;

ψ_k – the attack angles of the relevant wheel pairs and the rails (k=1, 2);

$2C$ – the truck wheelbase;

ρ, ρ_1, ρ_2 – the radiuses of the curve symmetry line, the inner rail and the outer rails;

G – the point of the truck turning relative to the vertical axis – the center pivot;

V – the direction of the truck movement at the right angle to the radial straight line that passes through the center pivot;

OXY – the absolute coordinate system;

$O_k X_k Y_k$ – the coordinate system associated with the dedicated wheel pairs.

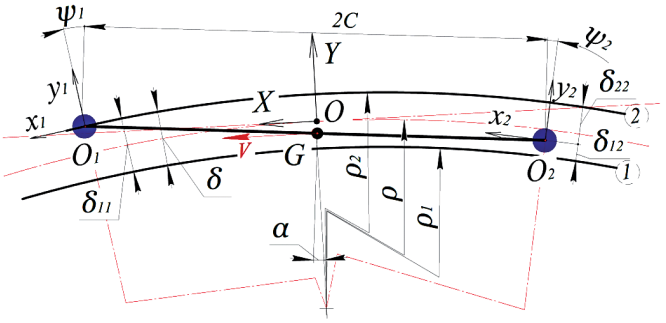

Figure 5.3. Computational Model of the Wagon Two-Axle Truck Insertion into the Curve at the Truck Free Arrangement in the Track

The directions of axes y_k coincide with the radial straight lines passing through the centers of the relevant wheel pairs.

The first wheel pair is a leading one and moves with flange pressed to the outer rail, while the other is in a free position. The actual position of the other wheel pair is determined by the calculations.

Figure 5.4 provides the diagram of the contact forces for wheels of wheel pairs:

а – the vertical cross sections in the contact planes;

б – the horizontal projections of the contact forces.

The following designations are used:

K_{ijk} – the designation for the relevant wheel-rail contacts: i – the contact number as per the type (the main contacts – $i = 1$, the flange contacts – $i = 2$); j – the designation of the contacts by the wheel number (left wheels – $j = 1$, right wheels $j = 2$); k – the contact designation by the wheel pair number (the first wheel pair – $k = 1$, the second wheel pair – $k = 2$);

N_{ijk} – the normal loads in the contacts;

P_{ijk} – the vertical components of the normal loads in the contacts;

H_{ijk} – the horizontal transversal components of the normal loads in the contacts in $O_k X_k Y_k$ coordinate systems;

S_{ijk}, S_{xijk}, S_{yijk} – the adhesion forces, their longitudinal and transversal components in the dedicated contacts within $O_k X_k Y_k$ coordinate systems;

F_x – the longitudinal external force coming from the body to affect the truck and the models of the tractive power necessary for overcoming the additional resistance to the movement in the curve; the force applied to the center pivot and the perpendicular one to the radius of the curve that passes through the center pivot;

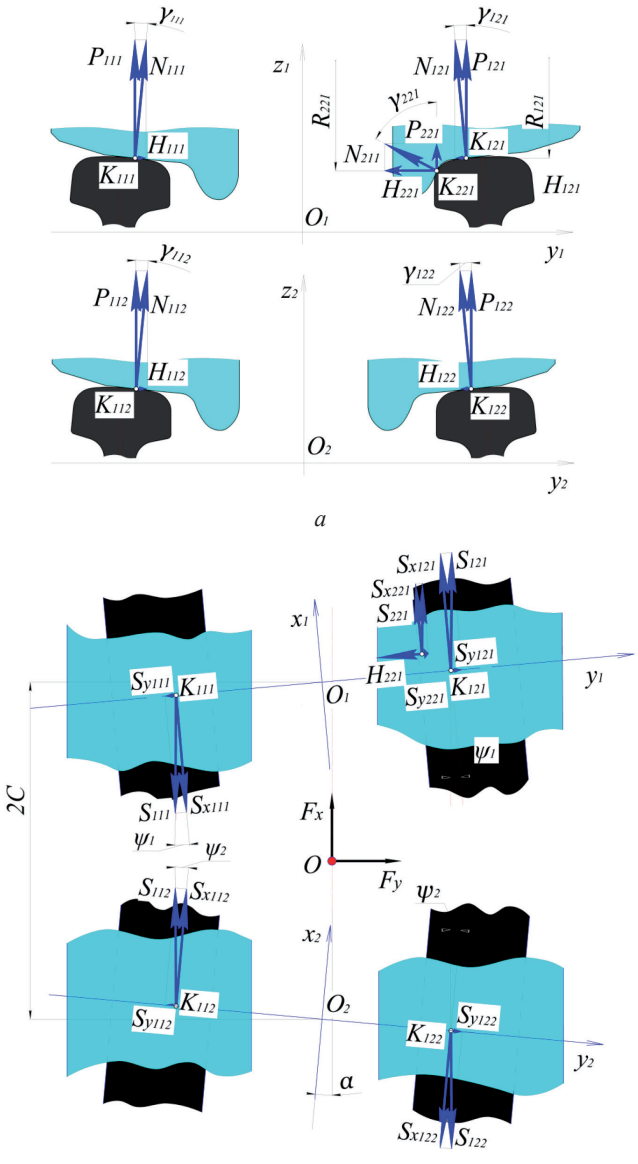

Figure 5.4. Diagram of Contact Forces for the Wheel within Wheel Pairs
a – the vertical cross sections in the contact planes;
b – the horizontal projections of the contact forces

F_y – the transverse force coming from the body to influence the truck and the models of the unbalanced centripetal inertia force.

Force F_y applied to the center pivot and directed along the curve radius that passes through the center pivot.

The principle of quasi-static dynamics can serve for the study on how the parameters of the truck and the track influence the resistance to the movement associated with the truck guidance by the rail track. The rolling stock is considered at its motion in the circular curve being affected by the contact track forces (including the forces of the resistance to the movement), the locomotive tractive power and unbalanced inertia forces which appear due to the circular motion.

5.2.2. The System of Equations for Truck Equilibrium when Guided into the Curve

The main vectors of the external force influence on the wheel pairs, namely the forces main vector $(\vec{F})$ and the main vector of the horizontal forces moments $(\vec{M}_G)$, are equal to zero:

$$\vec{F} = \vec{F}_k + \vec{F}_x + \vec{F}_y ;\ \vec{M}_G = 0 , \tag{5.5}$$

where $\vec{F}_k$ – the main vector of the components of the horizontal forces in the wheel-rail contacts.

Based on Figures 5.3 and 5.4, the relations can be written as follows:

$$\delta_{11} + \delta_{21} = \delta_{12} + \delta_{22} = \delta ;$$

$$\alpha = a\cos(\tau) - a\sin\left(\frac{C}{\rho_2}\right) + a\sin\left(\frac{\rho_2\sqrt{1-d^2}}{2C}\right); \tag{5.6}$$

$$\psi_1 = \frac{\pi}{2} - a\sin\left[(\rho_2 - \delta_{22})\frac{\sqrt{1-d^2}}{2C}\right];\ \psi_2 = \frac{\pi}{2} - a\sin\left(\frac{\rho_2\sqrt{1-d^2}}{2C}\right);$$

In equations (5.6):

$$d = \frac{2\rho_2(\rho_2 - \delta_{22}) - 4C^2 + \delta_{22}^2}{2\rho_2(\rho_2 - \delta_{22})}. \tag{5.7}$$

The adhesion forces in contacts K_{ijk} are calculated by the procedure provided in [75].

The main vector of the components of the horizontal forces in the wheel-rail contacts is expressed as below:

$$\vec{F}_k = \sum_{i,j,k=1}^{2} \left(\vec{H}_{ijk} + \vec{S}_{xijk} + \vec{S}_{yijk} \right). \tag{5.8}$$

The main vector of the moments of the horizontal forces relative to the vertical axis that passes through the center pivot (point *G*):

$$\vec{M}_G = \sum_{i,j,k=1}^{2} \left(\vec{H}_{ijk} l_{Hijk} + \vec{S}_{xijk} l_{Sxijk} + \vec{S}_{yijk} l_{Syijk} \right), \tag{5.9}$$

where l_{Hijk}, l_{Sxijk}, l_{Syijk} – the arms of the dedicated forces for the calculations of the moments relative to *G* point.

Recalling (5.5)–(5.9), system of the equilibrium equations can be developed as given below:

$$\begin{cases} \sum\limits_{i,j,k=1}^{2} \left(\vec{H}_{ijk} + \vec{S}_{xijk} + \vec{S}_{yijk} \right) = 0; \\ \sum\limits_{i,j,k=1}^{2} \left(\vec{H}_{ijk} l_{Hijk} + \vec{S}_{xijk} l_{Sxijk} + \vec{S}_{yijk} l_{Syijk} \right) = 0. \end{cases} \tag{5.10}$$

5.2.3. Calculation Results of the Resistance to the Movement Associated with the Control of Wheel Pairs by Rail Tracks: A Study on the Carriages of 18-100 Type

The solution of equation system (5.5) results in the dependence for the additional resistance to the movement associated with a wagon guidance by the rail track into the curve.

The following is accepted as the calculation input parameters: the motion speed, the curve radius, the outer rail lift, the wheel pair clearance in the track, the wagon loading.

The output data of the calculations are the dependences of the resistance to the movement on the above parameters.

Figure 5.5 shows the calculated dependences of the specific resistance to the movement in curve ω_r on motion speed *V*, curve radius ρ and outer rail lift *h*. In the form of lines, Figure 5.6 illustrates the calculated dependences of the specific resistance to the movement in curve ω_r on truck wheelbase *2C* and curve radius ρ for the motion speed fixed values of *V=30 m/s*, dedicated outer rail lift *h=120* mm and two variants of the clearance values for the wheel pair in the rail track (δ=20 mm and 40 mm).

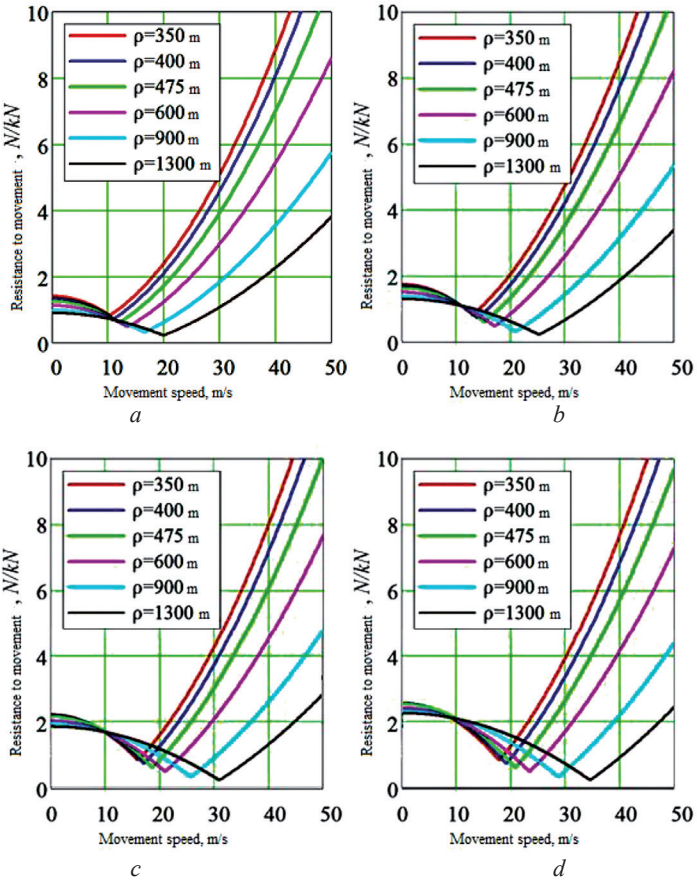

Figure 5.5. Calculation Dependences of the Specific Resistance to the Movement in Curve ω_r (*N*/*kN*) on Movement Speed *V* (m/s), Curve Radius ρ (m) and Outer Rail Lift *h* (mm): a – *h*=50 mm; b – *h*=80 mm; c – *h*=120 mm; d – *h*=150 mm

The dependences represented in Figure 5.6 demonstrate the dependence of the rolling stock resistance to the movement on the truck wheelbase and the wheel pair clearance in the rail track. The results obtained can be the ground for the truck rational parameters to be chosen while designing. These results can also be used when choosing the permissible parameters of the rails lateral displacement.

The mathematical modelling of the rolling stock guidance by the track in the curve is based on the quasi-static dynamics principles. The rolling stock steady motion is simulated in the circular curve: the speed is uniform, there is the influence of the track forces, the locomotive tractive force and the unbalanced inertia force. The special detailed consideration is given to the system of the

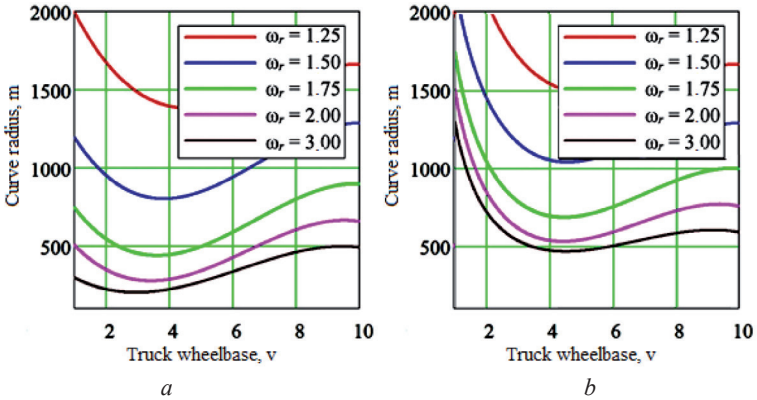

Figure 5.6. Calculated Dependences of the Specific Resistance to the Movement in Curve ω_r (*N*/*kN*) on the Truck Wheelbase and Curve Radius ρ (m) for two Variants of the Wheel Pair Clearance in the Rail Track: a – δ=20 mm; b – δ=40 mm (movement speed *V*=30 m/s; outer rail lift *h*=120 mm)

contact forces. The adhesion forces simulation is performed based on the procedure described in [75]. The arrangement of the truck remains free or loose in the circle. Its actual position is determined by the wheel pairs clearances in the track. The clearances values are defined during solving the equilibrium equations system. The kinematic resistance to the movement is defined as a force that should be applied to the center pivot for the other forces balancing.

The mathematical model and the resistance to the movement assessment procedure allows obtaining the calculation dependences of the resistance to the movement on the following parameters:

- the movement speed;
- the track parameters: the outer rail lift, the track radius, the deviation of the track width influencing the wheel pairs clearance in the track;
- the truck parameters: the truck wheelbase, the diameter and the profiles of the wheels, the geometric deviations of the wheel pairs position in the truck frame.

The calculated results prove the presence of the drastically evident minimal dependence of the resistance to the movement on speed (figure 5.5). However, this minimum does not correspond to the balance speed in the curve. The minimal speed is on average by 15–20 % less than the calculated balance speed.

The research has revealed one more important factor: the trucks with the wheelbase of between 2.5 - 6 m (refer to figure 5.6) show the least resistance to the movement. Thus, the truck wheelbase parameters of 18-100 are not the best ones from the standpoint of the resistance to the movement.

It draws us to the conclusion that the increase in the clearance of wheel pairs in the track from 20 mm to 40 mm increases the resistance to the movement in the curve as much as 25% (also refer to figure 5.6).

The elucidation of the nature of the resistance to the movement is relevant to the rolling stock guidance by the rail track and it offers certain challenges for reducing the kinematic resistance to the movement due to the design parameters of the rolling stocks and the track. The kinematic resistance to the movement can serve as an additional criterion for the optimal choice of the rolling stock mechanical part characteristics. The same is true for the permissible deviations from the parameters of the rolling stock and the track.

The analysis of the publications shows that the vast majority of the researches on the resistance to the movement with the rolling stock have been experimental ones.

The experiments objectives were related to the problem of obtaining the formulas for the traction calculations. By their very nature, they were passive, those that state the regularities associated with the resistance to the movement. The results presented in this book are active since they prove the possibility of influencing the resistance to the movement in the field of the rolling stock and the control is performed through the rail rolling stocks, namely the structural parameters of the truck arrangement and those of the track.

The obtained results show that the very component of the resistance to the movement associated with the track guidance acquires high value only in the curves with radiuses less than 350 m. Due to this, the study results can produce the maximum effect only on the railways with small radius curves. Additionally, the studies can be useful for the development and modernization of the urban rail transport.

The current research is an attempt to confirm the exploitability of the reduction in the resistance to the movement based on the analysis on how the design parameters influence the train performance. The research can be developed at least in three directions. The first one, based on the conventional schemes, is related to the choice of the rolling stock optimal design parameters. The second one is the research of truck arrangement perspective designs on the basis of so-called wheel pair controlled motion. The third direction is the study how the admissible deviations from the parameters of the rolling stock and the track affect the resistance to the movement. These are, first and foremost, the distortions and wheel pairs climbing in the trucks, the deviation of the wheels diameters, etc.

The first two of the said directions are related to the need for changes, sometimes essential, in the designs of the wheel pairs and the trucks. This can be quite problematic with regard to the modernization economic efficiency. More promising is the third direction, which is limited with the technological requirements for the rolling stock maintenance.

5.3. Method to Calculate the Kinematic Resistance to the Movement

The transversal displacement of the wheel pair relative to the track axis determines the radiuses of the wheel rolling surfaces. The difference in wheel radiuses, in its turn, determines the instantaneous radius of the rotation, at which the wheel pair can be rolled without slipping in the wheels-rail contacts. Such wheel pair motion is to be called the kinematic movement along the so-called equilibrium trajectory.

However, due to the interaction between the wheel pairs through the truck frame, the actual trajectory of the wheel pairs rolling differs from the equilibrium trajectory. A rather tight connection between the wheels leads to the circulation of power in the circuits of 'rail track-wheel pair' and the redistribution of the power flow between the wheels, as a consequence the increase in the resistance to the movement occurs. In the case of the locomotives, this also causes a deterioration of the adhesion properties. In the case of the wheel pairs group drive, the power circuit has several branching chains. The energy of the power circulation in the circuit is absorbed, mainly in the wheel-rail contacts, and partly in the dissipative connections of the trucks. The uneven distribution of the power flux between the wheels depends on several factors listed below:

- the rigidity of the adhesion characteristics;
- the rigidity of the axle, i.e. parameters of the wheels connection;
- the geometric characteristics of the wheel pair, including conicities and the diameters of the rolling surfaces, the track width and the truck wheelbase;
- the parameters of the longitudinal and the transversal connections in the axle boxes (the wheel pair with the truck frame);
- the radius of the track curve segment.

As it has been mentioned, the circulatory resistance is the result of the power flows circulation of the closed power circuits. The wheel-rail contacts act as decoupling nodal points. The level of circulating power is limited by the boundary value of the adhesion forces in the contacts, due to the complete slipping or the pseudo-slipping. Therefore, the resistance to the movement of the rolling stock under unsatisfactory conditions of the wheel-rail adhesion is lower than under good ones.

5.3.1. Reduction of Forces and the Moments of the Movement Resistance

The calculation of the kinematic resistance to the movement is based on the reduction of the horizontal contact reactions, or their moments to the gravity

center of the train. The reduction method employs the provision on the equality of the sum of the works performed by each of the considered contact forces on the possible displacements, and the work of the total force of the resistance:

$$A_W = \sum_{i=1}^{N} A_{F_i}, \tag{5.11}$$

where A_{F_i} – the work of i-force that caused the possible displacement;

A_W – the work of the reduced force of the kinematic resistance to the movement;

N – the number of reduced forces.

The current value of the reduced relative resistance to the movement can be determined according to formula below:

$$w_\kappa = \frac{\sum_{i=1}^{N} F_i V_i \cos(\vec{F}_i, \vec{V}_i)}{V_C Q}. \tag{5.12}$$

where F_i – the contact forces;

V_i – the absolute speed of relevant *Fi*-force application point;

V_C – the absolute speed of the rolling stock gravity center motion;

Q – the rolling stock weight.

Taking into account the structure of the contact forces (4.1) and recalling (4.7)-(4.9), we obtain expressions for the numerator of equation (5.12), which is a capacity sum of the contact forces:

$$\begin{aligned} F_i V_i \cos(\vec{F}_i, \vec{V}_i) = \sum_{i=1}^{2} [S_{xijkI} V^*_{sxijkI} + S_{xijkII} V^*_{sxijkII} + \\ +(S_{yijkI} + S_{yijkII} + H_{ijk})(V^*_{yijkI} - \dot{y}_{pijk}) + S_{zijkII} V^*_{sijkII}]. \end{aligned} \tag{5.13}$$

5.3.2. Impact of Carriage Truck Parameters on the Kinematic Movement Resistance

The study on the locomotives and the wagons of the full-scale production has allowed determining the main factors influencing the kinematic resistance to the movement, they are truck wheelbase, the profiles of the rolling wheels surfaces, the stiffness in the wheel pairs spring connections with the truck frame and the clearances in the axle box nodes.

In this section, we regard the example of a four-axle two-truck train in order to study the influence of above factors on the resistance to the movement in curved segments of tracks.

Figure 5.7 shows the dependences of the leading wheel pair to the rail angles of attack on the truck wheelbase and the curve radius for the clearance in rail track δ = 30 mm and 40 mm. As it is evident from the results obtained, when the clearance in the rail track exceeds 30 mm and the truck wheelbase is less than 3 m, the attack angles reach high values of up to 0.025 radian. Moreover, the dependence on the curve radius is insignificant.

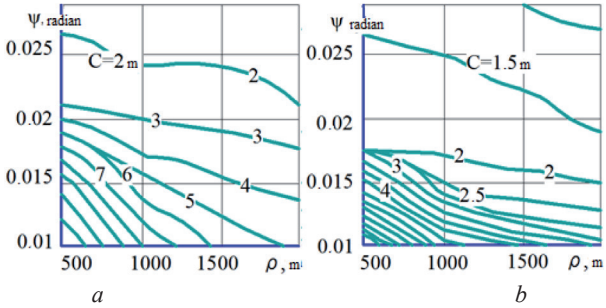

Figure 5.7. Dependences of the Leading Wheel Pair to Rail Angles of Attack on the Truck Wheelbase and the Curve Radius: a – δ =30 mm; b – δ =40 mm

In figure 5.8, we illustrate the profile maps to describe the equal level of the kinematic resistance to the movement as the dependence on the same values: truck wheelbase, the curve radius and the clearance in the rail track. The dashed lines stand for the minimum levels of the kinematic resistance to the movement. The smallest values of the kinematic resistance to the movement correspond to the truck wheelbase of 2.5 ... 8.0 m. The increase in the clearance in the track from 20 mm to 80 mm leads to the increase in the resistance in the curve by 25%.

The studies of the mathematical models of the locomotive and the wagons with different wheel profiles have shown a significant influence of the rolling surface shapes on the kinematics and the dynamics of the frictional interaction between the rolling stock and the track.

Figure 5.9 shows a histogram of the calculated kinematic resistance to the movement for 2TE116 rolling stock with different wheel profiles for the speed of 30 m/s in the curve of 1,000 m and the outer rail elevation of 120 mm.

It is difficult to give an unambiguous answer to the question of what exactly is that factor which influence is determining for the parameters of this interaction: the shape of the rolling wheel surface or the shape of the flange. However, we can say for sure that the higher values of the kinematic resistance to the movement are common for the profiles with the large angles of the conicity.

For example, the profiles with the flange cone of 70° are characterized by higher values of the resistance (1.30 ... 1.46 N/kN), while the respective values are lower (0.85 ... 1.08 N/kN) for the profiles with the flange cone of 60°. The

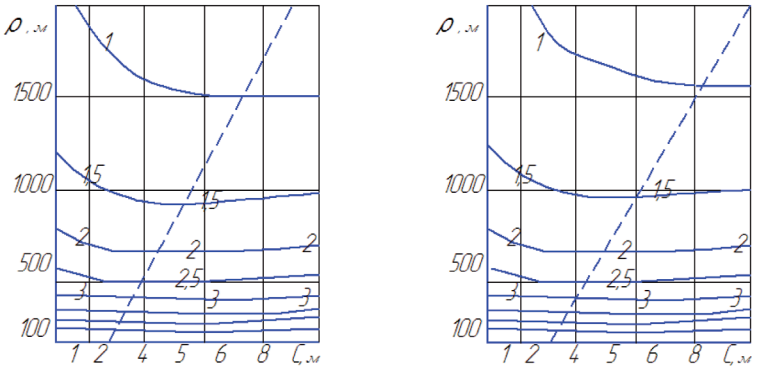

a *b*

Figure 5.8. Dependence of the Kinematic Resistance to the Movement on Truck Wheelbase (*C*), Curve Radius (ρ) and Rail Track Clearance (δ): a – δ = 30 mm; b – δ = 40 mm

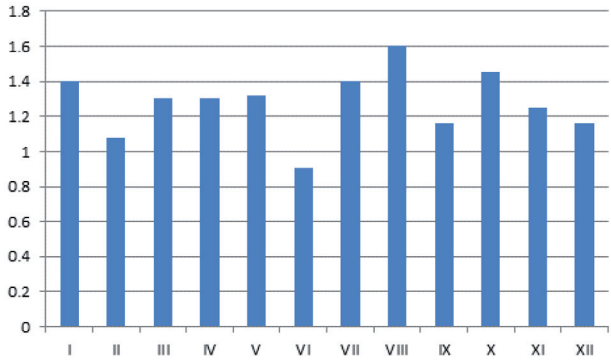

Figure 5.9. The Values of the Kinematic Resistance to the Movement: TE116 (N/kN) with different wheel profiles, the speed of 30 m/s, the curve of 1,000 m, the elevation of the outer rail of 120 mm; wheel profiles: I - Heimann-Lotter; II - standard German wheels until 1953; III – DBII (Germany); IV - I type (Germany); V - II type (Germany); VI and VII - R2 and R6 types, respectively (England); VIII – standard (Japan); IX and X – standard wheels and experimental wheels of Uni-Point type (USA); XI – Sc type (France); XII - standard wagon (Ukraine)

influence of the wheel pairs-truck frame longitudinal connection on the resistance to the movement parameters is studied within the range of the longitudinal stiffness of the axle box links ($Ж_{bx}$ = 1.00 ... 20.0 kN/mm).

Figure 5.10 shows the dependences of the kinematic resistance to the movement on the curve radius of the 200 ... 1000 m and the speeds of the movement with the stiffness of $Ж_{bx}$ = 1, 5, 10 and 20 kN/mm. The calculations

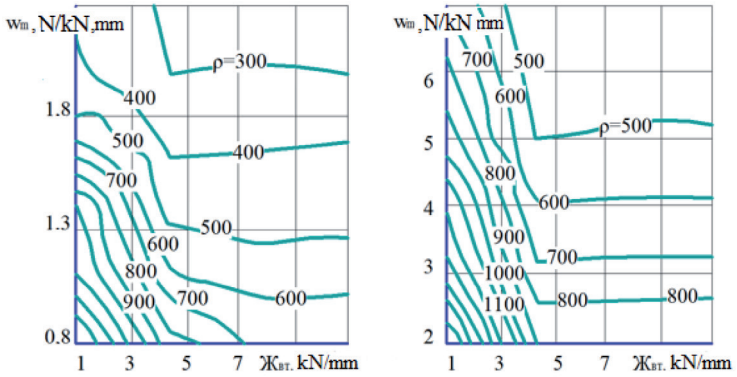

Figure 5.10. Dependence of the Kinematic Resistance to the Movement of the TE116 Rolling Stock on the Longitudinal Stiffness of Axle Box Links ($Ж_{bx}$) and the Curve Radius (ρ): a – V = 5m/s; b – V = 50m/s

results also indicate that at speeds higher than 15 m/s, the increase in the stiffness more than 5 kN/mm as much practically does not affect the parameters of the resistance to the movement, especially in small radius curves.

Within the limits of the longitudinal stiffness change in the axle box links from 5 kN/mm to 1 kN/mm, the resistance increase is observed by 1.5 ... 1.7 times higher. The minimal values of the resistance to the movement occur at combinations of the speeds and the curve radiuses, which are close to the equilibrium motion mode:

$$\rho = \frac{163}{h} \cdot V^2 ,$$

or at h = 120 mm:

$$\rho = 1.36 \cdot V^2 . \qquad (5.14)$$

The sharp drop in the resistance to the movement in the region of the equilibrium curve is related to the leading wheel pairs attack angles being close to the minimum absolute values. Curve 2 $\left(\rho = 0.675 \cdot V^2\right)$ in Figure 5.14 describes the combination of the speed and the curve radius for the maximum allowable comfort norms of the unbalanced centripetal acceleration of a = 0.75 m/s^2. However, it is difficult to indicate the optimal value for the stiffness of the longitudinal connection in the axle box node. The kinematic resistance to the movement in coordinates ρ(V) is strongly influenced by the speed of the movement. The value of $Ж_{bx}$ = 4.2 ... 7.5 kN/mm could be regarded as the optimum value for the equilibrium motion mode. For the comfort zone, this value is $Ж_{bx}$=3.6 ... 6.8 kN/mm, while for the movement with the speeds higher than the comfort speed – $Ж_{bx}$=8.0...12.0 kN/mm.

6 WAYS TO IMPROVE CONTROLABILLITY AND REDUCE THE RESISTANCE TO THE MOVEMENT OF RAIL CARRIGES

The analysis on the structure of the rolling stock resistance to the movement indicates its dependence on the factors and currently it is difficult to change the significant part of the latter. First of all, they are the state of rail tracks, which require large capital costs for maintenance and repair. Moreover, it is not possible to significantly reduce the resistance to the movement due to parameters of the wheel-rail contact. On the contrary, with the current tendency of increasing the wheels diameter with simultaneous increase in axial loads, we are to expect the increase in the resistance to the rolling motion.

For the high-speed rolling stock, the aerodynamic resistance becomes decisive with great potential for its reduction.

This is confirmed, in particular, by the fact that up to 90% of publications dedicated to the resistance to the movement over the past 40 years have been addressing the area of the rolling stock aerodynamics study. Unfortunately, for Ukrainian railways, especially for urban railroad transport, this area is not yet relevant.

A large reserve for reducing the resistance to the movement with the rolling stock by means of replacing the plain friction bearings for rolling bearings has already been consumed, therefore its further research in terms of the resistance to the movement is not promising. However, the study on the components of the rail rolling stock resistance to the movement allows us to make a conclusion on certain prospects availability for reducing this type of resistance, due to the reduction in the kinematic resistance caused by the comprehensive interaction of the wheel pairs dynamic system with the rail track when the rolling stock is guided by the track. Moreover, within the framework of this area, the comprehensive research is required on the frictional interaction of the rolling stock and the track and the search on their basis of new engineering solutions for the truck arrangement designs that are capable of allowing the control over the kinematics and the dynamics of the wheels-rail frictional interaction. This primarily relates to the

studies on the horizontal forces in the wheel-rail contacts, the forces of this kind arise when the rolling stock is guided by the rail track.

Furthermore, the development of rolling stock truck arrangement designs is associated with two main problems. The first one is the stability and the level of the horizontal impact on tracks for high-speed movement. The second one is the resistance to the urban rail transport insertion into small radius curved tracks. Both problems are united with a common problem of transversal controllability of rolling stocks.

With the frame design to provide the rolling stock movement, the opportunities for it to be steered around the small radius curves were very limited due to the parallelism of all wheel pairs axles and relatively small clearances in the rail track. The transition into the truck designs was the first step for implementing the principle of rolling stock guided movement. Truck rolling stocks are able to cope with the curve radiuses of 6 ... 8 times smaller than those common for frame rolling stocks.

6.1. Linked Carrieges Design Development

Jointed trucks are employed with many rolling stocks of mass production. At first, it was an imposed engineering solution, because the longitudinal efforts were transmitted through jointed means located on the truck frameworks, for example, electric locomotives of *VL8, VL22, VL23*, and others. The disadvantage of rigid longitudinal attached connections between the trucks is the increase in the inertia moment when the group of the connected trucks turns, which consequently increases the lateral impact on the track. However, along with the disadvantages, the attached trucks have a number of advantages associated with the improved steering around the curved tracks. From this standpoint, the attached connections between the trucks, in most cases spring ones, able to transmit the horizontal transversal forces from one truck to the other have been widely applied again for the recent past years.

There are many design types of spring attached connections between trucks, but the majority of them has one-spring or two-spring devices with horizontally located springs.

For example, in K-series of electric locomotives *(Siemens-Schuckertwerke and Krupp)*, the spring unit is connected to a single truck, while its rod passing between the springs and the ball insert case is connected to another truck (refer to Figure 6.1). Depending on the direction of the trucks relative displacement, the right spring or the left spring is compressed, transmitting the reciprocal horizontal forces from one truck to the other.

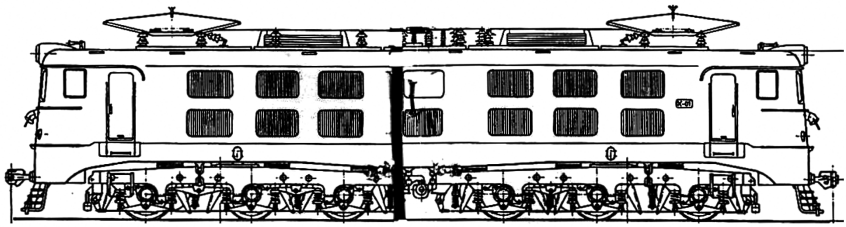

Figure 6.1. K (Kaiser) Electric Locomotive Manufactured by *Siemens-Schuckertwerke and Krupp*

VL80 electric locomotives are equipped with one-spring device of the same operating principle. The spring attached connections between trucks are used in electric locomotives of ChS2, Re2/2, and others.

It is believed that the spring connection between trucks significantly reduces the guiding efforts in the small radius curves of both the front and the rear trucks, although when driving in curves with the radiuses exceeding 600 m and in the straight sections of tracks it is ineffective and sometimes harmful. Therefore, a transversal clearance is usually made in a spring connection to exclude the trucks interaction when they all experience small deviations.

6.2. Carriages with Radial Installation of Wheel Pairs

The advantage of the traditional wheel pairs is their ability to self-adjustment with respect to the track axis and the ability to achieve the certain movement speeds without flanges touching the rails. One of the conditions for wheel pair ideal rolling in the curve, i.e. its movement without wheels slipping relative to the rails, is its radial installation in the track.

According to the generally accepted view, the trucks with wheel pairs able to align themselves radially in curves have a number of advantages over rolling

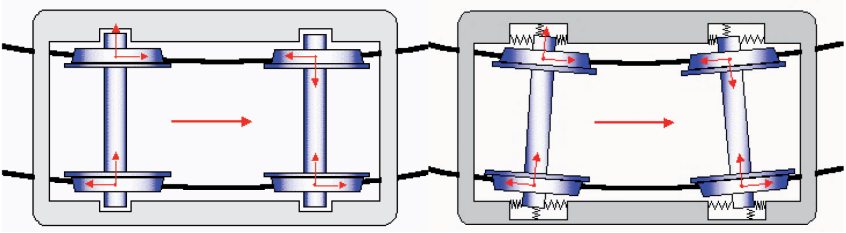

a *b*

Figure 6.2. Rolling Stocks of the Traditional Design (*a*) and Rolling Stocks with Radial Wheel Pairs (*b*) [146]

stocks with conventional 'fixed' wheel pairs. The latter generated greater loading on the rails.

Many theoretical and experimental studies have proved that the radial installation for wheel pairs can significantly reduce the parasitic slipping in the contacts, the load on the flange contacts and consequently decrease the flange wear and the resistance to the movement.

The wheel pairs with the trucks of the traditional design do not have the guiding mechanism for the axis rotation in the plane. Contrary to popular belief, in the ideal case, the wheel flanges should not touch the rails. The flanges should be a preventive measure against the wheels derailing. The wheel pairs, as a rule, have a fairly fixed connection with the trucks frames with respect to the rotation in the horizontal plane.

The idea to apply adaptable wheel pairs and to enjoy their alignment in the truck along the axis radiuses of the rail track in the railroad sphere was definitely inspired by the automotive industry. The possibility to control the motion trajectory by means of the track clearance and to drive the train in any modes without the wheel flange-rail contacting turned out to be very attractive one. This would make it possible to significantly reduce lateral sliding and wear in the contacts and to decrease the resistance to the movement.

The radial installation of the wheel pairs in the truck frame reduces the contact forces in the flange contacts of the wheels with rails. As a consequence, there is a reduction in the wear of the wheels and the rails as well as the decrease in the resistance to the movement, this also improves the rolling stocks guidance in the track curved segments.

6.2.1. HTCR-II Trucks Locomotives Developed by Electro-Motive Diesel

One of the contemporary developments for the sphere of rolling stock with the trucks controlled guidance by rail track is HTCR-II, the three-axle locomotive developed by the Electro-Motive Diesel (Figure 6.3). The letter R in the truck index indicates a modification with the radial alignment of the wheel pairs in the curve.

6.2.2. Truck of 2TE25k Locomotive Being Studied

The another example of the radial truck is an experimental 2TE25k locomotive truck, developed by *All-Russian Scientific-Research and Design-Technological Institute* and built at *Bryansk Machine-Building Plant* (refer to Figure 6.4).

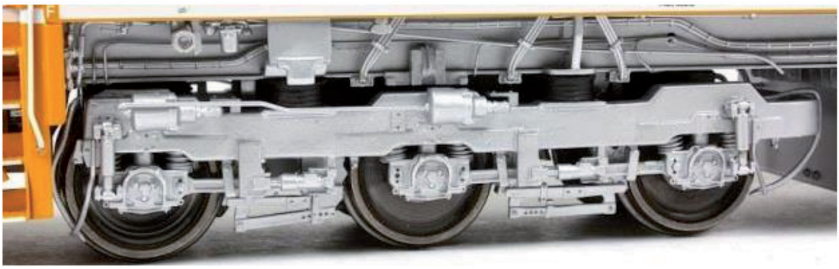

Figure 6.3. Locomotive Three Axle Truck. *HTCR-II Trucks* (*Electro-Motive Diesel Company*) with the Wheel Pairs Radial Alignment

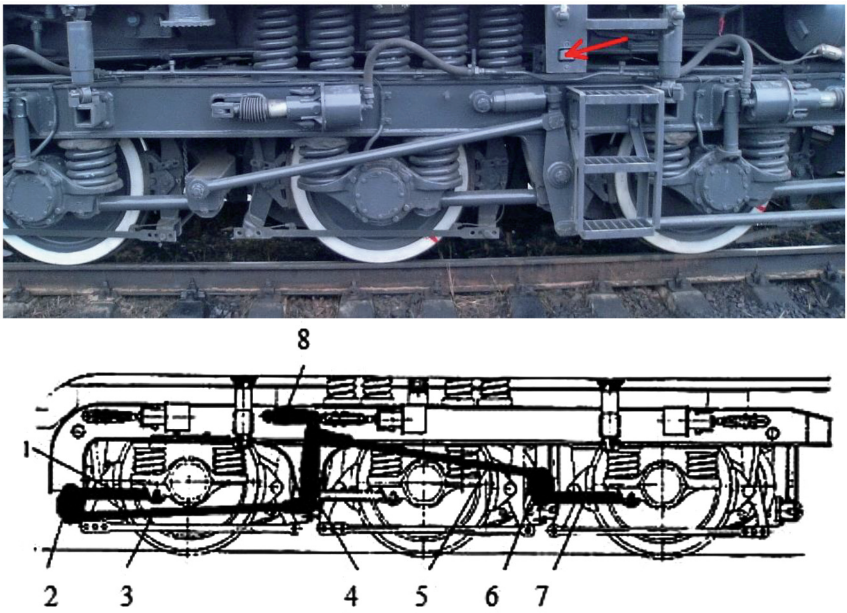

Figure 6.4. 2TE25k Locomotive Truck Design with Controllable Position of the Wheel Pairs in Curves

The mechanism of radial alignment consists of as follows: link (1) and (7) of the outermost axle boxes are connected with transverse equalizers (2) and (6). Rods (3) and (5) are connected with the equalizers ends while the opposite ends of the rods are connected with vertical two-arm lever (4). The lever upper end extension is connected to the hydraulic shock absorber (8). The trucks with the wheel pair radial installation are characterized by the lesser resistance to the movement and the lesser flange wear when movement in the curved track segments.

Nevertheless, despite all these advantages, the trucks with wheel pairs radial installation have not been used extensively due to the complexity of the mechanism to control the wheel pairs positions, and consequently, their high cost.

6.2.3. Wheel Blocks of Talgo High-Speed Spanish Electric Trains

The wheel blocks of high-speed Spanish trains *Talgo* (Figure 6.5) can be considered as the most advanced implementation of the principle of radial wheel pairs. The application of the body pendulum tilting along with the radial wheel pairs in *Talgo* trains allows increasing the train speed in the track curved sections.

At this, the negative impact of centrifugal unbalanced acceleration on the passenger travel comfort is reduced.

In this case, it is particularly important that the body tilt occurs automatically under the action of the gravity and the centrifugal force and does not require the use of a complicated servo drive with electronic control, onboard gyroscopes, as the tilt occurs in systems of rolling stock body forcible tilt.

The truck arrangement of Talgo passenger wagons is constructed without the use of the conventional wagon truck and wheel pair. This engineering solution

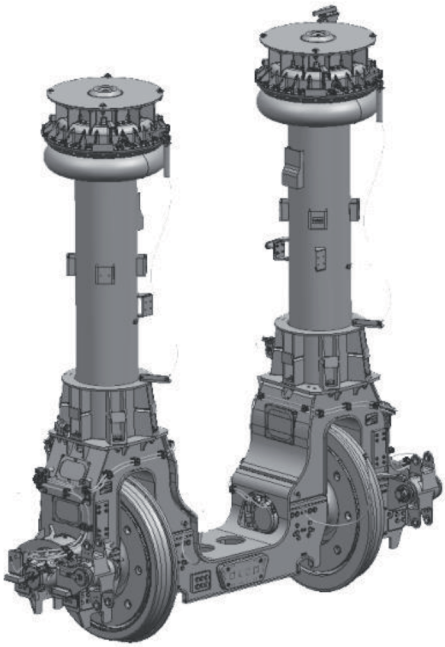

Figure 6.5. Wheel Block of *Talgo*, Spanish High-Speed Electric Train

is based on the Talgo-designed wheel block. The rigid steel frame of the wheel block is made in the form of a yoke in which the wheel assemblies are fixed. Moreover, the wheels are not connected to each other with any rigid axle and can rotate with different angular speeds, which prevents the slipping of the wheels while moving in curves, on the contrast to the conventional design of the wheel pairs with which the wheel slipping often takes place. The operation of the 'the wheel block radial arrangement' system in the curved sections of the track allows increasing the service life of the train truck arrangement elements while reducing the wear of the rail facilities.

The system of 'the wheel block radial arrangement' is installed on all wheel assemblies (except for the final wagons) and consists of the longitudinal rods, the transverse rods and the equalizers that make up the system to ensure the automatic radial alignment of the wheel blocks when entering the curve of the rail track. The use of air suspension in combination with the systems of the pendulum tilt of the body and 'the wheel block radial arrangement' in the curves allows ensuring the high degree of the wagon running smoothly and consequently the significant increase in the passenger comfort.

6.2.4. Technical Solutions for Designs of Wheels with Radial Installation of Wheel Pairs

There are a large number of engineering solutions for the trucks wheel pairs position control. Some of them have been developed as real rolling stocks, however, most of them remains to be the paper projects. All of them can be classified into three groups according to the actuating mechanisms operating principle used for the wheel pair yaw. The first group includes the trucks with the wheel pairs installed in a position close to the radial one, which is achieved due to the guiding forces that arise in the wheel-rail contacts.

The second group includes structures based on the control action of the inertial forces. The third group designs use the principle of forcible turning the wheel pairs in order to improve their steering around the curved sections of the track.

Trucks with the radial alignment of wheel pairs is achieved due to the guiding forces in the wheel-rail contacts. Re4/4-46 trucks of the electric trains can serve as an example of the trucks with the wheel pairs capable of self-arrangement due to the guiding forces.

A similar scheme is described in patent [151] 'Two-axle truck' (Figure 6.6). The dual self-arrangement truck comprises frame (1), bracket (2) and tractive

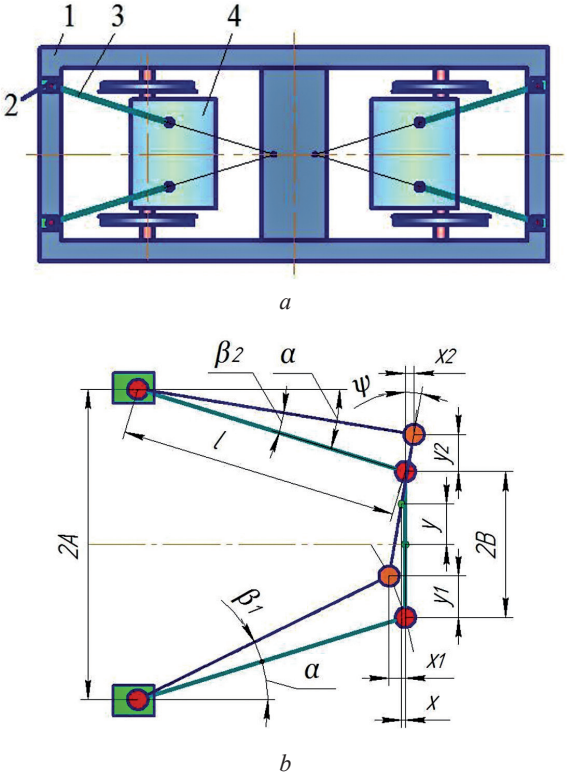

Figure 6.6. Two-Axle Truck (a.c. 1206153) [151]

motor (4). Each motor (4) is connected to frame (1) by four spring draw rods (3), which are mounted with slopes towards the truck gravity center. Moreover, draw rods (3) form a pivoted truncated pyramid, symmetric to this gravity center.

During the truck motion, the draw rods move under the action of transverse guiding forces acting on the wheel pairs. In this case, the gravity center of the wheel-motor block is displaced in a transversal direction, which eliminates the wheel pairs oblique setting. When moving in a curve, the wheel pair is arranged in the position close to the radial one, as a result of the action of the contact forces and the inertia forces of the rolling stock elements.

The relations between transversal displacements of the wheel pair (y), angular rotation (ψ) and longitudinal displacement (x) can be expressed as follows:

$$y_1 = l\left(\sin\alpha + \beta_1\right) - A + B\,;\;\; y_2 = A - B - l\cdot\sin\left(\alpha - \beta_2\right)\,;$$

$$x_1 = l\left[\cos\alpha - \cos\left(\alpha + \beta_1\right)\right];\ x_2 = l\left[\cos\left(\alpha - \beta_2\right) - \cos\alpha\right]; \qquad (6.1)$$

$$\psi = \frac{x_1 + x_2}{2B + y_1 - y_2}.$$

As an example of the most simple variant of the wheel pairs spring connection with a truck frame can be considered as a self-alignment wheel pair, shown in Figure 6.7. With its spring grouping (1), wheel pair (2) is connected with frame (3). The cradle suspension is created; it is with suspension axles (4), which intersect above the axle of the wheel pair.

The Liechty truck structure belongs to the same group (refer to Figure 6.8). Wheel pairs (1) are installed to yaw along with the controlling guides (2). Guides (7) can rotate relatively to the truck frame around pivots (3). Both guides (7) are connected in middle point (4) by angle lever (5) with bracket (6) of body (8).

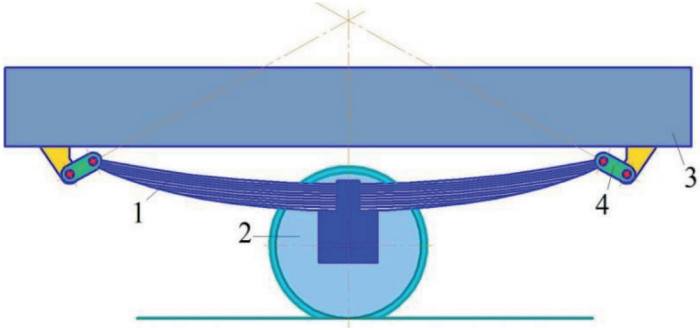

Figure 6.7. Self-Alignment Spring-Based Wheel Pair

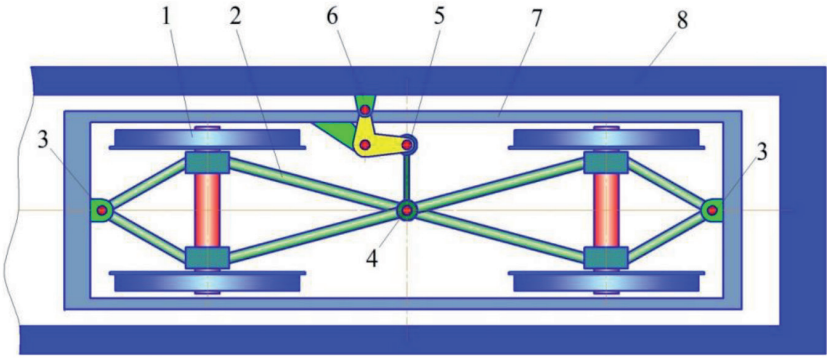

Figure 6.8. Liechty Truck

The two-axle truck with radially adjustable wheel pairs with cross-linkage is reported in European patent EP 2157007 A1 [147]. The two-axle truck consists of two cross-wires that are diagonally connected by the both wheel pairs within the truck and contains L-shaped dimensional adapters (3) (refer to Figure 6.10). They are connected by two crossed draw rods (4) and (7), which are firmly connected to axle box (1) through carrier of axle boxes (2). Dimensional adapter arms (3) do not lie in the same plane and therefore dimensional adapter (3) has at least one other bend, through which its points of connection with axle box carrier (2) and draw rod (4) and/or (7) will get into the desired position [147].

The steering railroad truck (patent US 8276522 B2) [148]. This truck includes a frame, two or more wheel pairs, and steering linkage that connect wheel groups to support motion control (refer to Figure 6.9).

The truck is equipped with sensors for monitoring yaw angle and yaw velocity. The output signal of the sensor is processed to determine the curvature of the track and to determine the train speed and the vehicle body velocity.

The processor actuates the alignment rams to adjust the body position relatively to the frame in response to the track curvature and the current frame position to increase the stability of the wheel pairs.

Figure 6.10 shows an embodiment of the construction of a two-layer connection of the truck with body (10), equipped with frame (11), wheel pairs

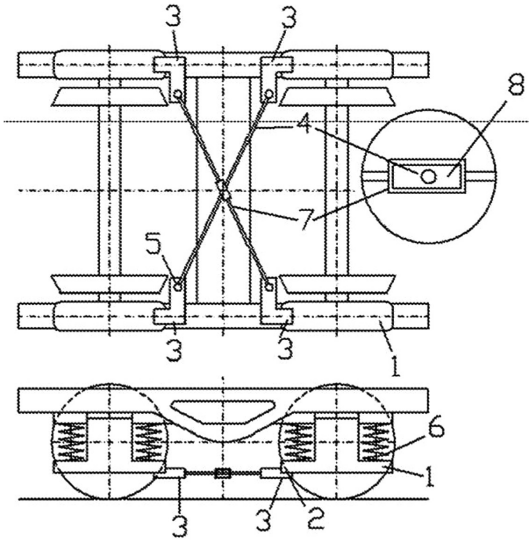

Figure 6.9. Truck with Axles Radial Arrangement. Patent EP 2157007 A1 [147]

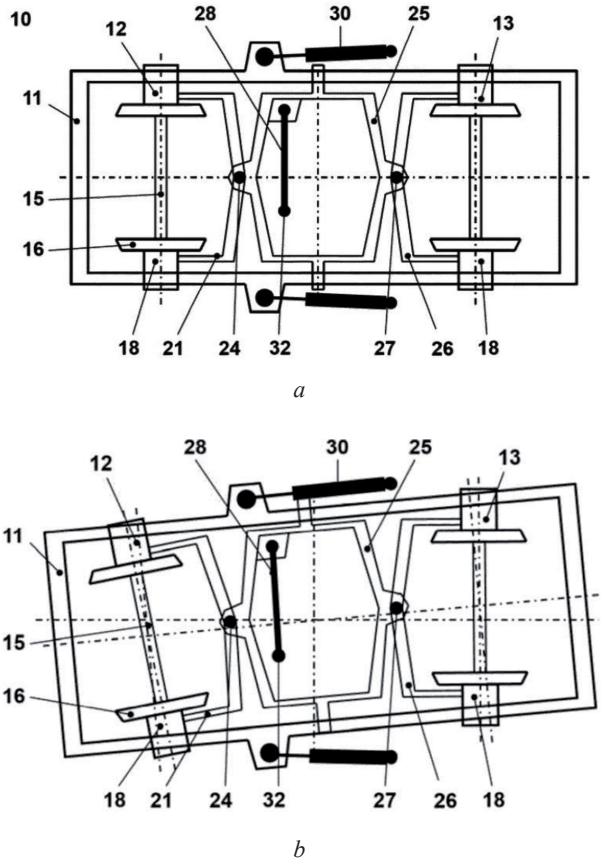

Figure 6.10. Truck with Wheel Pairs Capable to Radial Alignment in Curve. US Patent Code 8276522 B2 [148] – Variant 1

(12), (13). Front wheel pair (12) and rear wheel pair (13) include axles (15), conical wheels (16) and wheel axle boxes (18). Front wheel pair (12) is connected with swivel frame (21) through axle boxes (18).

Swivel frame (21) is connected through pivot element (24) with intermediate frame (25). Intermediate frame (25) is substantially rectangular and is also connected to another frame (26) through pivot element (27). Swivel frame (26) is connected to axle boxes (18) of another wheel pair (13). Intermediate frame (25) is connected to the vehicle body by coupling (28).

Thus, wheel pairs (12) (13) are connected so that the orientation of front wheel pair (12) affects the orientation of rear wheel pair (13).

When truck (10) moves along the curved track, wheel groups (12) and (13) move so that wheels (16) of wheel pairs (12) and (13) touch the flanges at the same positions. When front wheel pair (12) moves together with frame (21), this causes intermediate frame (25) turns, which results in frame (26) turning and directing other wheel pair (13) in a position that is symmetrical to the position of first wheel pair (12) with respect to the transversal axis of frame (11). Intermediate frame (25) yaws transversely due to the connection with body (28), when front wheel pair (12) follows the track curved segment.

Furthermore, truck (10) has alignment rams (30) that connect truck frame (11) with the body. Alignment rams (30) are arranged longitudinally on the opposite sides of frame (11). Alignment rams (30) may include a pneumatic, hydraulic or electric actuator that responds to the output signals of the sensors indicating the truck position in the curve.

When truck (10) enters the track curved segment, the processor processes the output signal of the sensor according to the program and triggers the draw rods (30) operation so that the supports for equalizer (30) coincide to reduce wheels slipping (16). When truck (10) moves along the curve, internal rod (30) is shortened, while the outer one is lengthened. The design allows wheels (16) guidance by the track at minimum levels of the wheels and the rails wear and the minimal values of the resistance to the movement.

Truck alignment rams (30) response to the track curvature estimation. The use of alignment rams (30) in this mode is a semi-active method for controlling the wheel pairs motion.

Figure 6.11 illustrates variant 2 of the three-axle truck design reported by US patent No. 8276522 B2) [148].

Alternatively, alignment rams (30) can be activated from the train position input and the database of the rail curvature, the centrifugal signal, and the difference in truck yaws (10). The data on the track curvature may come from a GPS receiver and be processed along with rail curvature database. Alignment rams (30) response to calculated truck deviation (10) in accordance to the track curvature. This operating mode is a complete active control method and can be used to control trucks motion (10) in curves. Truck (50) has frame (51) and wheel pairs (52), (53), (54). Truck (50) is connected with the body via alignment rams (70). Wheel pairs (52), (53), (54) have axles (56), conical wheels (57) and axle boxes assemblies (58). Front wheels (51) have swivel frame (61) connected by pivot mechanism (62) with intermediate frame (63). Intermediate frame (63) joins the other swivel frame (65). Swivel frame (61), intermediate frame (63), and another swivel frame (65) are interconnected by pivots (62).

The railroad truck with the wheel pairs radial control (US patent 5375533 A). US patent No. 5375533 A [149] proposes an engineering solution for a three-axle

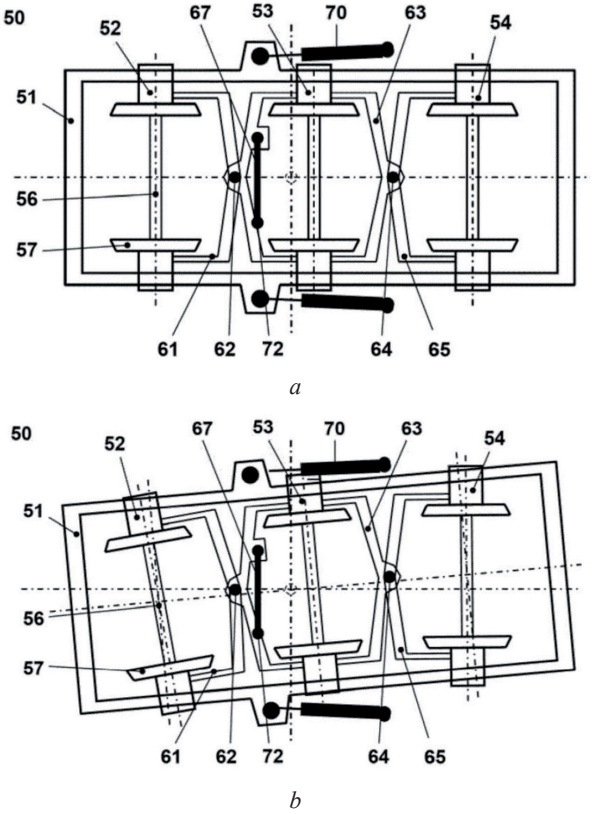

Figure 6.11. Truck with Radially Arranged Wheel Pairs in Curves. US Patent Code 8276522 B2 [148] - Variant 2

truck capable of radial alignment of the wheel pairs. The rear wheel pairs are installed in a radial position by means of the longitudinal guide rods positioned with a slope to the longitudinal direction of the vehicle. The intermediate wheel pair is displaced in the transversal direction due to the centrifugal force in the curve. The oblique arrangement of the longitudinal guiding rod provides the longitudinal displacement of the axle box assembly, which is located in opposite directions to the left and to the right. However, the intermediate wheel pair is not a part of the control in this process. It is specifically transversely directed, regardless of the outermost wheel pairs. Moreover, such a design operates in the context of the radial orientation for wheel pairs only in those cases where there is an excess of the centrifugal force. At low motion speeds, this noticeable effect will be absent.

Figure 6.12 depicts two variants of the truck arrangements of the three-axle truck according to US patent No. 5375533 A [148]. When the truck enters the curve, the middle wheel pair (3) is displaced in transversal direction. Levers (4) of the middle set rotate around supports (6) fixed on the truck arrangement frame. In this case, the rear wheel pairs are set at angle (1) with respect to the transversal axis of the truck, and their geometric axes are oriented approximately in the direction to the center of the curve. When traveling at relatively high speeds and thus with relatively high transversal acceleration, the centrifugal force makes the frame of the truck arrangement (or running gear in the dedicated patent) undergo the influence of the shear force oriented towards the outside of the curve.

Let us consider the truck of a railroad vehicle patented as EP 0161729 A1 [148]. In order to control the wheel pairs hunting oscillations in the track straight segments, the wheel pairs are interconnected through two attachments, each of

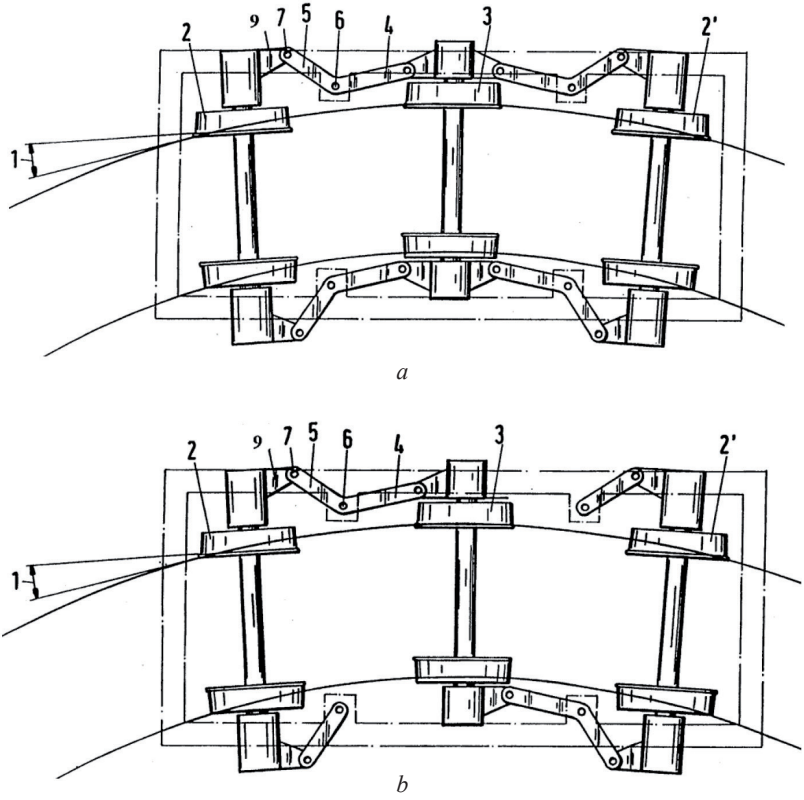

Figure 6.12. Three-Axle Truck with Radial Installation of the Wheel Pairs. US Patent 5375533 A [148]

which is coupled with the cross-coupling mechanism. The railroad wagon truck (1) comprises frame (2) and two wheel pairs (3).

The wheel pairs rotate in bearings (4). Wheels (5) of wheel pairs (3) move along rails (6). Each ram (4) has rotary bracket (7), which is connected to central part (9) of vertical lever (10) by means of spherical axis (8).

The upper end of lever (10) is pivotly suspended to neck (13) of frame (2) by means of spherical rod (12). Necks (13) are supported by spring pack (14) on axle box assemblies (4). Lower end (15) of each lever (10) is connected by means of spherical axle (16) with transversal rods (17).

Rods (17) are crossed with each other and connect levers (10) arranged diagonally opposite each other.

Thus, they form the so-called cross anchor. Spherical axles (16) can shift each other in the direction of arrows (18). These are the means to achieve a steady turn of wheel pairs (3) in the horizontal plane. Crossings (17) are arranged at a low level or at least a much lower level than axles level (19) of wheel pairs (3).

A railroad truck with a frame and two controllable axles (EP 0387744 A2) [150]. The truck in Figure 6.14 comprises frame (10) and two controlled axles (20), each of which is mounted on frame (30). Each axle is installed in the axle box

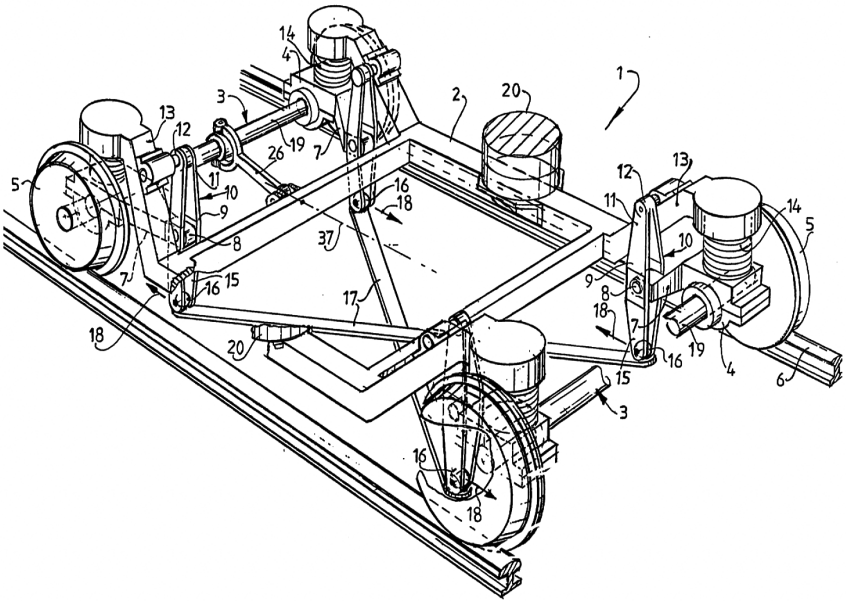

Figure 6.13. Railroad Vehicle Truck with the Controllable Position of the Axles. Patent EP 0161729 A1 [149]

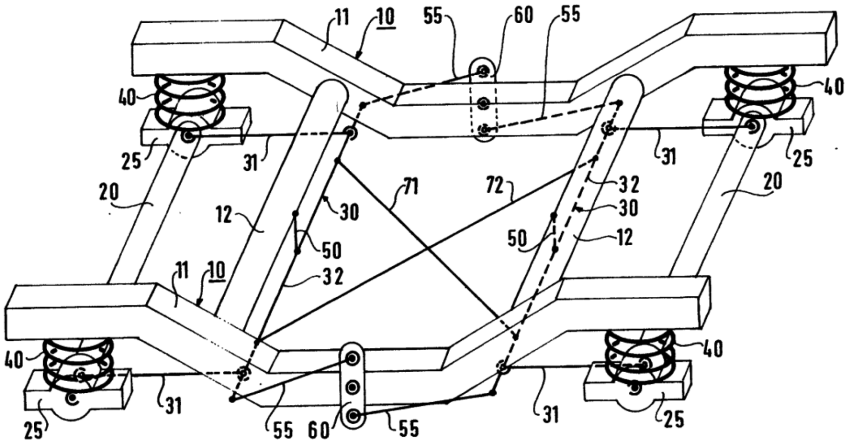

Figure 6.14. Railroad Truck with Controllable Axles Position. Patent EP 0387744 A2 [150]

pair (25) connected to the frame via primary spring suspensions (40) and vertical connecting rod (50).

The both frames are connected by two diagonal rods (71), (72). Transversal rods (32) are connected with a pair of links (55) by central levers (60). Levers (60) are pivotly installed on frame (11). When levers (60) make a turn, the wheel pairs make a turn with respect to the horizontal plane for their radial installation in the track.

CONCLUSIONS AND RESULTS

The reported study addresses the reduction of the rolling stock resistance to the movement, which is associated with the guidance of the railroad trains by tracks and enables the following conclusions and results.

1. The existence of the component of the resistance to the movement in railroad rolling stocks due to the wheel pairs guidance by rail tracks is substantiated. The authors term this kind of resistance as the kinematic resistance to the movement.

The nature of the kinematic resistance to the movement is revealed. The kinematic resistance to the movement is caused by the group interaction of the multi-axle wheel systems of rolling stocks with rail tracks. The origin of this resistance lies in the discrepancy between the geometric and kinematic parameters of each wheel contacting and the kinematic parameters of the entire rolling stock motion. The kinematic resistance to the movement is associated with circulatory processes of the closed power circuits, formed by the elements of the truck and its wheels and those of the track.

2. In the current publication, we suggest the method of the closed power circuits analysis for mechanical transmission of power within the rail rolling stock. The kinematic diagrams of the drive and the wheel pairs guidance include the closed power circuits formed by the wheel pairs and the track subsystem. Moreover, their characteristic features are quite uneven distribution of the power flows among the circuit branches and the circulation of the flows within the circuits.

The parasitic power flows are the cause of the increase in mechanical losses and the decrease in the efficiency of the multi-axle wheel mover. The level of the mechanical losses depends on the characteristics of the kinematic pairs. We introduced the circulation coefficient to estimate the level of the losses in the closed circuits. The main circulating flows that determine the level of the kinematic resistance to the movement of rail rolling stocks are the flows in the axial and the inter-axial closed power circuits. The circulation energy is absorbed in the decoupling nodes, especially in the wheel-rail contacts. In this case, the wheel-rail contacts act as friction dampers with a high degree of dissipation.

The coefficients of circulation in the specified circuits are of greatest importance when the rolling stocks are moving in the curves of medium and small radiuses, which have the values of 0.85 ... 1.0.

3. With this publication we also report on the procedure has been developed for mathematical modeling of two-point contact between the wheel and the rail as a statically undetermined system of support. The contact elasticity of the material and the spatial geometry of the rolling surfaces profiles have been taken

into account. The laws of the distribution of the vertical and the normal loads, the longitudinal and the transversal forces, and sliding velocities in contacts have been revealed and developed as the functions of the mutual positioning of the wheel and the rail in the spatial coordinate system. The procedure of translating for the main and the flange contacts has been expressed as a linear dependence of the vertical load on the relative transversal displacement of the wheel and the rail within the two-point contact zone.

The comparative analysis between the results of the integration of the rolling stock motion equations and various descriptions of the contact interaction has showed the expediency of taking into account two-point contacting when simulating the movement of rolling stocks in the mode when the flange touches the wheels and the rails.

4. Based on the analysis of the closed power circuits and geometrical characteristics of wheel-rail contacting, the procedure for simulating the kinematic resistance to the movement has been developed. The mathematical models suitable for the majority of the designs of the mass production rolling stock have been developed, among them are as follows: steam engines, electric locomotives, electric and diesel locomotives, passenger and freight wagons.

5. Based the two-point contacting features, the description of the frictional wheel-rail interaction has been refined to make it more precise. This allowed obtaining a satisfactory level of mathematical modeling reliability and evaluation of the kinematic resistance of the rolling stocks to the movement, as well as assessing the impact of the design factors. As the main criterion for the simulation validity, was assumed the kinematic resistance to the movement, which can be estimated by experimental characteristics when an additional resistance to the movement in curves. As the additional criteria, are accepted the trajectory parameters of the rolling stock motion (according to the analyzed publications on horizontal dynamics).

6. The mathematical models results have revealed the characteristics of the kinematic resistance to the movement for the mass production rolling stock.

The following results were obtained:

• rolling stock kinematic resistance to the movement in the main line curves is commonly within the range of 20 ... 50%, depending on the speed and parameters of the track; this value makes up to 80% of the total resistance to the movement in the curves with radius of 30 m... 80 m (typical for urban rail transport);

• the formulas to calculate the resistance to the movement in the curves used in traction calculations do not reflect the dependence between the specific resistance to the movement and the design features and the motion modes, but give the error of 1.5 ... 2.5 times;

• in case of the conventional truck arrangement, the rolling stocks with two-axle trucks have the specific kinematic resistance to the movement by 15% ... 30% lower than the rolling stocks with three-wheel trucks;

• the profiles of the wheel rolling surfaces with a larger angle of conicity are characterized by higher values of the resistance to the movement. In particular, under equal conditions and at the angle of the wheel flange cone of 60°, the resistance to the movement of the four-axle rolling stock is 1.3 ... 1.6 times lower than that at the wheel flange angle of 70°.

7. The analysis of the guiding force factors of the rolling stocks entering the track curves has indicated that the controllability of the rolling stocks by the rail track is a rigid characteristic associated with the transversal elasticity of rail lines. The longitudinal forces of adhesion play the role of guides only in curves with the radius of more than 1000 m ... 1250 m. On the contrary, in the curves of the medium and the small radiuses, they cause the resistance to the movement. The components of the transversal adhesion forces can act as the controllability factors only in case of the oblique wheel pairs arrangement when the first wheel pair is climbing the inner rail. In other installations, this factor causes the moment of the resistance when the train is steering around the curve. In this case, the dependence of the resistance moment on the attack angle is unstable, which manifests itself in the climbing wheel pair being prone to racheting.

8. Taking into account the high level of the transversal sliding and the transversal coupling rigidity characteristics, these forces can be considered as the main resistance factor in the entire range of the curve radiuses. Furthermore, the only really acting guiding factor is the flange gravitational forces.

9. When rolling stocks move in the curves, the approximately linear relationship between the guiding forces and the kinematic resistance to the movement is observed. It has been revealed that the rolling stock with lesser value of the resistance to the movement creates the lesser horizontal effect on the rails. Thus, the reduction in the influence on the track can be achieved through the use of the integral criterion for steering controllability quality, that is, the kinematic resistance to the movement.

10. Eventually, in the current paper we have proposed the principle for the truck arrangement design to develop the rolling stock with low resistance to the movement, based on reducing the circulation coefficient in the axle and the inter-axle closed power circuits. The certain limits of the power circulation reduction can be achieved by reducing the circuit stiffness. However, in pseudo-stationary modes of the circuit operation, for example, when moving in curves, the limitation of the circuit flows can only be made by introducing the drive and the wheel pair guidance of decoupling node points into the kinematic chains.

These methods allow reducing the kinematic resistance to the movement by 15% ... 60%, which corresponds to the reduction in the total resistance to the movement by 8% ... 20%, as well as fuel and electricity economy for trains by 5% ... 12%.

REFERENCES

1. Dobronravov A. G. (1858) *Obshchaya teoriya parovykh mashin i teoriya parovozov* [General Theory of Steam Engines and Theory of Steam Locomotives]. Sankt-Peterburg.
2. Lopushinskyi V. (1880) *Soprotivlenie parovoza i vagona dvizheniyu i deystviyu parovoy mashiny parovoza* [Resistance of Steam Engines and Wagons to the Movement and the Influence of the Engines]. Sankt-Peterburg.
3. Ermakov L. (1960) *Dani i rozrakhunki, shcho vidnosyat'sya do vzhivannya parovoziv (1809-1959)* [Data and Calculations Relating to Locomotives Operation 1809-1959)]. Moscow: Moscow Institute of Railway Engineers.
4. Borodin A. (1893) *Sluzhby podvizhnogo sostava Yugo-Zapadnykh zheleznykh dorog v period desyatiletiya 1880 - 1889 gg* [The Rolling Stock Services of the Southern-Western Railways of the Decade 1880 - 1889]. Kiev.
5. Petrov N. (1892) *O naivygodneyshey skorosti tovarnykh poezdov* [About the Most Advantageous Speed for Goods Train]. Sankt-Peterburg.
6. Petrov N. (1879) *Parovozy* [Locomotives]. Sankt-Peterburg.
7. Petrov N. (1898) *Soprotivlenie poezdov na zheleznykh dorogakh* [Train Resistance at Railways]. Sankt-Peterburg.
8. Romanov A. D. (1893) *Parovozy* [Locomotives]. Sankt-Peterburg.
9. Smirnov S. (1895) *Kurs podvizhnogo sostava i tyagi* [Lecturing Course on Rolling Stock and Traction]. Sankt-Peterburg.
10. Lomonosov Yu. (1912) *Tyagovye raschety i prilozheniya k nim graficheskikh metodov* [Traction Calculations and Appendixes with Graphical Methods]. Sankt-Peterburg.
11. Davis W. J. (1904) Train resistance. *The Street Railway Journal*. Vol. 24. No. 23, p.p. 1000-1003.
12. Schmidt W. J., Dunn H. H. (1918) Passenger Train Resistance. *University of Illinois bulletin.* No. 110, p. 4.
13. Schmidt E. (1910) Freight Train Resistance: Its Relation to Car Weight. *Bulletin 43*, p. 144.
14. Schmidt E. C., Marquis F. W. (1912) The Effects of Cold Weather upon Train Resistance and Tonnage Rating. *Bulletin 59*. p. 25.
15. Dunn H. H. (1914) The Tractive Resistance of a 28ton Electric Car. *Bulletin 74*. p. 45.
16. Schmidt E. C., Dunn H. H. (1916) The Tractive Resistance on Curves of a 28-ton Electric Car. *Bulletin 92*. *Of the Engineering Experiment Station of the University of Illinois*. p. 54.
17. Edward C. Schmidt (1927) Freight Erain Curve Resistance on a One-Degree Curve and on a Three-Degree Curve. *University of Illinois Bulletin*. Vol. XXIV. July 12. No 45.
18. Rochard B., Schmid F. (2000) A Review of Methods to Measure and Calculate Train Resistances. *Proceedings of the Institution of Mechanical Engineers, Part F: Journal of Rail and Rapid Transit.* Vol. 214. No 4. p.p. 185-199.

19. Armstrong A. (1910) Electric Traction. *Standard Handbook for Electrical Engineers*. *Section 13*. p.p. 947-1085.

20. Davis W. J. (1926) The Tractive Resistance of Electric Locomotives and Cars. *Gen. Electr. Rev*. p. 29.

21. Yu. V. Lomonosov (1915) *Tyagovye raschety: 2-izd.* [Traction Calculations. 2-nd Edition]. Odessa.

22. Karachan B. (1958) Raschet dopolnitel'nogo soprotivleniya dvizheniyu ot krivykh [Calculation of the Additional Resistance to the Movement in Curves]. *Zheleznodorozhnyy transport* [Railway Transport]. No 4.

23. Gurskiy P. (1944) Soprotivlenie dvizheniyu chetyrekhosnykh tsistern [Resistance to the Movement of Four-Axle Tank-Cars]. *Zheleznodorozhnyy transport* [Railway Transport]. No 12.

24. Astakhov P. (1948) Osnovnoe soprotivlenie tovarnykh vagonov v srednezimnikh usloviyakh [Main Resistance of the Freight Wagons under Average Winder Conditions]. *Tekhnika zheleznykh dorog* [Railway Equipment Magazine]. No 9.

25. Vedenisov B., Komarov A, Nadezhin S. (1950) Povyshenie skorosti dvizheniya, moshchnosti i effektivnosti tyagovykh sredstv transporta [Increase in the Movement Speed, Power and Efficiency of the Transportation Means Traction]. Moscow: USSR Academy of Science. No 1.

26. Sharonin V, Proskurin Yu, Pinn V. (1961) Issledovanie soprotivleniya dvizheniyu gruzovykh i passazhirskikh vagonov na rolikovykh podshipntikakh [Study on the Resistance to the Movement of Freight and Passenger Wagons Operating on Roller Bearings]. *Trudy TsNII* [Journal of Central Scientific and Research Institute]. No 221.

27. P. Gursky (1956) Soprotivlenie dvizheniyu passazhirskikh vagonov na bol'shikh skorostyakh [Resistance to the Movement of Passenger Wagons at High Speeds]. *Vestnik VNIIZhT* [Vestnik of the Railway Research Institute]. No 3.

28. Baranov A. (1963) Osnovnoe soprotivlenie vagonov na rolikovykh podshipnikakh. [Main Resistance Generated by Wagons with Roller Bearings]. *Vestnik VNIIZhT* [Vestnik of the Railway Research Institute]. No 4.

29. Rules of Traction Calculations for Train Operation. Moscow: Transport. 1985. 287 c.

30. Schmidt E. (1927) Freight Train Curve Resistance on a One-Degree Curve and on a Three-Degree Curve. *University of Illinois Bulletin*. Vol. XXIV. July 12, No 45.

31. Amelin S., Andreyev G. (1986) Ustroystvo i ekspluatatsiya puti [*Railway Design and Operation*]. Moscow: Transport. p 238.

32. Armstrong A. H. (1910) Electric Traction. *Standard Handbook for Electrical Engineers.* Section 13. p.p. 947-1085.

33. Astakhov P. N., Stromski P. P. (1962) Opredelenie osnovnogo soprotivleniya dvizheniyu podvizhnogo sostava na eksperimental'nom kol'tse [Determination of the Main Resistance to the Movement of the Rolling Stock on the Experimental Loop]. *Vestnik VNIIZhT* [Vestnik of the Railway Research Institute]. No 6. p.p. 60-78.

34. Rochard B. P., Schmid F. A. (2000) Review of Methods to Measure and Calculate Train Resistances. Proceedings of the Institution of Mechanical Engineers. Part F. *Journal of Rail and Rapid Transit*. Vol.214. No .4. P.185–199.

35. *Practical Guide to Railway Engineering. Chapter 2.* Railway Industry Overview. Available at: https://www.arema.org/publications/pgre/Practical_ Guide/PGChapter2.pdf

36. Fayet P. (2008) *Modélisation des réseaux électriques ferroviaires alimentés en courant alternatif*. PhD thesis. Ecully: Ecole centrale de Lyon.

37. Mlinarić T. J., Ponikvar K. (2011) Energy Efficiency of Railway Lines PROMET. *Traffic & Transportation*. Vol. 23. No 3. p.p. 187-193.

38. Economics of Railway Engineering and Operation. AREMA Manual for Railway Engineering. *American Railway Engineering and Maintenance-of-Way Association.* 1999. 232 p.

39. Astakhov P. N. (1966) Soprotivlenie dvizheniyu zheleznodorozhnogo podvizhnogo sostava [*Tractive Resistance of the Rolling Stock*]. Moscow: Transport. No 311. 179 p.

40. Armstrong D. S., Swift P. H. (1990) Lower Energy Technology. *Identification of energy use in multiple units. Report MR VS 077. Part A.* 20 July. Derby: British Rail Research.

41. Radosavljevic (2006). Proceedings of the Institution of Mechanical Engineers. *Journal of Rail and Rapid Transit. Part F.* Vol. 220. p.p 283-291.

42. Lysyuk V. S. (2002) *Prichiny i mekhanizm skhoda kolesa s rel'sa. Problema iznosa koles i rel'sov* [Causes and Mechanisms of Derailing. Wheels and Rails Wearing resistance]. Moscow: Transport. 216 p.

43. Markov D. P. (2003) Zadir bokovykh poverkhnostey rel'sov i grebney koles [Torn of Lateral Surfaces with Rails and Wheel Flanges]. *Vestnik VNIIZhT* [Vestnik of the Railway Research Institute]. No 3. p.p. 30-35.

44. Markov D. P. (2004) Tipy katastroficheskogo iznashivaniya, voznikayushchie na kolesno-rel'sovykh stalyakh [Types of Catastrophic Wearing of Wheel-Rail Steels]. *Vestnik VNIIZhT* [Vestnik of the Railway Research Institute]. No 2. p.p. 30-35.

45. Boschetti G., Mariscotti A. (2012) The Parameters of Motion Mechanical Equations as a Source of Uncertainty for Traction Systems Simulation. *XX IMEKO World Congress Metrology for Green Growth September 9-14*. Busan. Republic of Korea.

46. Bouden F. P., Teybor D. (1968) Trenie i smazka tverdykh tel [Friction and Lubrication of Rigid Bodies]. Moscow: Machine building. 543 p.

47. Morozov A. M, Kramarenko P. Yu. (1975) Uproshchennaya metodika opredeleniya osnovnogo udel'nogo soprotivleniya dvizheniyu lokomotiva kak povozki [Simplified Procedure to Determine the Main Specific Movement of the Locomotive as the Type of the Truck Arrangement]. *Trudy VNITI* [Journal of Scientific and Research Institute of Military Orientation]. No 42. p.p. 86-91.

48. *Ishlinskiy A. Yu. (1954) Rassmotrenie voprosov ob ustoychivosti ravnovesiya uprugikh tel s tochki zreniya matematicheskoy teorii uprugosti* [Review on Equilibrium Stability from the Standpoint of Mathematical Theory of Elesticity]. *Ukrainian Mathematical Journal. Vol.6.* No *2. p.p. 140-146.*

49. Palmgren A. (1945) *Ball and Roller Bearing Engineering*. Philadelphia, SKF Industries Inc. 431 p.

50. Tabor D, Amer J. (1956) The Mechanism of «Free» Rolling Friction. *Soc. Lubricat. Engrs*. No 6. p.p. 379–386.

51. Tomlinson J. A. (1929) A Moleculur Theory of Friction *Philos. Mag. Ser.* 7. No 198. p.p 905–939.

52. Pinegin S. V. (1969) Kontaktnaya prochnost' i soprotivlenie kacheniyu [Contact Strength and Resistance to Rolling]. Moscow: Machine Building. 243 p.

53. Pinegin S. V. (1976) Trenie kacheniya v mashinakh i priborakh [Rolling Friction in the Machines and Devices]. Moscow: Machine Building. 264 p.

54. Akhmatov A. S. (1963) Molekulyarnaya fizika granichnogo treniya [Molecular Physics of the Boundary Friction]. Moscow: State Publishing House of Physical and Mathematical Literature. 482 p.

55. Deryagin B. V., Korotova N. A., Smigla V. P. (1973) Adgeziya tverdykh tel [Rigid Body Adhesion]. Moscow: Science. 280 p.

56. Blokhin Yu. (1973) Issledovanie soprotivleniya kacheniyu detaley mashin v shirokom diapazone skorostey [Study of the Resitance to Rolling of Machine Details with a Wide Range of Speeds]. PhD thesis report. Moscow: Institute of Mechanical Science of USSR Academy of Sciences. 17 p.

57. Blokhin Yu. (1972) Koeffitsienty treniya kacheniya gladkikh tsilindrov pri predel'noy nesushchey sposobnosti maslyanogo sloya [Coefficients of Rolling Friction for Even Cylinders at Boundary Capability of Oil Layer]. Moscow: Mechanical Science. No 3. p.p. 85-89.

58. Drutovski R. C. (1965) The Roll of Microslip for Freely Rolling on Bodies. *J.Bsic. Trans.ASME. S.D*.V.87. p.p 724-728.

59. Johnson K. L. (1962) *Tangential Traction and Microslip in Rolling Contact Phenomena*. Amsterdam: Ed.by Bidwell Elsevier Publishing Company. p.p. 6-28.

60. N. A. Korolyova (1965) Izmenenie poverkhnostnogo sloya stal'nykh detaley pri obkatyvanii pod nagruzkoy [The Changes in the Surface Layer of the Steel Parts under the Load]. *Mechanical Science*. No 3. p.p. 66-75.

61. Tadao Ohyama, Seigo Uchida (1994-6) Behavoir of Traction Force between Wheel and Rail from Microslip to Gross Sliding: Some Experiments under Water Lubrication with Static and Dynamic Contact Loads. *Trans. Jpn. Soc. Mech.Eng.* Vol. 60, No 574. p.p. 207–212

62. Drutovski R. C. (1965) The Roll of Microslip for Freely Rolling on Bodies. *J.Bsic. Trans.ASME. S.D*. Vol. 87. p.p. 724-728.

63. Konvisarov D. V. (1952) K teorii kacheniya [To Rolling Theory] Report of USSR Academy of Sciences. Vol. XXXIII: Mechanics. No 3.

64. Konvisarov D. V., Pokrovskaya A. A. (1955) *Vliyanie radiusov krivizny tsilindricheskikh tel na ikh soprotivlenie perekatyvaniyu pri razlichnykh nagruzkakh* [Influence of Radiuses of Cylindrical Bodies on their Resistance to Rolling at Various Loads]. No 43.

65. Горячева И. Г. Kontaktnaya zadacha kacheniya vyazkouprugogo tsilindra po osnovaniyu iz togo zhe materiala [Contact Problem for Viscoelastic Cylinder Rolling on the Surface of the Same Material]. *Journal of Applied Mathematics and Mechanics*. Vol. 37. No 5. p.p. 925-933.

66. Goryacheva G., Galina L. A. (1978) Kontaktnye zadachi teorii uprugosti pri nalichii iznosa [Contact Problems for Elasticity Theory at Wearing Phenomenon]. *Theory of Friction, Wearing and Standardization Problems*. p.p. 251-265.

67. Goryacheva G., Galina L. A. (1980) Kontaktnye zadachi i ikh prilozhenie k teorii treniya i iznosa [Contact Problems and their Application for Theory of Friction and Wearing]. *Trenie i Iznos* [Friction and Wear]. Vol. 1. No 1. p.p 105-119.

68. Reynolds O. (1876) On Rolling friction. *Philos. Trans. Roy. Soc*. Vol. 166. p.p 155-175.

69. Kheyman Kh. (1957) Napravlenie zheleznodorozhnykh ekipazhey rel'sovoy koleey [Guiding of Railway Trains by Tracks]. Moscow: State Publication House on Railway Literature. 415 p.

70. Pieringer A., Baeza L., Kropp W. (2015) Modelling of Railway Curve Squeal Including Effects of Wheel Rotation. *Noise and Vibration Mitigation for Rail Transportation Systems.* Springer, Berlin, Heidelberg. p.p 417-424.

71. Dusza M. (2015) The Wheel-Rail Contact Friction Influence on High Speed Vehicle Model Stability. *Transport Problems*. Vol.10. No 3. p.p. 74-86.

72. Zeng J., Wei L., Wu P. Safety Evaluation for Railway (2016) Vehicles Using an Improved Indirect Measurement Method of Wheel-Rail Forces. *Journal of Modern Transportation*. Vol. 24. No 2. p.p. 114-123.

73. Tkachenko V. P., Sapronova S. Y., Maliuk S. V., Kulbovskyi I. I. (2016) Studying the Structure of Railway Rolling Stock Resistance. *Metallurgical and Mining Industry*. No 11. p.p. 30-36.

74. Tkachenko V., Sapronova S. Refinement of the Structure of Motion Resistance of railway vehicles. *Proceedings of IX International Scientific Conference Transport Problems*. Katowice-Sulejów: Politechnika Śląska. p.p. 216-222.

75. Golubenko A. Sapronova S., Tkacenko V. (2007) Kinematics of Point-to-Point Contact of Wheels with Rails. *Transport Problems*. Vol. 2, No 3. p.p. 57-61.

76. Tkachenko V., Sapronova S. (2007) Steerability of Railway Vehicles. *Transport Problems*. Vol.2. p.p. 9-16.

77. Heathcote H. L. (1921) The Ball Bearing in Making under Test and Service. *Proc. Inst. Auto-Engineers*. Vol. 15. p.p. 569–622.

78. Tkachenko V. P. (2009) Do optimizatsiï sistemi normativno-dopuskovikh parametriv znosu grebeniv bandazhiv lokomotiviv [On Optimization for Normative Allowance Parameters of Bandage Locomotives Flange Wearing] / *Zaliznichniy transport Ukraïni* [Railway Transport of Ukraine]. No 1. p.p. 37-39.

79. Kutsenko S. M., Slashchev V. A. (1968) Matematicheskaya model' zheleznodorozhnogo ekipazha, dvizhushchegosya po pryamomu uchastku puti s uchetom vzaimodeystviya grebney koles s rel'sami [Mathematical Model for Railway Vehicles to Move on the Track Straight Sections with Account to the Wheel Flange-Rail Interaction]. *Trudy VNITI* [Journal of Scientific and Research Institute of Military Orientation]. No. 31. p.p. 83−91.

80. Ershkov O. P. (1966) Raschety poperechnykh gorizontal'nykh sil v krivykh [Calculation of Transversal Horizontal Forces in Curves]. *Trudy Vsesoyuz. nauch.issled. in-ta zh.-d. transp*. [Journal of the Railway Research Institute]. Moscow: Transport. No 301. p. 235.

81. Minov D. K. (1965) *Povyshenie tyagovykh svoystv elektrovozov i teplovozov s elektricheskoy peredachey* [Enhancing Traction Properties of Electric-Diesel Trains with Electric Transition]. Moscow: Transport. 267 p.

82. Kravchenko A. I. (1972) Ob upravlyaemom napravlenii zheleznodorozhnykh ekipazhey pri dvizhenii v krivykh [On Controllable Guiding of Railway Trains in Curves]. *Materialy n.-t. konf. «Povyshenie ekspluatatsionnoy nadezhnosti lokomotivov v usloviyakh dorog Urala i Sibiri»* [Proceedings of Scientific and Engineering Conference "Enhancing Operational Dependability of Locomotives under Conditions of Ural and Siberia"]. p.p. 224-228.

83. Kashnikov V. M. (1975) Opredelenie funktsii upravleniya zheleznodorozhnym ekipazhem pri vkhode v krivuyu [Defining the Function of Railway Vehicle Control at Entering the Curve] *Voprosy konstruktsii i dinamiki lokomotivov i povyshenie nadezhnosti tormozov* [Issues of Railway Locomotive Design and Dynamics and Dependability of Braking Systems]. No. 115. p.p. 3-10.

84. Kashnikov V. M. (1982) *Основы теории управляемого движения локомотивов в рельсовой колее* [Fundamentals of Controllable Motion of Locomotives in Railway Track]. Rostov-na-Donu. 30 p.

85. Kashnikov V. M. (1983) *Upravlenie dvizheniem zheleznodorozhnykh ekipazhey v krivykh uchastkakh rel'sovoy kolei* [Control over Railway Vehicle Movement in Railway Curves]: PhD thesis. Rostov-na-Donu. 394 p.

86. Patent of the Russian Federation. No 2090406 Device for Self-Alignment of Railway Wheel Pairs of Railway Vehicles. Grinevich V. P., Dmitriev A. S. MKI B61 F 5/38. appl. 20.9.07, Bull. No 26.

87. General Motors Three-Axle Radial Stiring Bogie for Heavy Haul Locomotives. *Pap. 10th Int. Wheelset Congr. "Sharing Lates Wheelset Technol. Order Reduce Coats and Improve Railway Prod"*. Sidney, 27 Sept. 10 Oct., 1992. Nat. Conf. Publ. 1992. No 92/10. p.p. 97-100.

88. Sheffel' Kh. (1989) Radial'no ustanavlivayushchiesya kolesnye pary elektrovozov [Radial Wheel Pairs of Electric Trains]. *Zheleznye dorogi mira* [*Railways of the World*]. No 2. p.p. 74–76.

89. Kobayashi H. (2000) The New Bogies for Diesel - Trans Japan Railways *Quarterly Report of RTRI*. No 1. p.p. 16 – 20.

90. Upadhyay R. (2000) Reduced Wear Wheels and Rails. *International Railway Journal*. No 7. p.p. 33–34.

91. Chuprakov E. V. (2016) Snizhenie iznosa koles i rel'sov za schet differentsial'nogo vrashcheniya kolesnykh par netyagovogo podvizhnogo sostava pri dvizhenii v krivykh uchastkakh puti [Reduced Wheel and Rail Wear due to Differential Wheel Pair Rotation within Non-Traction Rolling Stock at Motion in Track Curved Section]: PhD thesis. Irkutsk: IrGUPS 225 p.

92. Tseglynsky K. Ju. (1913) *Kurs zheleznykh dorog. Obshchie svedeniya o zheleznykh dorogakh. Podvizhnoy sostav i usloviya prokhozhdeniya ego po rel'sovoy kolee. Proektirovanie zheleznodorozhnoy linii* [Railway Road Lecturing Course. General Information on Railways. Rolling Stock and Conditions of its Movement on Railway Tracks. Railway Track Design]. Moscow: Vladimir Chicherin Company Publishing House. No. I. 260 p.

93. Koroliov K. P. (1950) *Vpisyvanie parovozov v krivye uchastki puti* [Insertion of the Steam Engines into Railway Track Curved Sections]. Moscow: State Publication House on Railway Literature. 224 p.

94. Carter F. (1926) On the Action of a Locomotive Driving Wheel. *Proc. R. Soc. London* 112. p.p. 151–157.

95. Johnson K. L. (1964) The Effect of a Tangential Force upon the Rolling Motion of an Elastic Sphere upon a Plane. *J.Appl.mec*. V.31. No 2. p.p. 339-340.

96. Halling J. (1964) Microslip between a Rolling Element and its Track Arising from Geometric Conformity. *J. Mech. Engnr. Science*. Vol. 6. No 1. p.p. 64-73.

97. Hainess D. J., Olerton E. (1963) Contact Stress Distributions on Elliptical Contact Surfaces Subjected to Radial and Tangential Forces. *Proc. Inst. Mech. Engrn*. Vol. 177. No .4.

98. Kalker J. J. (1967) *On the Rolling Contact of Two Elastic Bodies in the Presence of Dry Friction*: Doct.Thesis. Delft University. 160 p.

99. Kalker J. J. (1973) Simplified Theory of Rolling Contact. *Mechanical and Aeronautical Engineering and Shipbuilding*. Delft Progr. Rep. 1P. S.C. p.p 1-10.

100. Barwell F.T. Einige Ergebnisse Uber Reibung und Verschreib unter besonderer Bezugnahme Auf die Reibzahlzwschen Raben und Schiene. Glasers Annalen. No 1, p.p. 1-3.

101. Mariama H, Ohyama T. (1998) Reibung bei Rollen berruhrung. *Beruhrung zwischen einen Rad und einer*.

102. Chap J. (1973) Modelove visetreni sklurovich charakteristik selesnicho dviokoli, pri zhenach a jejich frekvence. *SbornikVUD VSD*. No. 54. p. 57.

103. Patent of the USSR. A.S. 1444636, MKI G01 M 17/00. No 4112929. The Experimental Unit for Railway Vehicle Testing. Tkachenko V. P., Gorbunov N. I., Mikhaylov E. V. appl. 25.08.86, publ. 15.12.88, Bull No 46.

104. Golubenko A. L. Tkachenko V.P. (1984) Eksperimental'nye issledovaniya kharakteristik stsepleniya kolesa s rel'som na stendovoy ustanovke [Experimental Study on Wheel-Rail Adhesion at the Experimental Unit]. *Konstruirovanie i pr-vo transp. mashin* [Design and Rules for Means of Transportation]. No 16. p.p. 20-22.

105. Ling L, Dhanasekar M., Thambiratnam D. P., Sun Y. Q. Lateral impact derailment mechanisms, simulation and analysis. *International Journal of Impact Engineering*.2016. Vol.94. p.p. 36–49.

106. Leishman E. M, Hendry M. T., Martin C. D. Canadian Main Track Derailment Trends 2001 to 2014. *Canadian Journal of Civil Engineering*. Available at: https://doi.org/10.1139/cjce-2017-0076.

107. Liu X. (2015) Statistical Temporal Analysis of Freight Train Derailment Rates in the United States: 2000 to 2012. *Transportation Research Record: Journal of the Transportation Research Board*. No 2476. p.p. 119–125.

108. Liu X. (2017) Statistical Causal Analysis of Freight-Train Derailments in the United States. *Journal of transportation engineering*. Part A: Systems. Vol.143. No 2. p.p. 4-16.

109. Nadal M. J. (1896) Theorie de la Stabilite des locomotives, Part II: mouvement de lacet. *Annales des Mines*.Vol. 1. p.p. 232-245.

110. Ishida H., Matsuo M. (1999) Safety Criteria for Evaluation of Railway Vehicle Derailment. *Quarterly Report of RTRI*. Vol. 40. No 1. p.p. 18–25.

111. Ishida H., Miyamoto T., Maebashi E., Doi H., Iida K., Furukawa A. Safety Assessment for Flange Climb Derailment of Trains Running at Low Speeds on Sharp Curves. *Quarterly Report of Railway Technical Research Institute.* 2006. Vol. 47. No 2. p.p. 65–71.

112. Tkachenko V. P., Sapronova S. Yu. (2015) Otsinka stiykosti zaliznichnikh ekipazhiv vid skhodu z reyok [Estimation of Stability of Railway Vehicles against Derailing]. *Visnik SNU im. V.Dalya* [Journal of Volodymyr Dahl East Ukrainian National University]. No 1[218]. p.p. 266–271.

113. Shabana A. A. (2012) Nadal's Formula and High Speed Rail Derailments. *Journal of Computational and Non-Linear Dynamics*. Vol. 7. No 4., p.p. 41-93.

114. *Dukkipati R. (2000) Vehicle Dynamics. Narosa Publishing House. p.p. 227–228.*

115. Santamaria J., Vadillo E., Gomez J. (2009) Influence of Creep Forces on the Risk of Derailment of Railway Vehicles. *Vehicle System Dynamics. International Journal of Vehicle Mechanics and Mobility*. Vol. 47. No 6. p.p. 721–752.

116. Marquis B., Grief R. (2011) Application of Nadal limit in the Prediction of Wheel Climb Derailment. *Proceedings of the ASME/ASCE/IEEE 2011 Joint Rail Conference, Pueblo, CO*. JRC2011-56064. p.p. 273–280.

117. Ohno K. (2003) Research and Development for Eliminating Wheelclimb Derailment Accidents. *JR East Technical Review*. No 2. p.p. 46–50.

118. Bibel G. (2012) *Train Wreck – the Forensics of Rail Disasters*. Baltimore: Hopkins University Press. 368 p.

119. Uchida M., Takai H., Muramatsu H., Ishida H. (2002) Derailment Safety Evaluation by Analytic Equations. *Quarterly Report of Railway Technical Research Institute*. Vol. 43. No 3. p.p. 119–124.

120. Сокол Э. (2010) Вкатывание гребня колеса на острие остряка стрелочного перевода [Wheel Flange In-Rolling on the Pointed Part of Pointwork]. *Zaliznichniy transport Ukraïni* [Railway Transport of Ukraine]. No 5. p.p. 26–30.

121. Kardas-Cinal E. (2009) Comparative Study of Running Safety and Ride Comfort of Railway Vehicle. *Prace naukowe politechniki warszawskiej*. Z. 71. p.p. 75–84.

122. Iijima H, Yoshida H., Suzuki K., Yasuda Y. (2014) A Study on the Prevention of Wheel-Climb Derailment at Low Speed Ranges. *Quarterly Report of Railway Technical Research Institute*. No 30. p.p. 21–24.

123. Zeng J., Wei L., Wu P. (2016) Safety Evaluation for Railway Vehicles Using an Improved Indirect Measurement Method of Wheel-Rail Forces. *Journal of Modern Transportation*. Vol.24, No 2, p.p. 114–123.

124. Myamlin S, Lingaitis L., Dailydka S., Vaičiūnas G., Bogdevičius M., Bureika B. (2015) Determination of the Dynamic Characteristics of Freight Wagons with Various Bogies. *Journal Transport*. Vol. 30(1). p.p. 88–92. http://www.tandfonline.com/toc/tran20/30/1.

125. Miyamoto M. (1996) Mechanism of Derailment Phenomena of Railway Vehicles. Railway. *Technical Research Institute, Quarterly Reports*. Vol. 37. No 3. p.p. 147–155.

126. Molatefi H., Mazraeh A. (2016) On the Investigation of Wheel Flange Climb Derailment Mechanism and Methods to Control it. *Journal of Theoretical and Applied Mechanics*. No 2. p.p. 541–550.

127. Kardas-Cinal E. (2014) Selected Problems in Railway Vehicle Dynamics Related to Running Safety. The Archives of Transport. Vol. 31. No 3. p.p. 37–45.

128. A Technical Guide on Derailments. Government of India Ministry of Railways. Maharajpur Gwalior. Centre for Advanced Maintenance Technology. 1998. 133 p.

129. Burgelman N., Li Z., Dollevoet R. (2016) Effect of the Longitudinal Contact Location on Vehicle Dynamics Simulation. *Mathematical Problems in Engineering*. Available at: https://www.researchgate.net/publication/292185450_Effect_of_the_Longitudinal_Contact_Location_on_Vehicle_Dynamics_Simulation.

130. Costea D. M., Gaman M. N, Dumitru G. (2013) Considerations On Tribological Phnenomenons at the Wheel-Rail Contact Level, Specific To The Br 189 Class Locomotives. *Annals of the Faculty of Engineering Hunedoara*. Vol. 11. No 4. p.p. 181–188.

131. Pombo J., Ambrósio J. (2008) Application of a Wheel-Rail Contact Model to Railway Dynamics in Small Radius Curved Tracks. *Multibody System Dynamics*. Vol. 19, No 1. p.p. 91–114.

132. Golubenko A., Sapronova S., Tkachenko V. (2007) Kinematics of Point-To-Point Contact of Wheels with Rails. *Transport Problems*. Vol. 2. No 3. p.p. 57–61.

133. Sapronova S., Tkachenko V., Kramar N., Voron'ko A. (2008) Regularities of Shaping of a Wheel Profile as a Result of Deterioration of the Rolling Surface in Exploitation. *Transport Problems*. Vol.3. No 4. p.p. 47–57.

134. Fomin O., Kulbovskiy I., Sorochinska E., Sapronova S., Bambura O. (2017) Experimental Confirmation of the Theory of Implementation of the Coupled Design of Center Girder of The Hopper Wagons for Iron Ore Pellets. *Eastern-European Journal of Enterprise Technologies*. 5/1(89) p.p 11-18

135. Tkachenko V., Sapronova S., Kulbovskyi I., Fomin A. (2017) Research into Resistance to the Motion of Railroad Undercarriages Related to Directing the Wheelsets by a Rail Track. *Eastern-European Journal of Enterprise Technologies*. No 5/7 (89). p.p. 65-72

136. Татуревич А. А. (2003) Teoreticheskie issledovaniya ustoychivosti podvizhnogo sostava protiv skhoda ot vkatyvaniya grebnya kolesa na rel's [Theoretical Study on Stability of the Rolling Stock against Wheel Flange Climbing on Railway Track]. *Visnik DNUZTi* [Journal of Dnipropetrovsk National University of Railway Transport named after academician V. Lazaryan]. No 2. p.p. 133–137.

137. Martland C. Zhu Y., Lahrech, Sussman J. (2001) Risk and Train Control: A framework for Analysis. *Transportation Research Record: Journal of the Transportation Research Board*. No 1742. p.p. 25–33.

138. Amos P, Bullock D., Sondhi J. (2010) High-Speed Rail: The Fast Track to Economic Development. *The World Bank*. p.p. 1-28.

139. Tkachenko V. P. (1996) Kinematycheskoe soprotyvlenye dvyzhenyyu y eho mesto v obshchey klassyfykatsyy soprotyvlenyy dvyzhenyyu relsovykh ekipazhey [Kinematic Resistance of Engines and its Position in the Rolling Stock Engine General Classification of the Resistance to Movement]. *HNTB Ukrayny*– 6 p.

140. Baek K S., Kyogoku K., Nakahara T., Kyogoku K., Nakahara T. (2007) An Experimental Investigation of Transient Traction Characteristics in Rolling–Sliding Wheel/Rail Contacts under Dry–Wet Conditions. *Wear*. Vol. 263, No 1. p.p. 169-179.

141. Tkachenko V. (1994) Vehicle Railway Vibration Influence on the Train Traction Resistance. *Vibrations in Physical Systems: XVIth Symposium. Poznan*. p.p. 160.

142. Tkachenko V. P. (1998) Upravlyaemost' rel'sovykh ekipazhey [Controllability of Rail Vehicles]. *Zaliznichniy transport Ukraïni* [Railway Transport of Ukraine]. No 2-3. p.p. 37-41.

143. Tkachenko V. P. (1996) *Kinematicheskoe soprotivlenie dvizheniyu rel'sovykh ekipazhey* [Kinematic Resistance to Rolling Stock Movement]. Lugansk: East Ukrainian National University. 200 p.

144. Gorbunov N. I. (1987) *Povyshenie tyagovykh kachestv teplovozov za schet sovershenstvovaniya uprugikh svyazey telezhek* [Enhancing the Diesel Trains Traction Characteristics by Improvements in Truck Spring Connections]: PhD thesis report. Dnipropetrovsk National University of Railway Transport named after academician V. Lazaryan. Dnipropetrovsk. 19 p.

145. Yayati Jadhav. Why Don't the Wheels of a Train Skid while Carrying so Much Weight, even Though the Rail-Wheel Friction is Low? [Електронний ресурс]. Available at: https://www.quora.com/why-dont-the-wheels-of-a-train-skid-while-carrying-so-much-weight-even-though-the-rail-wheel-friction-is-low/

146. Patent EP 2157007 A1. Two-Axle Bogie for Railway Vehicle with Radially Adjustable Wheelsets with Cross Coupling. Valigursky J., Meltzer I., Moravcik M., Rydlo P. Appl. and owner. Tatravagónka A.S. No EP20090475002, appl. 11.05.2009; publ. 24.02.2010.

147. Patent of US 8276522 B2. Steering Railway Bogie. Simson S. Appl. and owner Central Queensland University.No US 12/527,899; appl. 21.02.2008; publ. 2.10.2012

148. Grant US5375533 A. Running Gear for Rail Vehicles with Radial Control of the Wheelsets. Schwendt L. Appl. and owner Abbhenschel Lokomotiven Gmbh. No US 08/213,372; appl. 14.03.1994. publ. 27.12.1994.

149. Patent EP0161729 A1. Bogie for a Rail Vehicle. Steur Wolfram De. Appl. and owner RMO-Werkspoor Services B.V. No EP19850200769. appl. 14.05.1985. publ. 21.11.1985.

150. Patent EP 0387744 A2. Railway Bogie Comprising a Frame and Two Steerable Axles. Gec Alsthom Sa. Appl. and owner Roland 5 Résidence du Clos d'Orléans Joly. No EP19900104617. appl. 12.03.1990; publ. 19.09.1990.

151. Patent of the USSR A.S. 1206153. MKI B61 F 5/00. Two-Axle Truck of Railway Vehicle. Gorbunov N. I., Mikhaylov E. V., Konyaev A. N., Golubenko A. L., Tkachenko V. P., Kramar' N. M. No 3728393; appl. 13.04.84; publ.23.01.86, Bull. No 3. 2 p.

Наукове видання

САПРОНОВА Світлана Юріївна
ТКАЧЕНКО Віктор Петрович
ФОМІН Олексій Вікторович
КУЛЬБОВСЬКИЙ Іван Іванович
ЗУБ Євген Петрович

РЕЙКОВІ ЕКІПАЖІ: ОПІР РУХУ ТА КЕРОВАНІСТЬ

Монографія

(Англійською мовою)

Формат 60x84 1/16. Папір офсетний. Друк
різографічний. Умовн.друк.арк.???
Наклад ??? Зам № ???

Видано та віддруковано в ???????
Свідоцтво суб'єкта видавничої справи ???????